UNIVERSITY OF AGDER

Electrification of the Utsira formation

Electric System Requirements for a Power Distribution Platform

Anders Ballari

&

Jan Sola Østensen

Master Thesis in Renewable Energy
University of Agder
Faculty of Engineering and Science

This Masters Thesis is carried out as a part of the education at the University of Agder and is therefore approved as a part of this education. However, this does not imply that the University answers for the methods that are used or the conclusions that are drawn.

Grimstad, June 3, 2013

Supervisors

Ben Bjørke
Dep. Renewable, Fossil & Energy Services
Siemens AS, Norway

Stein Bergsmark
Dep. Engineering and Science
University of Agder, Norway

Summary

The Norwegian oil and energy department instructs operators to look at the possibility for electrification of future offshore installations with power from shore. The offshore installations at the Utsira formation may be suitable for this due to a high power demand and the distance from shore.

The objective of this thesis has been to investigate requirements for an electrical power distribution system for these installations. A power distribution platform recieves power from the onshore grid through a HVDC link and distributes it through high-voltage AC cables to the offshore installations. The focus has been on the high-voltage AC part of the distribution system. Requirements and capacities for the following components have been investigated:

- Voltage source converter
- Transformers
- Circuit breakers
- HVAC Transmission cables

In addition the option of integrating an offshore wind power plant in the high-voltage AC distribution system has been evaluated, as well as the modifications required for the mentioned components and the topology of the distribution system.

A Simulink model of the distribution system was developed to test the solution for different load conditions. The offshore installations were modelled as a number of 28 MW induction motors with a power factor of 0.9. The voltage source converter was simplified to a constant power source and modelled as two PI controllers for power and voltage.

The system currents and voltage levels from the steady state analysis are regarded as good estimates for the future realization of the distribution system with only power from shore. Future steady state analysis of the distribution system should look to the values presented in this thesis in order to verify if their results are within reasonable range.

With a wind power plant (WPP) the system components must be able to withstand a higher short circuit current and the circuit breaker ratings must be modified. To avoid this, a current

limiter (Is-limiter) could be introduced, which will prohibit the short circuit current contribution from the wind power plant. A new transformer will be required within the distribution system, and the capacity must be equal to the maximum capacity of the wind power plant.

If the floating wind turbine technology evolves, a WPP together with power from shore should be capable of supplying offshore installations with power. The fast response and versatile control of the voltage source converter makes it well suitable for balancing the power of the WPP. The balancing would also require a maximum power reserve equal to the WPP capacity in the onshore grid.

The offshore installations at Utsira formation is planned to start production in 2016 and will be operational to 2060. These installation could either be run with gas driven turbines located on the platforms or be supplied with power from onshore. Global warming and the world's demand for gas may call for measures to supply future offshore installations with power from shore. This thesis has shown that there are few technological restraints for the electrification of the Utsira formation with power from shore.

Acknowledgements

Work on the thesis have been carried out in cooperation with Siemens AS and the University of Agder. It have been performed at the University of Agder and with telephone meetings with our supervisor in Siemens. The work have been done as a final assignment for our master degrees in renewable energy engineering.

We would like to express our gratitude to our supervisors Ben Bjørke, Siemens AS Norway and Stein Bergsmark, University of Agder for the useful comments, remarks and engagement through the learning process of this master thesis. Furthermore we would like to thank professor Hans-Georg Beyer, University of Agder for his help and comments on the wind power part of the thesis and Sverre Gilje, BP Norge AS for contributing with useful information regarding offshore electrification and allowing us to use previous work.

I, Anders Ballari want to thank my girlfriend Hanna for being in my life the last 3 years. Her contribution have been valuable to me. I want to thank my parents for the support since I became a student in 2006. My brother, Mats, also deserves a thanks for always giving me a good laugh, it has been important.

I, Jan Sola Østensen want to thank all my friends and familiy. I want to especially thank my girlfriend Janne for supporting me through the master thesis and my father Jens Inge for all his help and support through my whole education.

Contents

Abstract i

Acknowledgement iii

Contents iv

List of Figures viii

List of Tables xi

Abbrevations xii

1 Introduction 1

1.1 Motivation . . . 1
1.2 Field of Research . . . 2
1.3 Problem Definition . . . 2
1.4 Research Questions . . . 2
1.5 Report Outline . . . 3

2 Electrification of Offshore Installations at the Utsira Formation 5

2.1 Electrification of Offshore Installations . . . 5
2.1.1 Johan Sverderup . . . 7
2.1.2 Dagny . . . 7
2.1.3 Edvard Grieg . . . 8
2.1.4 Ivar Aasen . . . 9
2.1.5 New discovery . . . 9
2.1.6 Distribution Platform . . . 9
2.1.7 Norwegian Law . . . 10
2.2 Electric Power Distribution . . . 11
2.2.1 Voltage Source Converter . . . 11
2.2.2 Transformer . . . 12

2.2.3 Circuit breaker . . . 13
2.2.4 Current Limiter . . . 13
2.3 Utility System . . . 13
2.4 Electric Power Transmission . . . 14
2.5 Wind Power Plant . . . 15
2.5.1 Wind Turbine Power Production . . . 16
2.5.2 Power Production Variations . . . 17
2.5.3 Fault Current . . . 17
2.6 Induction Machine . . . 17
2.6.1 Squirrel Cage Rotor . . . 18
2.6.2 Moment of Inertia . . . 19
2.6.3 Consumption/Production . . . 19
2.7 Power Management . . . 20

3 Electrical Systems on the Distribution Platform 21
3.1 Offshore Installations Load Cases . . . 21
3.2 Distribution System . . . 22
3.2.1 Voltage Source Converters, Capacity and Requirements . . . 23
3.2.2 DST1 and DST2, Rating and Requirements . . . 23
3.2.3 Circuit Breakers, Capacity . . . 24
3.3 Utility System . . . 24
3.3.1 US, Consumption of Power . . . 25
3.3.2 UST1-6, Capacity and Requirements . . . 25
3.3.3 UPS, Capacity and Requirements . . . 26
3.3.4 Emergency Generators, Capacity and Requirements . . . 26
3.4 Power Management System . . . 26
3.5 Simulink Model Distribution System . . . 27
3.5.1 Voltage Source Converter . . . 27
3.5.2 Transformers . . . 28
3.5.3 Busbar . . . 29
3.5.4 HVAC Transmission Losses . . . 29
3.5.5 Asynchronous Motors, Loads . . . 29
3.5.6 Short Circuit Contribution . . . 31
3.5.7 System Frequency . . . 31
3.5.8 Utility System . . . 32

4 Integration of Offshore Wind Power 33
4.1 Wind Data Utsira Formation . . . 33

4.2 Wind Turbine . . . 34
4.3 Wind Power Plant Capacity . . . 35
4.4 Modifications to Distribution System . . . 36
4.4.1 DST3, Capacity and Requirements . . . 37
4.4.2 Circuit Breakers . . . 37
4.4.3 Power Management System . . . 37
4.5 Modifications Simulink Model . . . 38
4.5.1 Wind Power Plant . . . 38
4.5.2 Wind Turbine Asynchronous Generator . . . 39
4.5.3 Rotational Speed of Wind Turbine Rotor . . . 39
4.5.4 Rotational Speed of Wind Turbine Generator . . . 40

5 Simulations with Power from Shore **41**
5.1 Case 1 - Steady State with Peak Load . . . 41
5.2 Case 2 - Steady State Medium Load . . . 44
5.3 Case 3 - Steady State with New Discovery and Peak Load . . . 46
5.4 Short Circuit Current Contribution VSC . . . 49
5.4.1 Dagny after Transmission . . . 49
5.4.2 Edvard Grieg after Transmission . . . 51
5.4.3 Johan Sverdrup . . . 52
5.4.4 New Discovery . . . 53
5.5 Short Circuit Current Contribution Offshore Installations . . . 53

6 Simulations with Power from Shore and Wind Power Plant **57**
6.1 Steady State with Wind Power Plant and Peak Load . . . 57
6.2 Increasing Mean Wind Speed with Peak Load . . . 61
6.3 Wind Speed Reaching Critical High Point / WPP Stop in Production with Peak Load 63

7 System Units Requirements **66**
7.1 Transformers . . . 66
7.1.1 VSC Transformers, DST1 and DST2 . . . 66
7.1.2 WPP Transformer, DST3 . . . 67
7.2 HVAC Transmission Cables . . . 67
7.2.1 Short Circuit Current . . . 68
7.3 Circuit Breakers . . . 70
7.3.1 Power from Shore . . . 70
7.3.2 Power from Shore and Wind Power Plant . . . 70
7.4 Wind Power Plant . . . 71

8 Discussion **72**
8.1 Simulink Model . . . 72
8.1.1 Steady State Analysis . . . 72
8.1.2 Short Circuit Contribution VSC . . . 72
8.1.3 Wind Power Plant . . . 73
8.2 Offshore Installation Transformers . . . 73
8.3 Component Requirements . . . 73
8.4 Integration of a Wind Power Plant . . . 74
8.4.1 Power Reserve . . . 74
8.4.2 Wind Power Plant Capacity . . . 74
8.4.3 Voltage and Frequency Fluctuations . . . 74
8.4.4 Short Circuit Current . . . 74

9 Conclusion **76**
9.1 Conclusion . . . 76
9.2 Recommendations . . . 78
9.3 Further Work . . . 78

Bibliography **79**

Appendix A - Simulink Model **81**

Appendix B - Datasheets **101**

Appendix C - Electrical Drawings **107**

Appendix D - Simulation Results **113**

Appendix E - Estimations: Excel Sheets **138**

List of Figures

2.1 Overview of proposed solution[25] 6
2.2 Estimated power consumption for planned offshore installations.[25] 7
2.3 Consumption of power for the offshore installations at Dagny. ”Fase 1” and ”Fase 2” is dependent on gas production[11] 8
2.4 Estimated power consumption for the Edvard Grieg offshore installations.[23] . . . 8
2.5 Estimated power consumption for the installations at Ivar Aasen[18] 9
2.6 Overview of the Utsira formation area, section from map over the north sea.[25] . . 10
2.7 Offshore distribution system proposed for nodes offshore[27] 11
2.8 Simulation of VSC response to AC fault on the inverter side. Rec is rectifier side, Inv is inverter side.[6] 12
2.9 Equivalent circuit of a transformer. 13
2.10 Illustration of connection between offshore installations and onshore grid[25] . . . 14
2.11 Schematic of the power module.[5] 18
2.12 Schematic of the power module.[5] 19
2.13 Schematic of the power module.[5] 20

3.1 Single line diagram of distribution system 23
3.2 Single line diagram of utility system 25
3.3 The VSC block in the Simulink model 28
3.4 Transformer block in the Simulink model. This is the VSC transformer. 28
3.5 Overview of loads in the Simulink Model 30
3.6 Simulink block of the Asynchronous Motor. 30
3.7 Simulink block of the Asynchronous Motor. 31
3.8 Simulink block to calculate rotational speed. 32

4.1 Map of annual mean wind speed for Norway. The estimated location of Utsira formation is marked with blue.[4] 33
4.2 Estimated daily production for a wind turbine installed at the Ekofisk field and Frigg field.[15] 34
4.3 Overview of proposed solution with WPP.[25] 35

4.4 Total power balance in Norway during a very cold winter day.[29] 36
4.5 Single line diagram of modified distribution system 36
4.6 The Simulink block of the Wind Power Plant 38
4.7 Rotational speed of WT rotor and stator magnetic field. 39

5.1 System RMS voltages during steady state with peak loads. 42
5.2 Platform RMS voltages during steady state with peak loads. 42
5.3 Current in DS and load currents during steady state with peak loads. 43
5.4 Power produced and consumed during steady state with peak loads. 43
5.5 Frequency during steady state with peak loads. 44
5.6 Total active power consumption of the offshore installations. 44
5.7 Total apperant power consumption of the offshore installations. 45
5.8 RMS currents at the 110 kV level. 45
5.9 Platform voltages phase to ground at the 11 kV level. 46
5.10 System RMS voltage during steady state with peak loads. 47
5.11 Platform RMS voltages during steady state with peak loads. 47
5.12 Current in DS and ND load current during steady state with peak loads. 48
5.13 Power produced and consumed during steady state with ND and peak loads. 48
5.14 The impedance of Dagny with motor and transformer after short circuit. 49
5.15 The reactance the 28 MW motors for the whole simulation period. 50
5.16 System RMS currents 1 second after the short circuit. 50
5.17 Currents in the system straight after the short circuit. 51
5.18 System RMS currents 1 second after the short circuit. 52
5.19 System RMS currents 1 second after the short circuit. 52
5.20 System RMS currents 1 second after the short circuit. 53
5.21 Generated current by Johan Sverdrup inductive motors during short circuit. 54
5.22 Generated RMS current by Johan Sverdrup inductive motors during short circuit. . 54
5.23 Generated current by Edvard Grieg inductive motors during short circuit. 55
5.24 Generated RMS current by Edvard Grieg inductive motors during short circuit. . . 55
5.25 Generated current by Dagny inductive motors during short circuit. 56
5.26 Generated RMS current by Dagny inductive motors during short circuit. 56

6.1 Frequency during steady state with 13 wind turbines and peak load. 58
6.2 Frequency during steady state with 52 wind turbines and peak load. 58
6.3 Power produced and consumed during steady state with 13 wind turbines and peak load. 59
6.4 Power produced and consumed during steady state with 52 wind turbines and peak load. 59

6.5 DS active power and active power delivered by WPP and VSC during steady state with 13 wind turbines and peak load. 60
6.6 DS active power and active power delivered by WPP and VSC during steady state with 52 wind turbines and peak load. 60
6.7 DS active power and active power delivered by WPP and VSC during increasing mean wind speed with 13 wind turbines and peak load. 61
6.8 DS active power and active power delivered by WPP and VSC during increasing mean wind speed with 26 wind turbines and peak load. 62
6.9 DS active power and active power delivered by WPP and VSC during increasing mean wind speed with 52 wind turbines and peak load. 62
6.10 Frequency during WPP production stop with 13 wind turbines and peak loads. . . . 63
6.11 Frequency during WPP production stop with 52 wind turbines and peak loads. . . . 64
6.12 DS active power and active power delivered by WPP and VSC during WPP production stop with 52 wind turbines and peak loads. 64
6.13 DS active power and active power delivered by WPP and VSC during WPP production stop with 52 wind turbines and peak loads. 65

List of Tables

2.1 Per unit estimates for the transformers in the simulation model [14]. 13
2.2 A comparison between a offshore wind farm commissioned in 2009 and one to be commissioned in 2014.[2] 15
2.3 Coefficients used to calculate the power coefficient. 16

3.1 Cases with different load conditions. 22
3.2 Load currents for the different cases at 110 kV. 22
3.3 Transformers in the Simulink model. 29
3.4 Total impedances for the transmission cables. 29
3.5 Asynchronous machines in the Simulink model. 31
3.6 Overview of Motor Inertia. 32

4.1 Data for the Hywind turbine and the estimated HywindX turbine.[8] 34
4.2 Estimated short circuit current contributions from WPP in the case of a three phase balanced short circuit. 37
4.3 Parameters for the WT generator. 39

7.1 DS transformers capacity requirements for only VSC cases. 67
7.2 DS transformers capacity requirements for WPP cases. 67
7.3 Transmission cable capacity requirements with peak load. 68
7.4 Offshore installations contribution short circuit current. 68
7.5 Transmission cable minimum short circuit current requirements with only PFS. . . 69
7.6 Transmission cable minimum short circuit current requirements with WPP and without new discovery. 69
7.7 Minimum circuit breaker capacity with only VSC as power source 70
7.8 Estimated circuit breaker interruption currents with VSC and WPP as power sources 71

Abbrevations

AC	Alternating current
DC	Direct current
DP	Distribution platform
DS	Distribution system
DST	Distribution system transformer
EG	Edvard Grieg
HV	High-voltage
HVAC	High-voltage alternating current
HVDC	High-voltage direct current
IA	Ivar Aasen
IEC	International Electrotechnical Commission
JS	Johan Sverdrup
ND	New discovery
P	Active/Real power
PFS	Power from shore
PMS	Power management system
PSA	Petroleum Safety Authority
Q	Reactive power
rms	Root mean square
RQ	Research question
S	Complex power, apparent power
UPS	Uninterruptible power supply
US	Utility system
UST	Utility system transformer
VSC	Voltage source converter
WP	Wind power
WPP	Wind power plant
XLPE	Extruded layer of insulating crosslinked polyethylene

Chapter 1

Introduction

The Norwegian oil and energy department instructs operators to look at the possibility for electrification of future offshore installations with power from shore. The offshore installations at the Utsira formation may be suitable for this due to a high power demand and the distance from shore. There are several offshore installations planned at the Utsira Formation and the electrification would require an electrical distribution system offshore. This thesis investigates a possible solution of the electrical distribution system from a report on behalf of the Norwegian Petroleum Depertament. It will also determine requirements for the components within the electrical distribution system.

In addition, development in offshore wind power technology could make it possible to supply power to offshore installations with floating wind turbines. The thesis will investigate how integration of an offshore wind power plant will affect the distribution system. This include modifications of the distribution system topology and new requirements for the components.

1.1 Motivation

Electrification of offshore installation by using power from shore are considered to reduce the greenhouse gas emissions. Reduction of greenhouse gas emissions has high focus worldwide. In Norway there is already some offshore installations on the Norwegian continental shelf which are supplied with power from shore. These projects has shown a good result with regard to system performance and in reduction of the total emissions. Further investigation of electrification based on power from shore can ideally electrify all the offshore installations on the Norwegian continental shelf by use of distribution platforms similar to the platform which has been investigate in this thesis.

There is high focus both politically and within the energy industry to look at sustainable solutions. It is therefor an interesting case to see if the combination of an offshore wind power plant and the onshore grid could supply the Utsira Formation installations. Wind power could in the future be used instead some of the worlds coal and gas power plants.

1.2 Field of Research

Reports on the electrification of the offshore installations and impact studies of the planned installations at the Utsira Formation have been the base for the development of this thesis.

Theory on electrical power engineering has been used to develop a model to test a solution for the distribution system based on the reports, and to determine capacity requirements of the components within this solution. Laws and regulations from Statnett and Norwegian Oil Industry Association (IEC) has been used to find general requirements.

The course content of *ENE405-G Wind Power* has been used as a base for the solution to integrate offshore wind power. Some of the subjects in the course were development of power coefficent eqution for wind turbines, estimation of power production and wind speed distribution (Weibull).

1.3 Problem Definition

To supply the offshore installations with power from the onshore grid, both HVDC and HVAC technology will be used. There will be a link between the onshore grid and the distribution platform which is high voltage direct current (HVDC). At the largest offshore installation, Johan Sverdrup, a distribution platform (DP) will be built. Here the HVDC is converted to high voltage alternating current (HVAC) through a voltage source converter. The offshore installations at the Utsira Formation are connected to the distribution platform through HVAC transmission cables.

The thesis will focus on finding requirements for the voltage source converter at the distribution platform, and the transformers, transmission cables, and circuit breakers within the HVAC distribution system. The requirements will be found by modelling and simulation of the distribution system with estimated load conditions, and by looking at laws and regulations.

This thesis will also study modifications necessary for the distribution system to integrate offshore wind power. In this case the power output from wind turbines will be estimated from available wind turbine data and rough wind data.

1.4 Research Questions

In order to clarify the intentions for this thesis four research questions were defined at the start of the project.

The distribution platform serves as a distribution hub for the area. The distribution system components should be designed to handle the load conditions of the offshore installations.

RQ1 Components: What component types are needed for the distribution system?

RQ2 Requirements: What are the requirements for the components in the distribution system with regard to various load conditions?

RQ3 System: How can a distribution system be realized based on RQ1 and RQ2?

There is a lot of research on offshore wind power and in the future it might be a part of the electrification

of offshore installations. It may be beneficial to look at what modifications on the distribution platform would be needed to integrate offshore wind power. This would enable the distribution platform to distribute power both from the onshore grid, and offshore wind turbines when it is available.

RQ4 Offshore Wind Power: What adaptions to the distribution platform are needed to integrate offshore wind power?

Limitations

The thesis work has been carried out with the following limitations. This is done to limit the scope of the thesis.

- Onshore facilities and converter station are required, but will not be further investigated.
- HVDC transmission is suggest from shore to the distribution platform, but will not be investigated.
- Offshore converter station will be simplified since much of the technology is classified as confidential and it is also a complex part of the solution. The converter stations are considered ideal and without losses.
- Power from shore is regarded as a constant power source at the offshore distribution platform.
- Occuring harmonics within the system will not be investigated.
- Switchgear is simplified to only cover investigations of current ratings for circuit breakers.
- HVAC transmission is simplified to impedances.
- The HVAC transmission cable planned for Ivar Aasen is suggested to be laid via Edvard Grieg. These installations are simplified and simulated together as one platform.
- The loads at the offshore installations are simplified to be inductive motors.
- The wind power plant and wind turbines are simplified since the main focus of this addition are to look at modifications required by the electrical system and how it will affect the system.
- The thesis will not include a design for the PMS, only suggest PMS functionalities.

1.5 Report Outline

Chapter 2 contains background information and litterature considered relevant for this master thesis. It includes a description of the situation at Utsira formation and relevant plans for electrification. Relevant theory for the system components and functionality are also included in this chapter.

Chapter 3 presents proposed solutions for the electrical system on the distribution platform with power from shore. It includes load cases, components, system topologies, functionality and introduces a Simulink model developed for simulations of the system. Chapter 4 presents proposed modifications for the distribution system to be operational with a wind power plant connected. It includes wind power plant cases,

relevant information for the wind power plant, modifications required for the distribution system and introduces new blocks to the Simulink model.

Chapter 5 presents Simulink model simulation results with only power from shore. It includes graphs and observations relevant for the cases presented in Chapter 3. Chapter 6 presents Simulink model simulation results with power from both shore and a wind power plant. It includes graphs and observations relevant for the cases presented in Chapter 4.

Chapter 7 determines the system components requirements based on findings in the previous chapters. Chapter 8 covers a discussion of findigs and results presented in the previous chapters. Chapter 9 gives a conclusion of the topics investigated, recommendations and proposes future work.

Chapter 2

Electrification of Offshore Installations at the Utsira Formation

At the Utsira formation there have been two major discoveries of oil and gas, which today are known as the Johan Sverdrup field. Three other nearby discoveries Edvard Grieg (Luno), Ivar Aasen (Draupne) and Dagny (Gina Krog) are all planned to be developed for oil/gas production in the coming years. The operators of the four fields at the Utsira formation, Statoil, Lundin and Det Norske have agreed to investigate the option of supplying their offshore installations with power from shore. They are considering the option of using a high-voltage direct current (HVDC) transmission link from shore to the Johan Sverdrup field. Where the power will be distributed via HVAC transmission to the other fields.

2.1 Electrification of Offshore Installations

The main reason for electrifying offshore installations are to replace the gas turbines which are typically used for generating electric power offshore. Gas turbines use a process which releases large amounts of polluting gases and can also be highly inefficient. This depends on whether the waste heat is used or not. Operators owning and running gas turbines in Norway have to pay taxes per ton of polluting gas released. An important factor to look into before deciding on electrification of offshore installations with powerfrom shore is to investigate if the onshore grid has the spare capacity required and acceptable availability.[25]

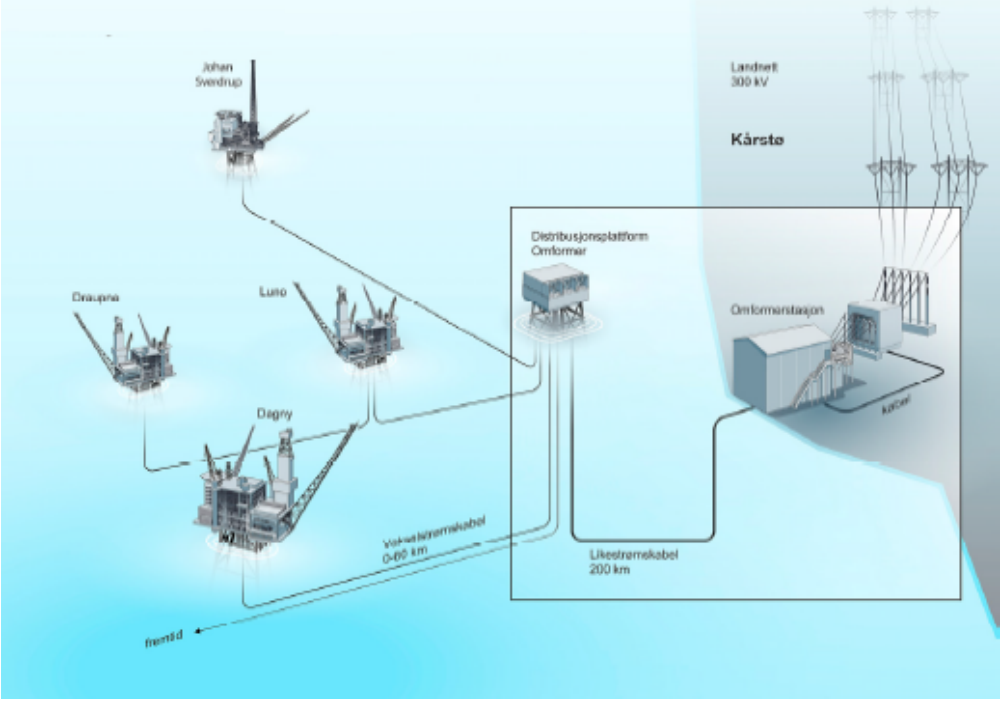

Figure 2.1: Overview of proposed solution[25]

The system required for electrifying offshore installations will mainly consist of a transmission system and a receiver station offshore. The distance between onshore point and offshore installations will in some cases require the use of HVDC technology. When HVDC technology is used it will require the voltage to be converted both onshore and offshore. If several offshore installations are to receive electric power from the same onshore point there will be a need for a distribution system offshore. If the power is sent from shore with HVDC technology it is usually converted to HVAC before it is distributed. The distribution system can be placed on either one of the offshore installations involved in the network or have an own platform dedicated for this system. This should be decided based on the power requirements and distances between oil platforms and onshore point.[27]

A similar oil field to the ones at the Utsira formation is Valhall operated by BP. Valhall have been connected to the onshore grid via Lista in Norway since 2010. The transmission cable length is 292 km and uses HVDC light (VSC) technology developed by ABB. The connection between Valhall and the onshore grid is a direct current (DC) link between the oil platform and a converter station onshore. Transmission capacity is 78 MW and the transmission system operates at + 0 / -150 kV asymmetrical DC voltage.[27]

Prior to the planning phase for delivery of power from shore to Valhall, solutions for distributing this to Ula, Gyda, Ekofisk 2/4J and Valhall through a distribution platform (DP) at Ekofisk 2/4G was discussed. This case is very similar to the case at the Utsira formation and solutions discussed may also apply for the offshore installations planned at the Utsira formation.[26]

Also Gjøa, an oil field operated by GDF SUEZ is connected to the onshore grid. Gjøa have been connected to the onshore grid via Mongstad in Norway since 2010. The transmission cable length is 100 km and uses HVAC technology. The transmission is lisenced to operate at 40 MW and the transmission system operates at 90 kV alternating current (AC) voltage. Troll A is also connected to the onshore grid and have a similar connection between the offshore installations and the onshore grid as Gjøa.[27]

The proposed gas turbine type for powering the offshore installations at the Utsira formation is GE LM2500+ delivered by General Electric. It is designed to produce a power output of 29 MW with a thermal efficiency of 38 %, see appendix B for datasheet of the model.

2.1.1 Johan Sverderup

The Johan Sverdrup (JS) field will have Statoil as licensed operator. Three offshore production platforms are planned at the Johan Sverdrup field. This will also be a main hub for processing and transport of oil and gas. The cluster of installations will be comparable with other large offshore installations in the North Sea. The production is estimated to be ongoing until 2060 and the first production installation is estimated to start-up in 2018. The other production installations will start-up every second year after 2018.

The installations at the Johan Sverdrup field are proposed to be powered by 6 GE LM2500+ gas-turbine driven generators. These could deliver around 170-180 MW of electric power. Figure 2.2 show the estimated power consumption for Johan Sverdrup, Dagny, Edvard Grieg and Ivar Aasen until 2059.[25]

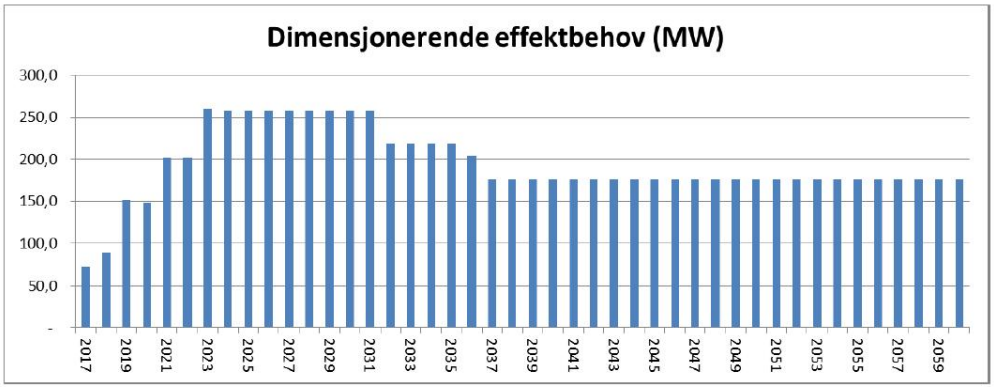

Figure 2.2: Estimated power consumption for planned offshore installations.[25]

2.1.2 Dagny

The Dagny field will have Statoil as licensed operator. This is a smaller field which initially was assumed to only contain gas, however in 2008 oil was discovered as well. One production platform is planned to be built together with a subsea unit for gas at a nearby field called Eirin. Startup of production will be around 2016/2017. A total of 300 million oil equivalents are estimated to be contained in the Dagny and Eirin field.

The installations is proposed to be powered by one GE LM2500+ gas turbine driven generator. The power consumption is estimated to be between 6 to 25 MW, depending on whether a compressor for gas injection is operational. The power consumption for injection of gas is estimated to be between 13-16 MW. Figure 2.3 shows the power consumption for the installations at Dagny until 2035.[11]

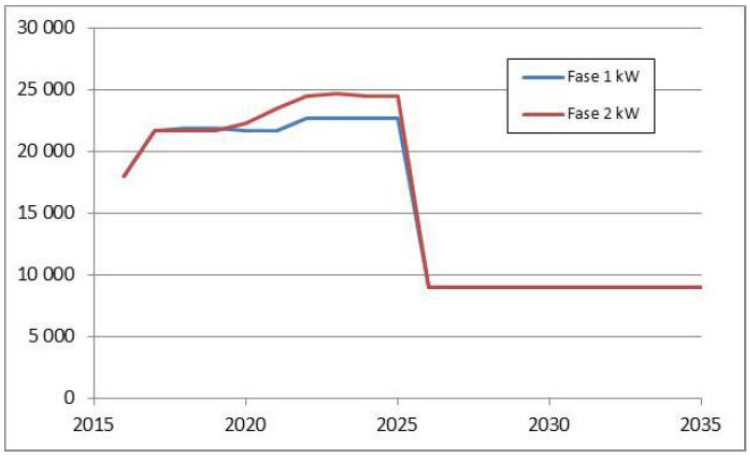

Figure 2.3: Consumption of power for the offshore installations at Dagny. ”Fase 1” and ”Fase 2” is dependent on gas production[11]

2.1.3 Edvard Grieg

The Edvard Grieg (EG) will have Lundin as licensed operator. One larger production platform is planned to be built with both oil and gas production. The peak production is estimated to be around 100 000 oil equivalents each day. The startup for production will be late in 2015.

The platform at Edvard Grieg is assumed to power the offshore installations at Ivar Aasen as well. It is proposed to use two GE LM2500+ gas-turbine driven generators to power the production platforms. The estimated electric power consumption for the Edvard Grieg platform will be 23 MW at normal load, and 13 MW for heating at normal load. Figure 2.4 show the estimated power consumption for the Edvard Grieg offshore installations until 2030.[23]

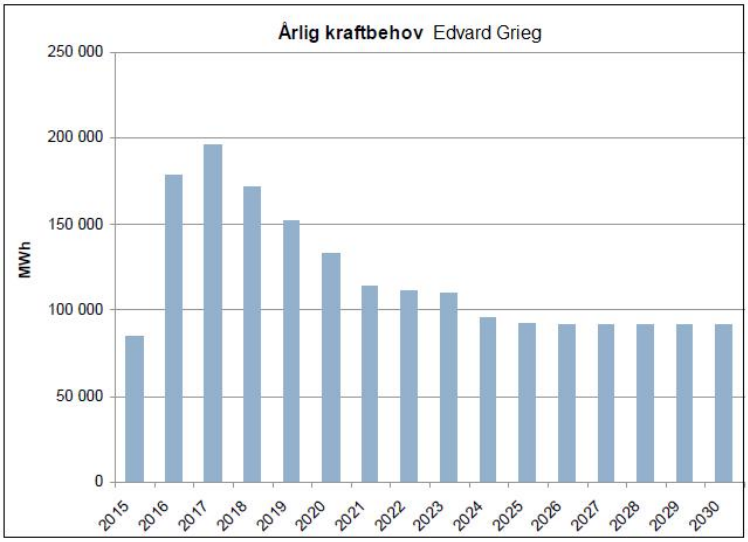

Figure 2.4: Estimated power consumption for the Edvard Grieg offshore installations.[23]

2.1.4 Ivar Aasen

The Ivar Aasen (IA) field will have Det Norske as licensed operator. This is a smaller field where one production platform and one subsea-unit are planned. These will be supplied with electric power from Edvard Grieg. The field is estimated to contain 150 million oil equivalents and production startup is estimated to be late in 2016.[24]

The electric power consumption for the Ivar Aasen field is estimated to be 22-25 MW. Figure 2.5 shows the power consumption for the installations until 2028.[18]

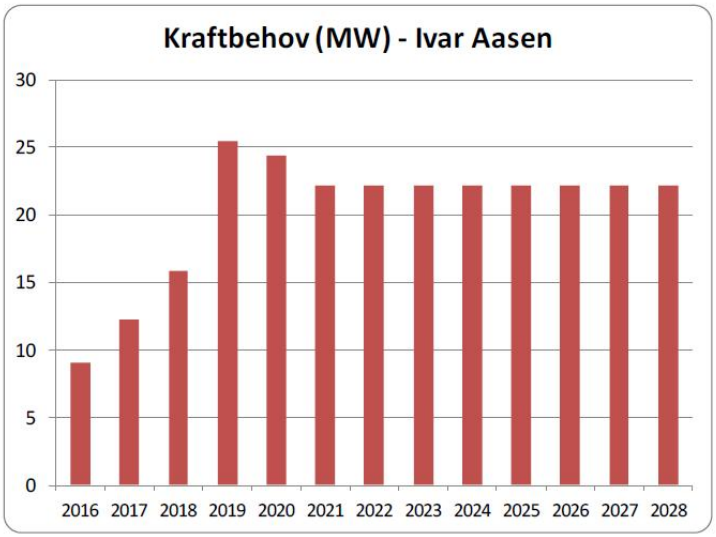

Figure 2.5: Estimated power consumption for the installations at Ivar Aasen[18]

2.1.5 New discovery

There could be new discovery (ND) of fields which contain oil and gas. The Norwegian oil and energy department assumed in a report that it could be similar to Dagny, and with start-up in 2032.[25]

2.1.6 Distribution Platform

The distribution platform is suggested to be placed at the Johan Sverdrup field, since it is expected to produce the longest and have the largest power demand. The distribution platform should be located nearby the first installation planned at the Johan Sverdrup field. The distance should be far enough to allow operation in the case of a gas leakage from the processing facility at this installation.[25]

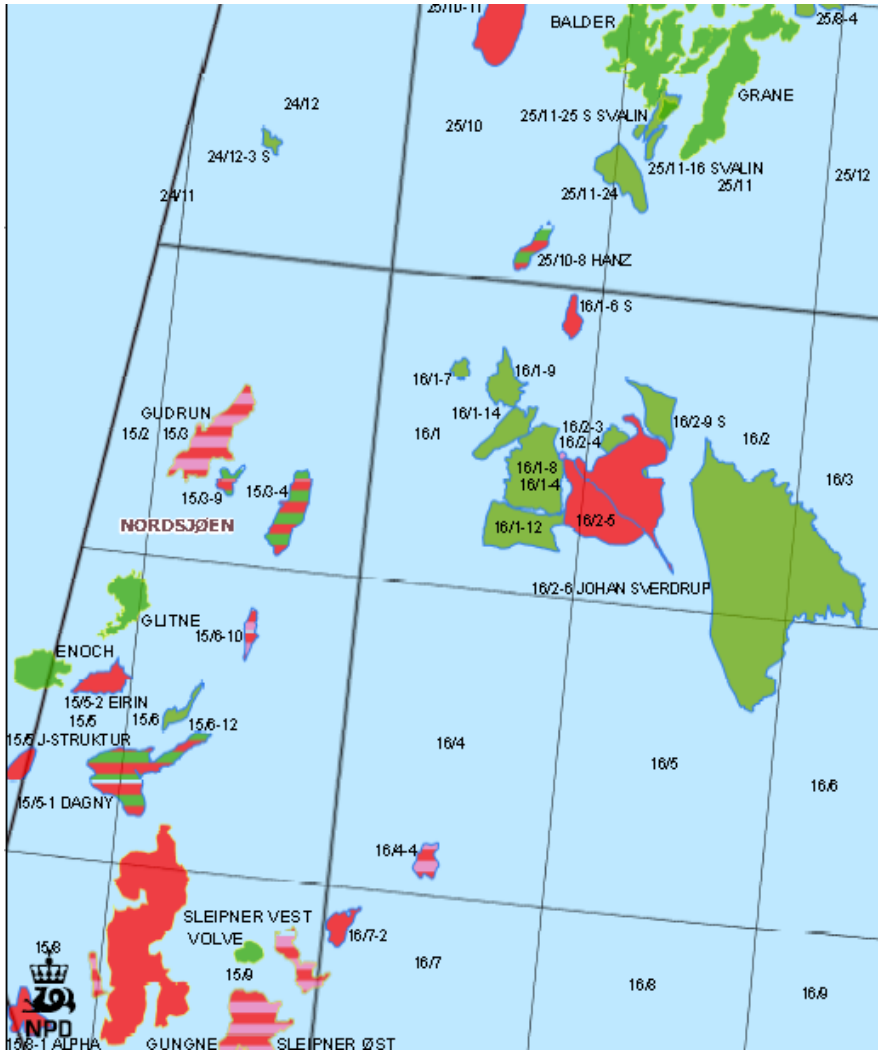

Figure 2.6: Overview of the Utsira formation area, section from map over the north sea.[25]

2.1.7 Norwegian Law

Norwegian law states that offshore electrical systems within Norway shall follow regulations from the Petroleum Safety Authority (PSA). PSA refers to and uses IEC standards. In addition to the IEC standards there are other recognized standards which are stricter and thereby also applicable. One of these are the NORSOK standard developed by Norwegian Oil Industry Association (OLF).[7]

Norwegian law also states that any electrical system connected to the Norwegian national grid shall follow regulations from Statnett. Statnett refers to the standard Funksjonskrav i kraftsystemet (FIKS) developed by themselves.[16]

2.2 Electric Power Distribution

An example of an offshore electrical power distribution system can be seen in Figure 2.7. This is similar to the distribution system which could be used at the Utsira Formation. The distribution system will consist of voltage source converters (VSC), transformers and switchgear.

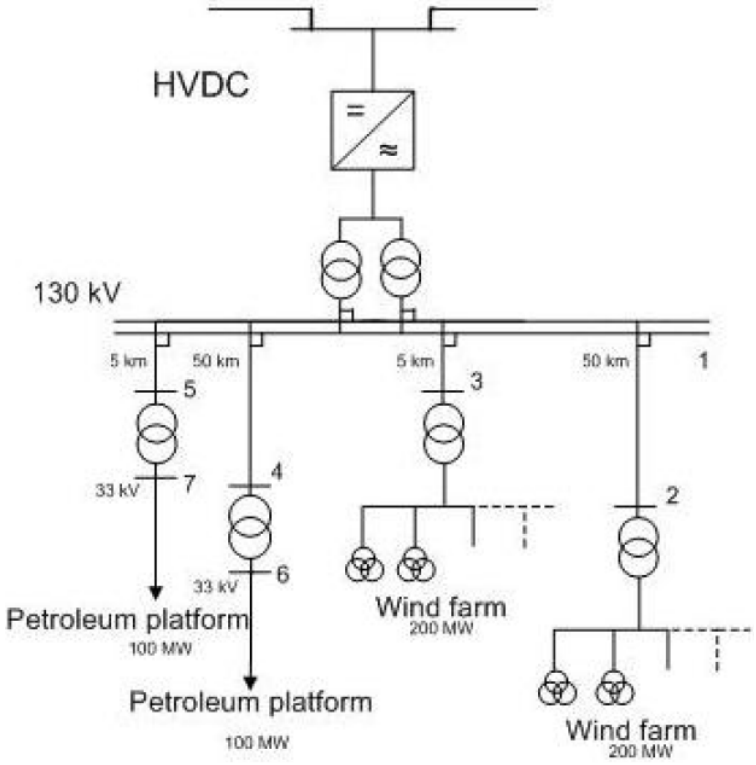

Figure 2.7: Offshore distribution system proposed for nodes offshore[27]

2.2.1 Voltage Source Converter

The voltage source converter is used to both rectify and invert the voltage. It is a self-commutated converter and can be black started. Four VSCs are proposed to be used for the HVDC link between shore and the distribution platform. A VSC use power transistors (IGBT) which can handle all power ranges. The VSC can be controlled with respect to amplitude and phase, and hence both the active (P) and reactive (Q) power can be controlled. This means that by proper control of the VSC there is no need for external devices to balance the reactive power. It can also supply reactive power without any supply of active power.[5]

The modern Voltage Source Converter from Siemens AG is based on HVDC plus technology. The HVDC plus technology uses the modular multilevel converter (MMC) approach, which are several power modules in series for each phase.

Fault Current

A fault current on the DC or AC side is experienced by the modules as a rapid rise in current. Since there are several modules for each phase, each of them only experiences a rise in current with a rate of a few tens of amperes each microsecond. The fault will be quickly detected by the controller and the IGBTs can be switched off before the current reach any critical value. This is an effective and reliable protection of the system. Circuit breakers must still be installed on the AC side, since the fault current can still flow through freewheeling diodes.[5]

During a short circuit on the AC side of the voltage source converter, it can be regarded as a current source. This is due to the fact that voltage and power output can be controlled. The fault current is limited by the thermal capacity of the power transistors. Figure 2.8 show a simulation of a VSC which experience an AC fault on the inverter side. It is important that the VSC have a large enough capacity to deliver the fault current on the AC side. This ensures that the fault is detected by the protection system.[1][6]

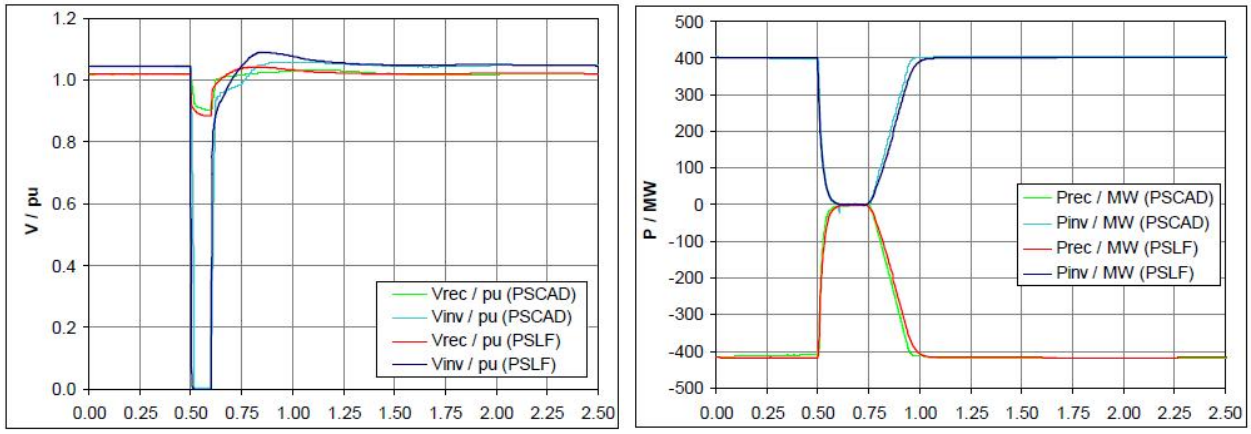

Figure 2.8: Simulation of VSC response to AC fault on the inverter side. Rec is rectifier side, Inv is inverter side.[6]

2.2.2 Transformer

The equivalent circuit of a transformer which represents one phase is shown in Figure 2.9. There is a voltage drop over every transformer in an electrical system, and a small active power loss which is converted to heat in the transformer. The transformer will also consume some reactive power. To represent these losses the equivalent circuit contains a magnetizing reactance and a resistance representing iron losses. For the primary and secondary side there is also a winding resistance and leakage reactance. These values are usually given in per unit by the transformer manufacturer, and a base for estimating per unit values are shown in Table 2.1.[13]

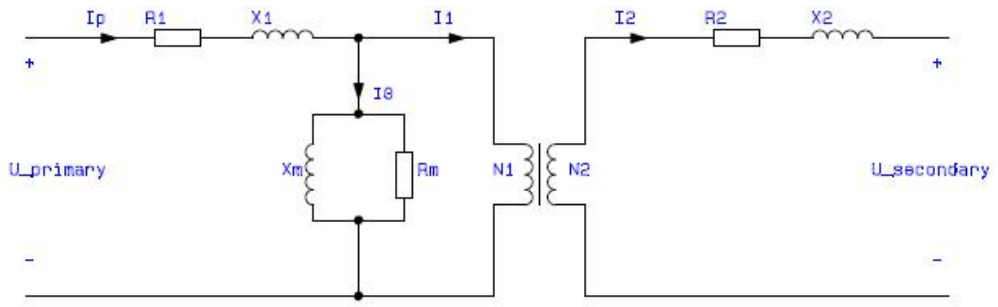

Figure 2.9: Equivalent circuit of a transformer.

Table 2.1: Per unit estimates for the transformers in the simulation model [14].

	1 MVA to 100 MVA
Primary winding resistance, R_1 [pu]	0.005 – 0.002
Secondary winding resistance, R_2 [pu]	0.005 - 0 .002
Primary leakage reactance, X_1 [pu]	0.03 – 0.06
Secondary leakage reactance, X_2 [pu]	0.03 – 0.06
Iron Core losses, R_c [pu]	50 - 200
Magnetizing reactance, X_m [pu]	100 - 500

2.2.3 Circuit breaker

The circuit breaker interrupt fault currents which can occur in power systems. When the current is interrupted the voltage across the inductance in series with the circuit breaker will work against a change in the current. An electric arc will occur in the breaking point until the air gap is sufficiently large making the arc die out. There will be a lot of energy which is converted to heat. This means the circuit breaker material must be able to withstand temperatures of several thousand degrees. The AC current is a sine wave which will become zero twice during a period which puts out the arc. Still the circuit breakers for AC current are designed to put out the arc with gas, vacuum or air pressure to break the current as fast as possible.[13]

2.2.4 Current Limiter

A current limiter (Is-limiter) is designed to reduce occuring short circuit currents. If there is a fault in the system it will be capable of detecting and limiting the occuring short circuit current during the first current rise. It does this by opening the circuit.[21]

2.3 Utility System

A utility system (US), normal power and emergency power, will be required on the distribution platform to supply power to different utilities needed on the distribution platform for operation and safety. Supply of power to these applications is essential in order for the distribution platform to operate correctly, it is also

required to ensure power to safety systems in the case of emergencies. The utility system will function as a distribution system for the mentioned applications.

There are several system utilities which should be included and need power on the distribution platform. These are control, safety, lighting, ventilation and telecom systems. The main power consumers within the utility system is however different types of pumps and high-voltage motors.[27]

The utility system should get its main supply of power from the distribution system. This should be done by connecting the utility system to the distribution system through a transformer.. The transformer will then supply the required power with desired voltage level.[27]

The utility system will need to include an emergency power system based on diesel generators. This system will be required to power the utility system during start-up and shut down periods, but also if the supply of power from shore fails or there is a fault in the connection between the utility system and distribution system transformers.[27]

2.4 Electric Power Transmission

The transmission between the onshore grid and the distribution platform is proposed to be HVDC. The transmission between the distribution platform and offshore installations is proposed to be HVAC. The suggested operating voltage of these transmission cables are 110 kV. Figure 2.10 shows an illustration of the transmission of power between the onshore grid and the offshore installations.[25]

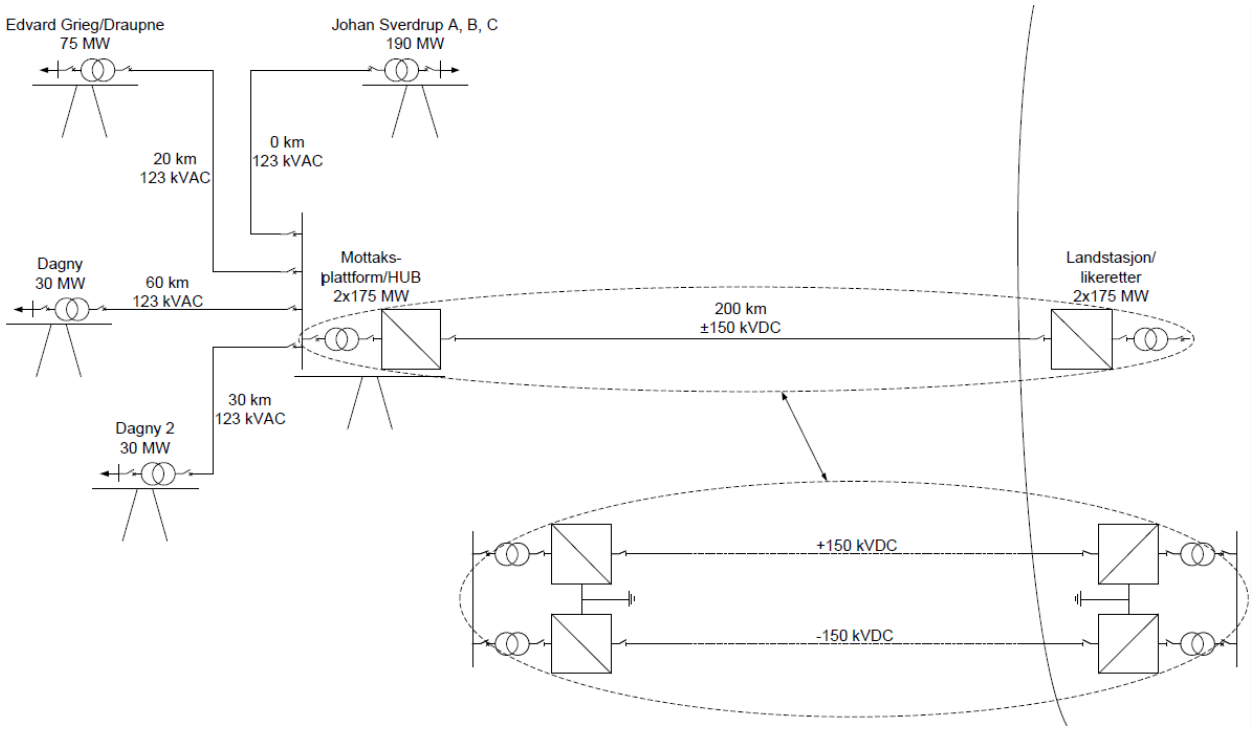

Figure 2.10: Illustration of connection between offshore installations and onshore grid[25]

The HVAC transmission cables require special design depending on length and capacity of maximum transferable power required. This report will base the HVAC transmission on a cable delivered by Nexans.

The cable is designed to handle the same voltage level which is suggested for the transmission cables at the Utsira formation. Also other characteristics of significance for the transmission lines are considered similar and hence it should be considered sufficient for use as an example in this report.

The cable considered is designed with a highest voltage level rating of 123 kV, this is sufficient due to the suggested operating voltage of 110 kV. The cable have a cross section of 3·1·500 mm^2. It uses XLPE as insulation which is common for sub-sea transmission. Due to the fact that the cable is not specifically designed for each transmission cable the specific ratings used for losses and impedance will not be 100 % accurate. The cable data is used to determine the expected electric power loss for each transmission cable. The active power loss for the cable are given as 79.9 W/m, see datasheet in appendix B.

The power losses due to transmission can be calculated with equation 2.1. The active power loss (W) is given by only applying the ohmic resistance of the impedance to the equation, while the reactive power loss (VAR) is given by only applying the reactance.

$$S_{losses} = I^2 \cdot Z \rightarrow Z = R + jX \tag{2.1}$$

S$_{losses}$ = Apparent power losses [VA].

I = Current [A].

Z = Conductor impedance [Ω].

R = Conductor ohmic resistance [Ω].

X = Conductor reactance [Ω].

2.5 Wind Power Plant

The water depth for today's offshore wind power plants (WPP) ranges approximately between 10-20 meters and they are found 5-25 km from shore. The installed capacity is between 90 - 200 MW, however larger offshore WPPs are on the horizon like *Gwynt y Môr* outside North Wales which will have an installed capacity of 576 MW in 2014. The increasing output is made possible by increasing the size of rotor blades. Table 2.2 shows a comparison of the once record breaking offshore WPP *Horns Rev II* and the mentioned *Gwynt y Môr*.[2]

Table 2.2: A comparison between a offshore wind farm commissioned in 2009 and one to be commissioned in 2014.[2]

	Gwynt y Môr, 2014	*Horns Rev II, 2009*
Installed capacity (MW)	576	209.3
Number of turbines	160	91
Diameter (m)	107	93
Generator capacity (MW)	3.6	2.3
Distance to shore (km)	13	27–35
Water depth (m)	12-33	9–17

All of todays offshore wind turbines are mounted to the seabed. This limits the depth of the water where

the wind turbines operate when considering the costs. However there is research looking into floating wind turbines which could be used to deliver electric power to many of the world's offshore installations.[3]

2.5.1 Wind Turbine Power Production

The power of the wind through circle with a given radius is shown in equation 2.2. A wind turbine can not extract all this power, and the amount of power extracted by it is limited by the power coefficient. The upper theoretical limit is around 59 % stated by Betz' Law. The equation for the power coefficient is individual for each wind turbine, but modern wind turbines can extract around 40-45 % of the wind power during optimal production. The maximum power output from a wind turbine is usually met at wind speeds around 12-13 m/s.[3]

$$P_{wind} = 0.5 \cdot p \cdot \pi \cdot R^2 \cdot u^3 \tag{2.2}$$

P$_{wind}$ = Power of wind through the area of the rotor blades [W].

R = Length of wind turbine blade [m].

u = Wind speed [m/s].

p = Air density [kg/m^3].

An example of a power coefficient equation for a wind turbine is shown in equation 2.3. The origin of the coefficients for the equation is a semester project in the course *ENE405-G Wind Power* at the University of Agder. The equation itself is from a book called *Windkraftanlagen im Netzbetrieb*.[28]

$$PowerCoefficient = C1 \cdot (C2–C3–C4) \cdot e^{C5} \tag{2.3}$$

Table 2.3: Coefficients used to calculate the power coefficient.

C1	0.5
C2	$\frac{R}{\lambda}$
C3	0.022
C4	5.6
C5	-0.17·$\frac{R}{\lambda}$

Table 2.3 shows the coefficents used to calculate the total power coefficient. Two of these are calculated by using the length of the wind turbine blade (R) and the tip speed radio (λ). The tip speed ratio is the ratio between the speed of the wind and the speed of the tip of the wind turbine blade. Equation 2.4 is used to calculate the ratio and it is determined by the rotational speed of the wind turbine rotor and the wind speed.[3]

$$\lambda = \frac{\omega_{rotor} \cdot R}{u} \tag{2.4}$$

$\boldsymbol{\lambda}$ = The tip speed ratio.

ω_{rotor} = Rotating speed of rotor shaft for wind turbine [m/s].

R = Length of wind turbine blade [m].

u = Wind speed [m/s].

2.5.2 Power Production Variations

When a wind turbine produces electric power during a period where the wind speed is not high enough to allow rated power production the power produced by the wind turbines will fluctuate. By increasing the number of wind turbines attached to the system the fluctuations will decrease. The fluctuations in each wind turbines power output will stay the same, but when the wind turbines power outputs are summarized they will overlap and decrease total power fluctuations. An increasing number of wind turbines will also make predictions of the total electric power output using national meteorological information more accurate.[3]

2.5.3 Fault Current

The most common type of generator in offshore wind turbines are induction generators. Immediately after a symmetrical short circuit the asynchronous generator can be regarded as a voltage source in series with a sub-transient reactance. This is the same case as for a synchronous generator. After around four cycles the flux will drop to zero which will also force the short-circuit current to zero. When looking at the contribution from a wind power plant, it can be regarded as one large generator with a capacity equal to the sum of all the wind turbine generators.[17]

The sub-transient reactance is usually around only 15-25 % of the nominal reactance. Hence the contribution to the short-circuit current can be 5-6 times larger than the root mean square (RMS) value of the load current immediately after the fault. The transient reactance is usually around 20-30 % of nominal reactance.[13]

Normally the wind turbine generators are either doubly fed induction generators or full conversion generators. These types of generators would have a smaller short circuit contribution compared to induction generators connected directly to the grid.[17]

2.6 Induction Machine

The generators installed in the wind turbines and the electric motors on the offshore installations are all assumed to be induction machines. These are also known as asynchronous machines. A voltage source connected to the asynchronous machine creates a revolving magnetic field in the stator. Conductors in the rotor cut the flux of this magnetic field. The result is a force pushing the rotor towards the rotational speed of the stators magnetic field. The speed of the rotating rotor determines the power output of the machine, and whether it runs as a generator or motor.[14]

2.6.1 Squirrel Cage Rotor

The induction machines of the offshore installations and the WPP are assumed to be squirrel cage rotor machines. The conductors in a squirrel cage rotor are solid copper or aluminum bars formed as a cylindrical cage. The equivalent circuit of a squirrel cage machine is shown in Figure 2.11. This circuit represent one phase of the machine.

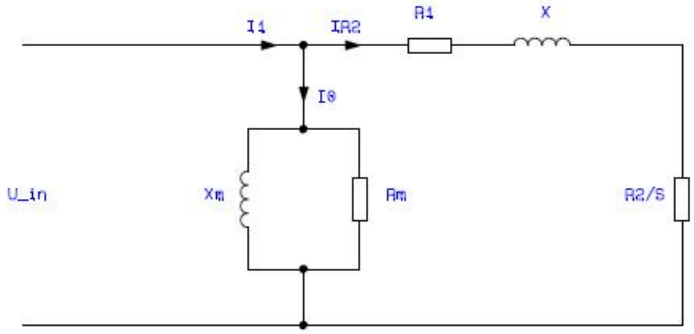

Figure 2.11: Schematic of the power module.[5]

The active power losses in the machine is represented by R_m and R_1 which is the magnetizing resistance and the resistance in the stator windings. The reactive power absorbed by the machine is represented by X which is the magnetizing reactance and the total leakage reactance. The rotor is represented by R_2/ s, where R_2 is the rotor resistance and s is the slip of the machine. The slip is calculated by equation 2.5. When the rotor is rotating faster than the magnetic field rotating in the stator, the slip become negative. In this case the the machine is in generator mode. When the rotor is rotating slower in the same direction, the machine is in motor mode absorbing active power. The short circuit contribution in motor mode will be the same as for generator mode, see Chapter 2.5.3.[14]

$$s = \frac{\omega_{sync} - \omega}{\omega_{sync}} \tag{2.5}$$

s = Slip.

ω_{sync} = Synchronous speed, rotating speed of magnetic field in stator [rad/s].

ω = Rotating speed of rotor [rad/s].

$$\omega_{sync} = \frac{4 \cdot \pi \cdot freq}{poles} \tag{2.6}$$

freq = Frequency of stator voltage [Hz].

poles = Number of poles in the induction machine.

2.6.2 Moment of Inertia

The inertia for the motors has been estimated with equation 2.7. The equation was derived using motors from a Siemens induction motor catalog which had the following parameters: 6 pole, 6,6 kV and 60 Hz motors, water cooled and for line connection [10]

$$J_{motor} = 0.00658 \cdot P_{motor}^{1.23} \tag{2.7}$$

J_{motor} = Moment of inertia in rotating mass of motor [$kg \cdot m^2$].

P_{motor} = Active power of motor [kW].

2.6.3 Consumption/Production

The power of a 28 MW asynchronous machine is shown in Figure 2.12. The synchronous rotational speed for the stator magnetic field of this machine is 125.66 rad/s. When the rotor speed is above this value, the negative power indicates the machine produce active power.

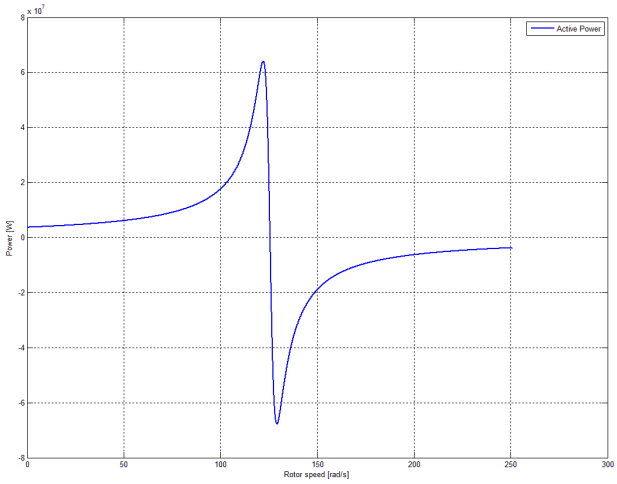

Figure 2.12: Schematic of the power module.[5]

The machine has potential for a higher power output than 28 MW, but it should operate around nominal speed to prohibit overheating. When the slip increase the value of R_2 / s fall. Since the voltage over the stator stay constant, the current in the machine increase. A high value of the slip can quickly make the machine overheat. Figure 2.13 show the reactive power and apparent power (S) of the machine, and illustrate how the current increase when the slip increase. Thyristor soft starters are often used to limit the starting current.[14]

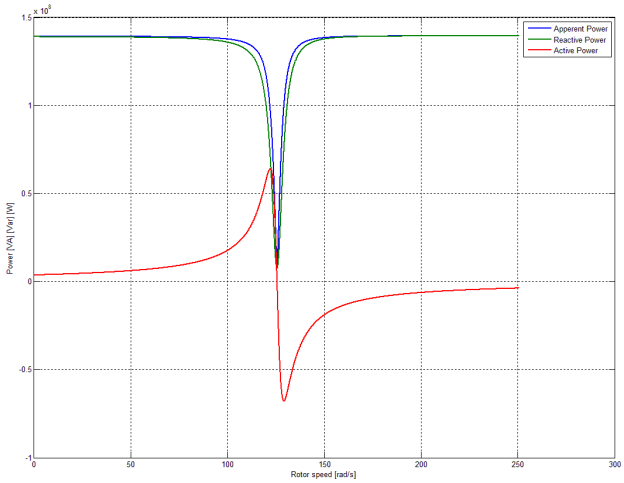

Figure 2.13: Schematic of the power module.[5]

2.7 Power Management

The power management of a power system ensures that there is always a balance between production and load by measuring the frequency. For the distribution system of the Utsira formation the converter station supplying power from shore will be the producing unit and must deliver power equal to the load of the offshore installations.

Even if the electric power system is monitored, the power management is made easier by estimating future changes for load and production. Large HV electrical motors should have planned start-up and shut down. This will ensure the power quality is not affected by problems such as starting large HV electrical motors. The estimation of power produced by offshore wind is complex, and power from this source can degrade power quality and even distort the frequency. The power management system relies on measurements of frequency and voltage from the electrical system, planned load changes and estimation of future production and load. The goal is to have constant frequency and power quality according to the consumers' needs.

Chapter 3

Electrical Systems on the Distribution Platform

There are two electrical systems on the distribution platfrom, a distribution system and a utility system. The distribution system, which is considered to be the main system, distributes the PFS between the offshore installations. The utility system system recieves power from the distribution system and distributes this to utilities on the platform.

3.1 Offshore Installations Load Cases

Three load cases have been investigated.

- Case 1 - Peak load is assumed when all the transformers on the offshore installations operate at full capacity. See Figure 2.10.
- Case 2 - Medium load consumption is assumed from 2037. See Figure 2.10.
- Case 3 - Peak load with a new discovery with a power demand equal to Dagny.

Table 3.1: Cases with different load conditions.

	Total	Losses HVAC Transmission	Johan Sverdrup	Dagny	Edvard Grieg and Ivar Aasen	New Discovery
Case 1, peak [MVA]	306	10.5	186.67	31.0	77.78	0
Case 2, medium [MVA]	181.5	10.5	93.33	31.0	46.67	0
Case 3, peak ND [MVA]	342.5	16	186.67	31.0	77.78	31.0

The estimated load currents in the transmssion cables and on the secondary side of the VSC transformers is shown in Table 3.2

Table 3.2: Load currents for the different cases at 110 kV.

	DST1 / DST2	Johan Sverdrup	Dagny	Edvard Grieg and Ivar Aasen	New Discovery
Case 1 [A]	775	980	163	408	-
Case 2 [A]	449	490	163	245	-
Case 3 [A]	857	980	163	408	163

3.2 Distribution System

Power from shore is recieved by two VSCs which inverts the HVDC to HVAC. These VSCs will be connected to distribution system transformers (DST) which will step down the voltage level. The two transformers will deliver the power through switchgear to the busbar. All the offshore installations are connected with HVAC transmission cables to the distribution platform.

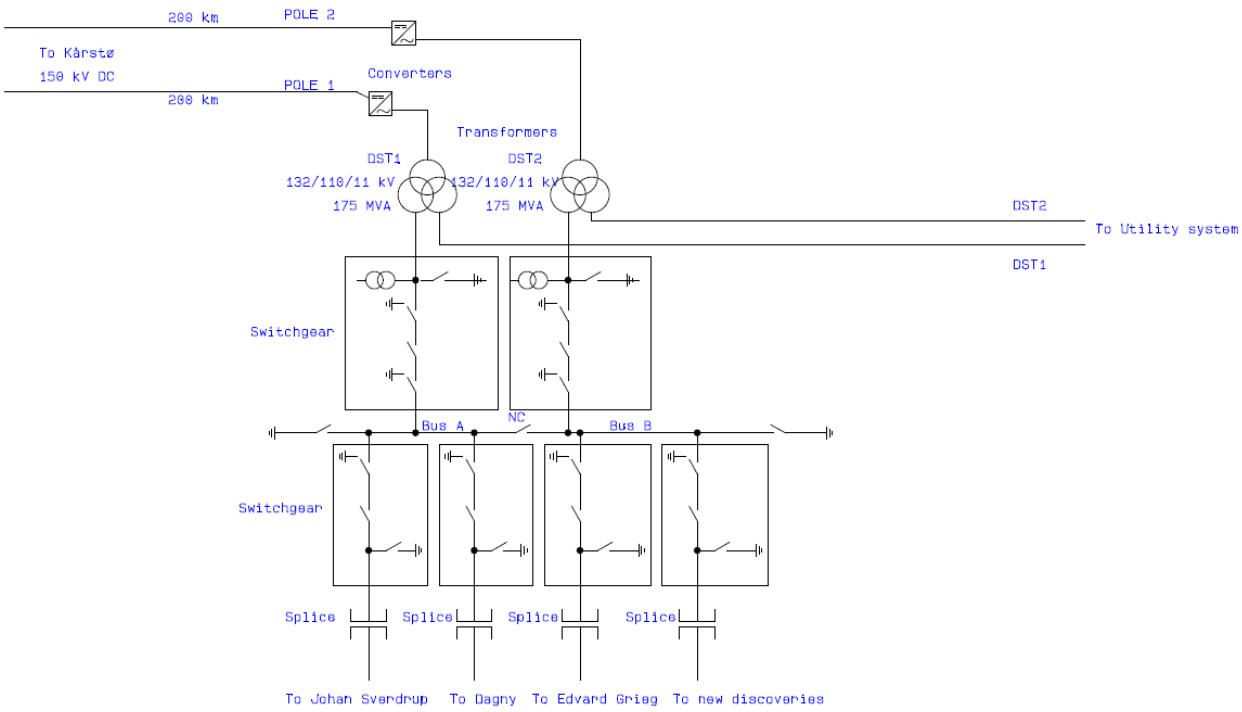

Figure 3.1: Single line diagram of distribution system

Two VSCs are used to ensure that the supply of power is not interrupted if there is a fault within one of the VSCs or transformers. This is according to the requirement for redundancy. If the connection between the distribution platform and offshore installations fails, local power plants at the offshore installations should work as a essential power supply.[19]

3.2.1 Voltage Source Converters, Capacity and Requirements

The capacity of the two VSCs at the DP must be around 175 MVA. The reactive power capacity seen from the converter transformer must be equal to a power factor less than 0.95 both for inductive and capacitive operation. A step of 5 % for the voltage should be handled within less than 0.5 seconds by the regulator of the VSC. This is valid until the voltage have reach 90 % of the steady state value. The voltage static must be possible to adjust from 0 – 10 %. The VSC is capable of going from delivering power equal to 100 % of its capacity to zero instantaneously. On the inverter side, the VSC should be able to deliver the reactive power demand of the system for realistic load conditions.[16][5]

3.2.2 DST1 and DST2, Rating and Requirements

The rating of the two three-winding transformers DST1 and DST2 must be around 175 MVA. The third winding is used to supply power for the utility of the distribution platform. The rating of the tertiary winding for the transformer will be equal to the power consumption at nominal load for the utility system for both DST1 and DST2.[25]

The NORSOK standard states that all parts of IEC 60076 shall comply with the transformers of the

system. Hence it will be important that the transformer could be loaded according to the IEC loading guide (IEC 60076-6) without overheating.[19]

The primary winding shall be isolated from earth. The secondary winding shall be directly earthed. The primary winding is a delta connection since it is isolated from earth. With a delta connection the current in each winding is dampened compared to the phase current by the square root of 3. The secondary and third windings are both wye connections.[16]

3.2.3 Circuit Breakers, Capacity

Six circuit breakers will be needed for the distribution system on the platform. They must be able to interrupt the total short circuit current with contribution from the VSCs and offshore installations. Due to limited space the circuit breakers would have to be compact and gas insulated. They should also be able to interrupt the capacitive charging currents of the HVAC transmission cables.[20]

3.3 Utility System

In order to integrate an efficient utility system on the distribution platform it will be required to split up the system to different voltage levels. The system will also need to include various switchgear between the branches. It is suggested that the voltage levels should be 11 kV, 690 V 400 V, 230 V and 48 V as it have been proposed for nodes offshore and in the NORSOK standard. The NORSOK standard states that the system will need both a normal operation power supply and emergency power supply which should be seperated. The proposed system in Figure 3.2 will include a normal operation power supply, an essenstial power supply and an emergency power supply[27].

- The highest voltage level in the US, 11 kV, shall be connected directly to the three-winding transformers of the main distribution system. The branch will contain the electrical equipment that requires above 400 kW power, such as pumps for cooling/fire etc. At this system voltage level one shall be able to feed the power directly to the applications attached.
- A system voltage of 690 V is used to supply small electrical motors/pumps and other electrical equipment requiring below 400 kW power. The branch shall be attached the 11 kV branch through transformers.
- The system voltage level on 400/230 V TN-S will be supplied through three transformers attached to the 690 V level branch. It will supply electrical equipment that requires below 3 kW power, such as single phase heaters. The NORSOK standard states that the system shall be symmetrically loaded.
- A voltage level of 230 V is used for such systems as switchboard control voltage and escape lightning. Both the control system and lighting system will be supplied through each their uninterruptible power supply (UPS) connected to both normal operation power supply and emergency power supply.
- There is also required a voltage level of 48 V DC, which shall provide power to the telecommunication system. It should be fed from both normal operation power supply and emergency power supply through an UPS.

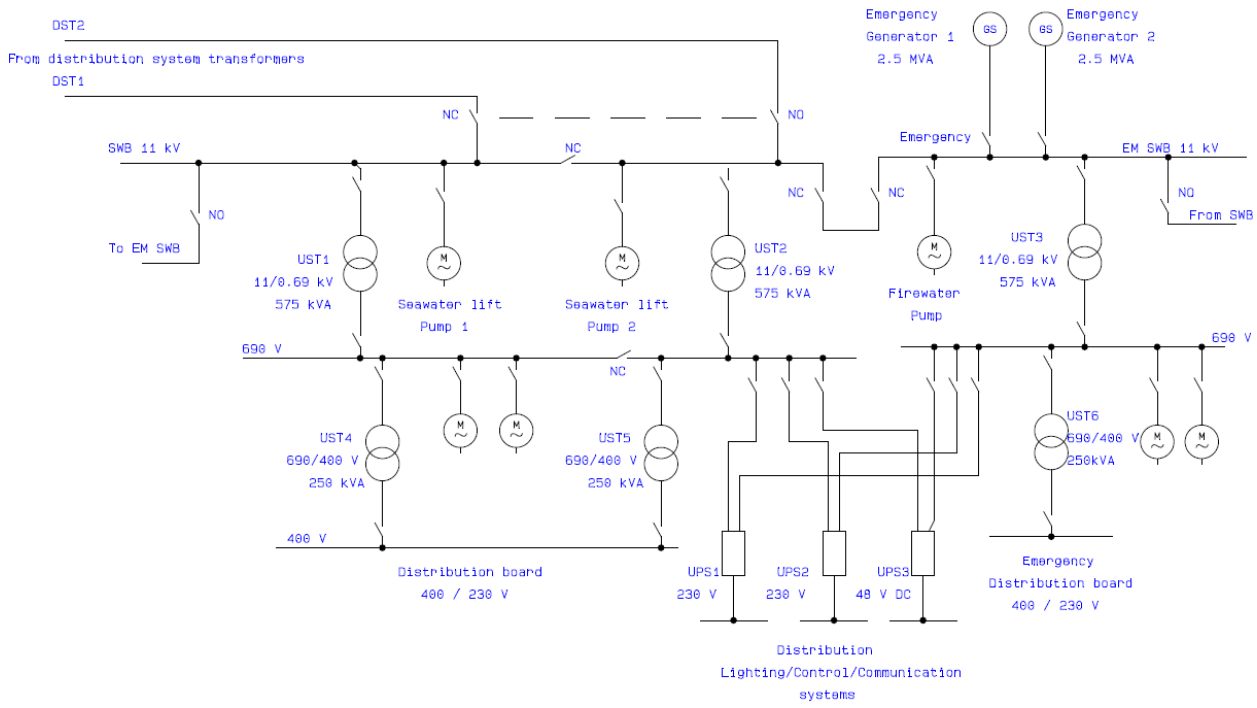

Figure 3.2: Single line diagram of utility system

3.3.1 US, Consumption of Power

The main consumer of the US will as previously stated be the seawater lift and firewater pumps. Frank Mohn AS delivered 4 x 3700 m^3/h with differential heads on 165 mlc to cover firewater requirements on the Gjøa platform, see appendix B. It is estimated that one firewater pump of same type as delivered to Gjøa will be sufficient for the distribution platform. The power required by one pump is given as 2240 kW, by assuming a power factor of 0.9 the apparent power needed to operate one pump is calculated to approximately 2.5 MVA. It is suggested to use two seawater lift pumps for normal operation. It is assumed that these will require the same amount of apparent power as the firewater pump. Total required power for these pumps will therefore be 5 MVA.

It is estimated that the remaining loads will be approximately the same as suggested in the Norwegian power project report, ie 575 kVA. Hence will the total power consumption of the US be estimated to approximately 6 MVA for normal operation and 3 MVA for emergency operation.

3.3.2 UST1-6, Capacity and Requirements

The three transformers connected to the 11 kV branch on primary side, ie UST1, UST2 and UST3, shall both have an estimated capacity of 575 kVA. The maximum earth fault current for these transformers shall be limited to 20 A per transformer.[19]

The three transformers connected to the 690 V branch on primary side, ie UST4, UST5 and UST6, shall all have an estimated capacity around 250 kVA. The maximum earth fault current for these transformers shall be limited to 100 A per transformer.[19]

All six transformers shall due to the NORSOK standard be high resistance earthed.[19]

3.3.3 UPS, Capacity and Requirements

The NORSOK standard states that for the lighting, control and telecommunication systems there are required to have UPS systems in case of power interruptions or power failure. To ensure redundancy the UPS systems should be connected to both normal operation power supply and emergency power supply. It is specified that the UPS systems shall have a capacity to supply emergency power for a minimum period of 30 minutes. It is suggested that it should be sized to accommodate power requirements for 120 minutes. The UPS should operate in on-line and thus continuously provide power to the attached system. All UPS systems in the utility system should be isolated and directly earthed. Each UPS should also have a by-pass breaker to be used for service/maintenance purposes and also be equipped with earth fault detection.[19]

3.3.4 Emergency Generators, Capacity and Requirements

The emergency generators should be diesel driven and is needed as redundancy in case of power failure in the main system. It is therefore required to be independent of the main supply system. Thus shall it be arranged in parallel with the main supply system and have capacity to power required emergency units. During black start, the PFS converter station will require cooling water, ventilation, control voltage etc. which will be supplied from the emergency system[19].

NORSOK standard states that it shall be capable of supplying emergency power for at least 18 hours. The generator shall start automatically and deliver power directly to the busbar in case of failure in the main system. The neutral conductor shall be high resistance earthed and maximum earth fault current shall be limited to 20 A.[19]

The generator should be attached to the 11 kV voltage branch and will operate at the same voltage level. The total generator capacity is required to be 1.5 - 2 times larger than estimated load and will also have to be customized to the amount of inductive load. Due to capacity requirements it is suggested to use use two generators with a capacity of 2.5 MVA, and in total 5 MVA.[19]

3.4 Power Management System

The active power consumption used on the various offshore installations will need to be measured and used to determine the power needed from the grid. A fiber cable is laid together with the HVDC and HVAC cables. This will enable communication between the DP, onshore converter station and the production platforms.

Identification of large consumers on each platform will be important in order to plan startups. Hence before starting large HV electrical motors the PMS shall check the active or reactive power reserve to determine if the system can handle the new load at once or wait until the power have been adjusted. Power availability restrictions for reasons such as single pole failure in the HVDC system must be automatically dealt with by adjusting the power of the other pole.

The PMS shall monitor voltage interruptions, system voltage, system frequency and active power. It is required by the IEC standard that the PMS shall be capable of delivering sufficient active and reactive power without varying the offshore system voltage outside limits. The system voltage steady state limits are + 6 % and - 10 %, while transient limits are +/- 20 %. Continous cyclic voltage variations shall be limited to 2% and the voltage transient recovery time is defined as maximum 1.5 seconds. The platform voltage should be kept stable by compensating for voltage drops in the distribution system. The PMS shall enable startup of large consumers or restart of platform after black out without bringing the frequency outside limits. The frequency steady state limits are +/- 5 % and transient limits are +/- 12.5 %. Continous cyclic frequency variations shall be limited to 0.5% and frequency transient recovery time is defined as maximum 5 seconds.[12]

The PMS shall include load shedding and fast load shedding functionalities. If the system detects any occuring faults with the power transmission/distribution leading to insufficient capacity, the system shall automatically start load shedding of motors and other electrical applications.

3.5 Simulink Model Distribution System

The equivalent circuits for a transformer and induction machine presented in Chapter 2, have been used to create a Simulink model of the distribution system. The model considers one phase of the system, and it is assumed that the load and production is balanced between all three phases. Also all the induction machines are assumed to be 6 pole machines and the system frequency is 60 Hz. The blocks in the simulink model is explained in details in this section. An overview of the Simulink model can be seen in appendix A.

3.5.1 Voltage Source Converter

It was stated in Chapter 2.2.1 that the VSC power output of the voltage source converter could change instantaneously. In addition the voltage output is controllable. Two PI controllers can simulate the voltage and power output of the VSC since the operation is very versatile. The job of the VSC is to maintain the system frequency by adjusting the electric power transmitted from the onshore grid. It must also maintain the correct voltage level across the loads, and compensate for voltage drops over the transmission cables and transformers. Figure 3.3 show the VSC modeled in Simulink. The rotational speed of the magnetic field in the system is compared to the synchronous rotational speed when the frequency is 60 Hz. One of the offshore installations is chosen for voltage control and the VSC maintains the nominal voltage level over this installation.

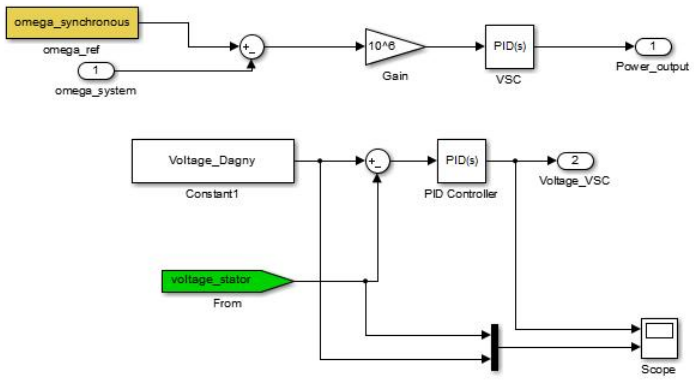

Figure 3.3: The VSC block in the Simulink model

3.5.2 Transformers

Figure 3.4 show the inputs and outputs of the transformer block. To calculate the currents and the losses inside the transformer, the block requires the voltage on primary side, and the total load on secondary side. The output of the transformer is the voltage on the secondary side, the current on the secondary side, the active power losses and reactive power consumed. The block also calculates the total load seen from the primary side, which includes the transformers internal losses and the load connected to the transformer on the secondary side. This load is required when calculating the total load seen by the VSC transformer in the Simulink model.

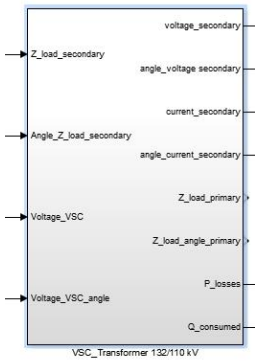

Figure 3.4: Transformer block in the Simulink model. This is the VSC transformer.

There are in all 5 transformers in the Simulink model of the system. The two 175 MVA three windings transformers for the VSC, seen in Figure 3.1, is replaced by one 350 MVA transformer assumed to be two windings. This is done to simplify the simulation model. Each of the offshore installations transformers have a rating based on the maximum power consumption in Figure 2.11. The wind power plant, which is introduced in Chapter 4, has an ideal transformer to simplify the calculating of the total load seen by the VSC. A list of the system transformers and their parameters are shown in Table 3.3

Table 3.3: Transformers in the Simulink model.

Name	VSC Transformer	JS Transformer	EG Transformer	Dagny Transformer	WPP Transformer
Capacity [MVA]	350	190	75	30	WPP Capacity
N1 / N2	132/110	110/11	110/11	110/11	110/6.9
R_1 and R_2 [pu]	0.006	0.006	0.002	0.002	ideal
X_1 and X_2 [pu]	0.04	0.07	0.06	0.06	ideal
R_x [pu]	500	500	150	150	ideal
X_m [pu]	200	200	70	70	ideal

3.5.3 Busbar

The busbar in the DS is implemented into the simulink model to simulate the total current at all time flowing through the busbar. The busbar block will calculate the current using the inflowing current from both the VSC and the WPP introduced in Chapter 4.

3.5.4 HVAC Transmission Losses

The transmission cables is implemented into the Simulink model to simulate the voltage drop, active power lost and reactive power consumed. In total there are 2 transmission cable blocks for case 1 and 2, and 3 blocks for case 3. Since Johan Sverdrup will be placed next to the distribution platform the voltage drop between the distribution platform and Johan Sverdrup is considered negligible. The transmission block will simply function as an impedance in series between the distribution platform and load. The total cable impedance will vary due to variations in distances, see Table 3.4. The impedance used is taken from the example cable introduced in Chapter 2.

Table 3.4: Total impedances for the transmission cables.

Platform	Base impedance [Ω/km]	Distance from DP [km]	Total transmission impedance [Ω]
Dagny	0.073 + j0.12	60	4.38 + j7.2
Edvard Grieg	0.073 + j0.12	20	1.46 + j2.4
New Discovery	0.073 + j0.12	30	2.19 + j3.6

3.5.5 Asynchronous Motors, Loads

The offshore installations are assumed to have large asynchronous motors to drive process/drilling equipment. Figure 3.5 show the number of asynchronous motors for each load and their capacity.

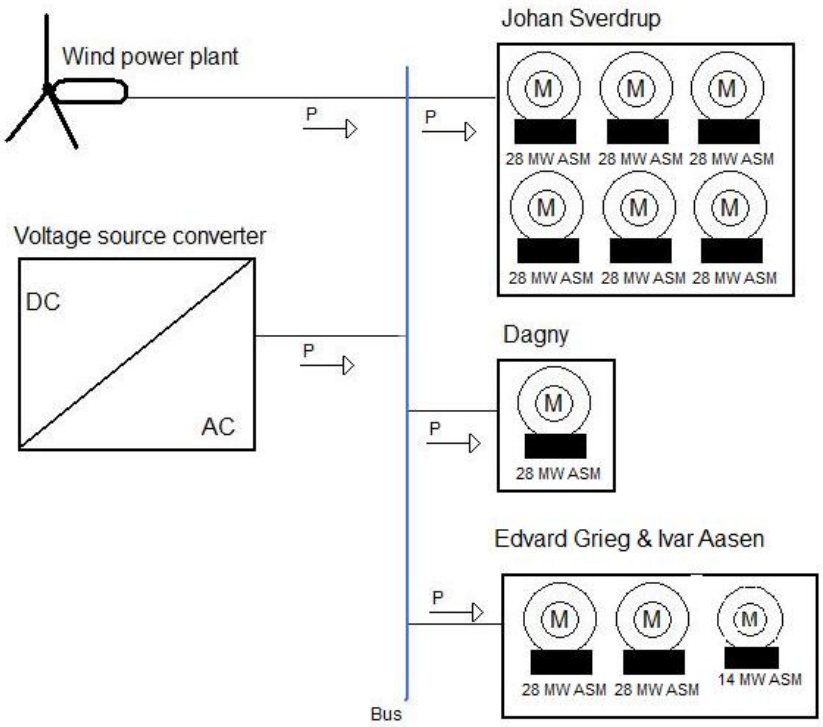

Figure 3.5: Overview of loads in the Simulink Model

The Simulink block of the asynchronous motor is shown in Figure 3.6. The input of the asynchronous motor is the stator voltage, the systems rotational speed and the rotational speed of the load. In Figure 3.6 the rotor speed is equal to the value which makes the asynchronous motor consume the nominal active power. The outputs are used to determine the performance of the motor and how much reactive power it consumes. In addition the total impedance of the motor is available for use if it is coupled with a transformer.

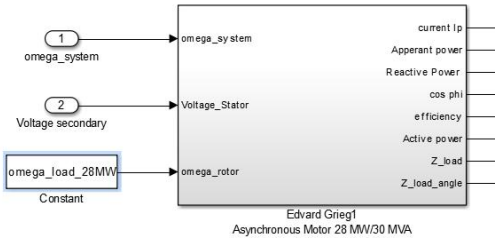

Figure 3.6: Simulink block of the Asynchronous Motor.

The parameters of the asynchronous motors in the system are shown in Table 3.5. The calculation of these parameters are based on an example 3800 kW squirrel cage motor in *Electric Machines, Drives and Power Systems* (chap 15.6) [14].

Table 3.5: Asynchronous machines in the Simulink model.

Capacity [MW]	28	14
Stator voltage line to line [kV]	11	11
Frequency [Hz]	60	60
Poles	6	6
Power factor nominal	0.9	0.9
Efficiency [%]	97.5	97.5
Stator and rotor resistance, R_1 and R_2 [pu]	0.014	0.0195
Total leakage reactance, X [pu]	0.216	0.229
Magnetizing resistance, R_m [pu]	88.89	64.21
Magnetizing reactance, X_m [pu]	3.82	3.66

3.5.6 Short Circuit Contribution

The asynchronous motor block in the previous section is not useable for simulation of the short circuit contribution of the asynchronous motor. To determine the contribution from the offshore installations a premade block from Simulink/SimPowerSystems was used in the Simulink model. Figure 3.7 shows the block and the parameter settings. These are the same as presented in Table 3.5.

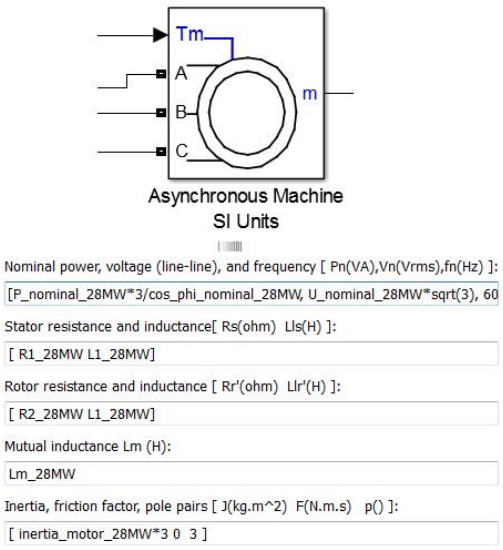

Figure 3.7: Simulink block of the Asynchronous Motor.

3.5.7 System Frequency

The acceleration of the rotational speed of magnetic fields in the motors are given by equation 3.1. The rate of acceleration depends on the total inertia of the system and power produced/consumed. When the

production and consumption is equal there is no acceleration. This rotational speed determines the system frequency.

$$J_{total} * \frac{d\omega}{dt} = \frac{P_{prod}}{\omega} - \frac{P_{load}}{\omega} \tag{3.1}$$

J_{total} = Total moment of inertia of the system[$kg \cdot m^2$].

P_{prod} = Total power produced [W].

P_{load} = Total load of system [W].

The total power is the power output of the voltage source converter. The total load is all the offshore installations, the utility system of the distribution platform and power losses in transformers and cables. The total moment of inertia is the total rotating mass in the system. Figure 3.8 shows the Simulink block which calculates the rotational speed of the system.

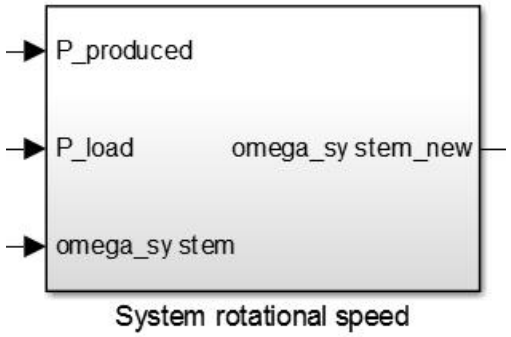

Figure 3.8: Simulink block to calculate rotational speed.

Total Inertia in System

The total inertia in the system is the sum of rotating mass in the asynchronous motors installed at the offshore installations which is 4742.2 $kg \cdot m^2$ and derived from Table 3.6.

Table 3.6: Overview of Motor Inertia.

Nominal Power [MW]	28	14
Inertia Motor [$kg \cdot m^2$]	503.1	214.5
Number of Motors	9	1

3.5.8 Utility System

The US is implemented into the simulink model to simulate the power demanded and delivered to the US. It will simply consume the needed apparent power (6 MVA) from the DST. The block calculates/measures the current required to supply this consumption.

Chapter 4

Integration of Offshore Wind Power

Future development in offshore wind power technology might open possibilities to supply offshore installations in water depths of 100 meters or more with power from wind turbines. There is often a high mean wind speed on the location of offshore installations, and focus towards sustainable technologies are increasing. Today Statoil has already made a prototype of a floating wind turbine which could be used at the water depths at the Utsira Formations called Hywind. In addition the capacity of the traditional offshore wind power plants in water depths around 20 m is increasing. It is therefor worthwhile to explore the possibilities of supplying the offshore installations at the Utisra formation with wind power.

4.1 Wind Data Utsira Formation

The mean annual mean wind speed around the Utsira Formation is estimated to be around 10 – 10.5 meters per second.[4]

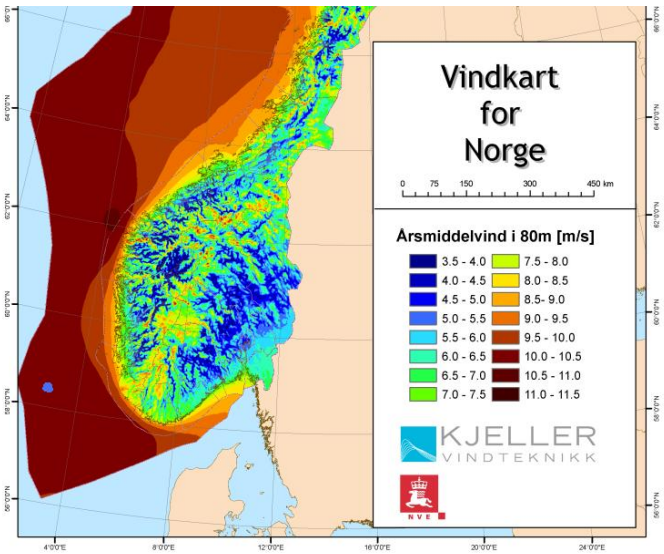

Figure 4.1: Map of annual mean wind speed for Norway. The estimated location of Utsira formation is marked with blue.[4]

The daily power production at the Frigg and Ekofisk field presented in Figure 4.2. Frigg is closest to the Utsira Formation field, and the power production at both fields could be assumed to be similar. The figure shows that a wind power plant in the North sea will have a higher production during the winter months than the summer months. It would produce around 35-45 % of its installed capacity daily during the winter months.[15]

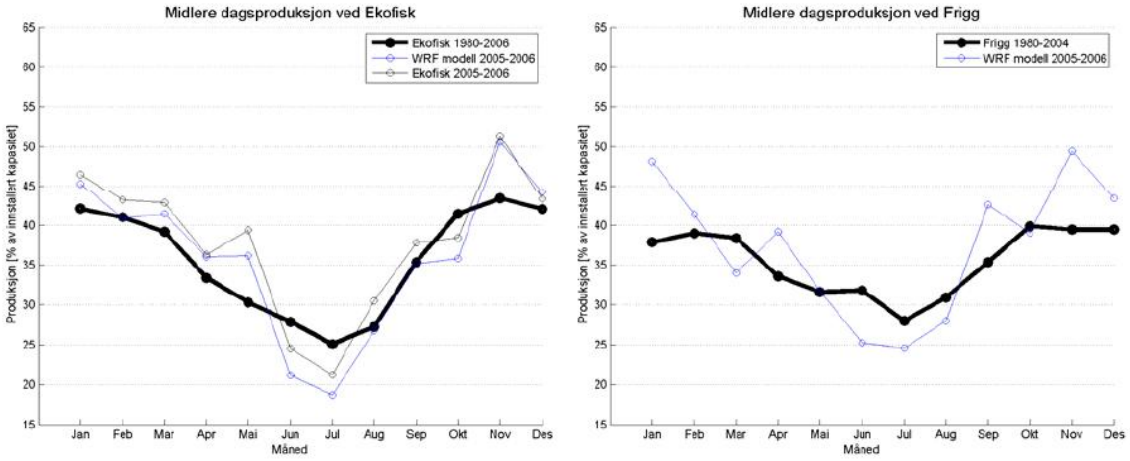

Figure 4.2: Estimated daily production for a wind turbine installed at the Ekofisk field and Frigg field.[15]

4.2 Wind Turbine

The water depth of the Utsira formation is around 115 meter and floating wind turbines are the most realistic option for a wind power plant.. The Hywind wind turbine developed by Statoil is the first full scale prototype of a floating wind turbine. This turbine is the base for the estimated wind turbine, HywindX, which could be used to supply the offshore installations. The rotor diameter of the HywindX turbine presented in Table 4.1 is derived by using the equations from Chapter 2.5.2 to get a 6 MW output at wind speeds around 12 m/s.[8]

Table 4.1: Data for the Hywind turbine and the estimated HywindX turbine.[8]

	Hywind	HywindX
Turbine size (MW)	2.3	6.0
Turbine weight (tons)	160	
Turbine height (m)	65	100
Rotor diameter (m)	82.4	140
Water depths (m)	200	200

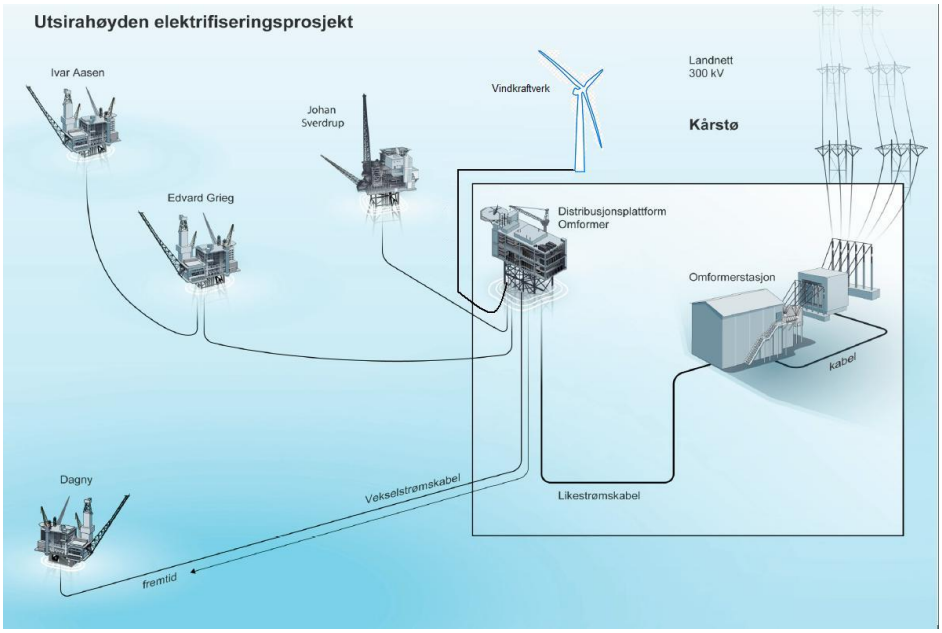

Figure 4.3: Overview of proposed solution with WPP.[25]

4.3 Wind Power Plant Capacity

Three different capacities of the WPP will be tested to see how they affect the system. It is assumed that the WPPs will only consist of HywindX turbines.

- WPP1 consisting of 13 wind turbines with total capacity of 78 MW. For this case the wind power (WP) would be a supplement to the PFS in most operational situations.
- WPP2 consisting of 26 wind turbines with total capacity of 156 MW. For this case the wind power would be the main power source for the offshore installations when the WPP is producing at full capacity.
- WPP3 consisting of 52 wind turbines with total capacity of 312 MW. For this case the wind power plant could supply the offshore installations alone when the WPP is producing near to full capacity. It is also likely that some power will be transmitted back to shore during good wind conditions.

When defining the power production capacity of the wind power plant, the power reserve in the grid must be considered. The reserve must be capable of balancing the capacity of the wind power plant. The power from shore would be from the Rogaland region, which has a large hydro-power plant capacity and there is also a gas fired power plant at Kårstø. Hence the largest capacity wind power plant could be realistic. The power reserve only need to be the full capacity when the wind speeds are very low or if the wind speeds are above 25 m/s[22]

Figure 4.4 shows that the total power reserve in Norway is around 1200 MW during a very cold winter day. There is also a surplus of 2200 MW avalible for transmission to neighbouring nordic countries and the continental Europe. For normal load conditions in the Norwegian grid there should be enough power avalible to balance the wind power plant production.[29]

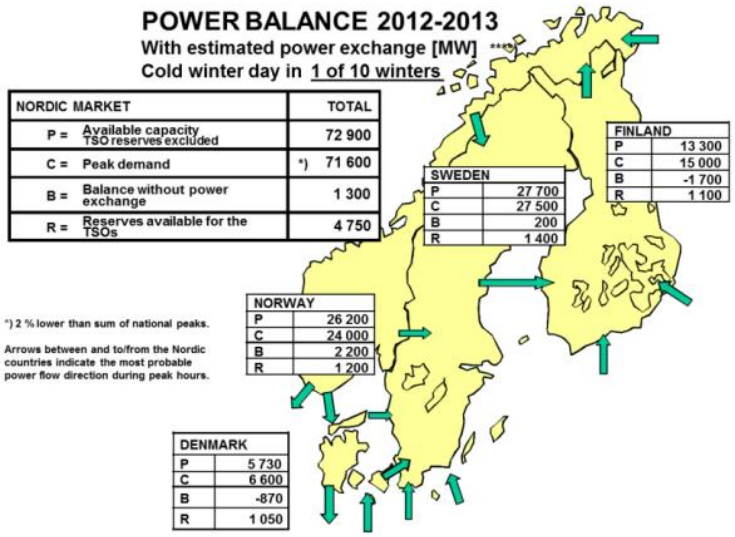

Figure 4.4: Total power balance in Norway during a very cold winter day.[29]

4.4 Modifications to Distribution System

Modifcations must be made in the distribution system in order to integrate wind power. A single line diagram of the modified distribution system can be seen in Figure 4.5.

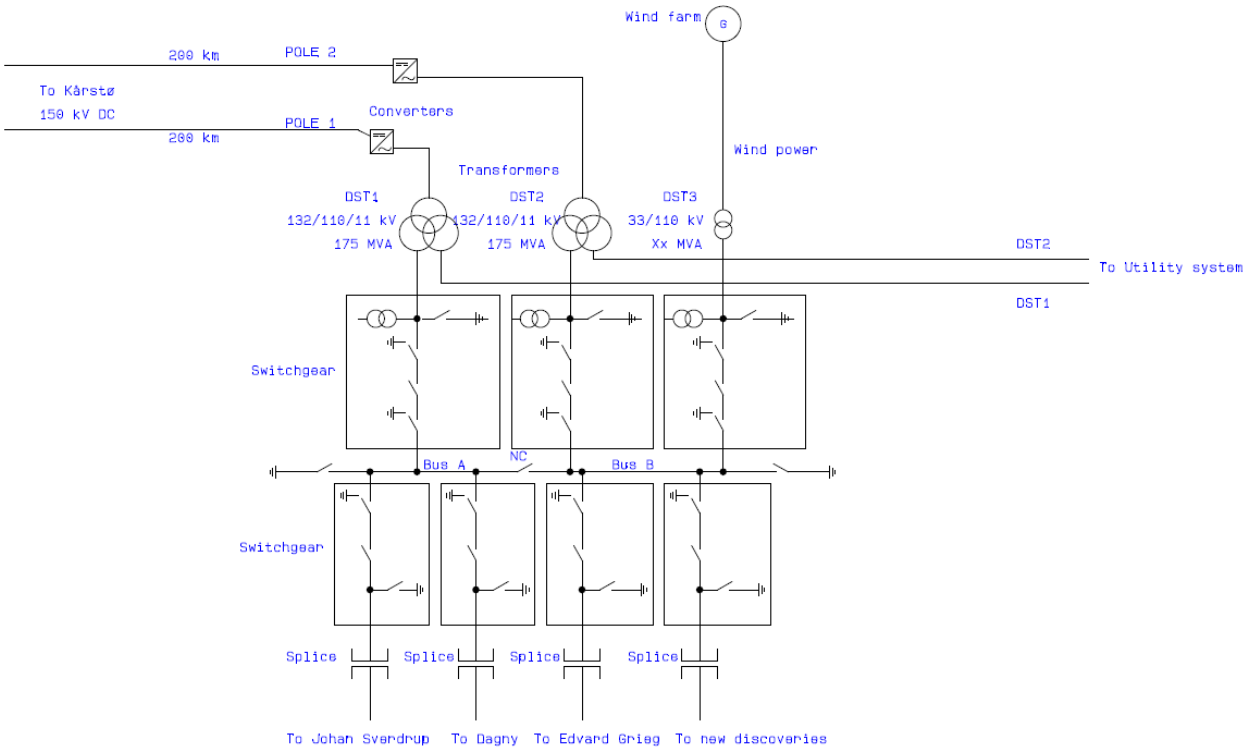

Figure 4.5: Single line diagram of modified distribution system

A new Transformer (DST3) is introduced to step up the voltage of the WPP plant to 110 kV. Usually the collector voltage for a WPP is around 30 kV. The requirements for the switchgear must be revised since the WPP will change the values for short-circuit currents.[3]

4.4.1 DST3, Capacity and Requirements

The capacity of DST3 will be equal to the capacity of the WPP. The requirements for DST3 will be the same as for the transformers connected to the Voltage Source Converter.

4.4.2 Circuit Breakers

An estimation of the sub-transient and transient short circuit current contributions due to a three phase symmetrical short circuit is shown in Table 4.2. The estimation assume the Wind Power Plant is producing at full rated capacity at the occurrence of the short circuit. The short-circuit current is seen on the 110 kV side of DST3. The estimation is shown i appendix E.

Table 4.2: Estimated short circuit current contributions from WPP in the case of a three phase balanced short circuit.

	Sub-transient Short Circuit Contribution Wind Power Plant [A]	Transient Short Circuit Contribution Wind Power Plant [A]	Load Current Wind Power Plant [A]
WPP1	4035	3362	409
WPP2	8069	6724	819
WPP3	16138	13449	1638

The contribution to the short circuit current from the WPPs is relativly large. As a result the circuit breakers for the transmission cables to the offshore installation must probably be upgraded. An alternative to upgrading components are to implement a current limiter (Is limiter) which restrict the short circuit current.

4.4.3 Power Management System

The PMS will need to be modified if wind power is to be integrated into the distribution system. The system will still have the same functions, however the power flow into the system will now also need to be balanced between power from the onshore grid and wind power. Hence will the power generated from the WPP be the basis of the power needed and the onshore grid shall deliver the remaining power needed for the offshore consumers. Due to variations in the wind the power generated at the WPP will vary and therefore the PMS shall be able to adjust the power received from the onshore grid continuously. The variations in wind can also to some degree be estimated based on the weather forecasting.

In order for the PMS to determine the needed power from the onshore grid the power generated at the WPP shall be measured at both the WPP and the DP. Communication between the WPP and DP PMS will therefore be important to determine power needed from shore. The communication between the WPP and DP will be enabled by a fiber cable laid together with the transmission cable.

The PMS shall if necessary initiate load shedding or fast load shedding in the event of occuring faults with the WPP transmission or generation. The PMS shall further adjust the missing electric power to be delivered from shore in order to continue operation.

The requirements for the system voltage and system frequency will stay unchanged from Chapter 3.4.

4.5 Modifications Simulink Model

The Simulink model will have a Wind Power Plant block in addition to the VSC block to deliver power. In the bus-bar block the active power from the WPP is subtracted from the active power demand of the loads. The result is that the WPP always will deliver all its produced power to the loads while the VSC deliver power to adjust the power balance in the system. It is assumed that the WPP will supply its own reactive power.

4.5.1 Wind Power Plant

The wind power plant consists of three blocks shown in Figure 4.6. The wind turbine block builds on the equation presented in Chapter 2. The asynchronous generator block is equal to the asynchronous motors from Chapter 3.

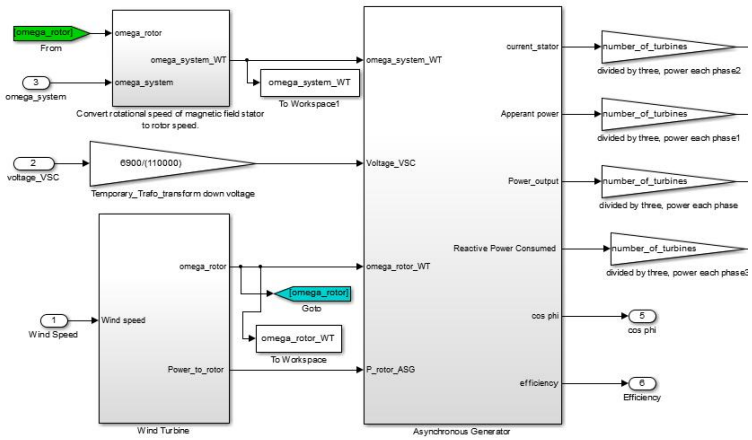

Figure 4.6: The Simulink block of the Wind Power Plant

4.5.2 Wind Turbine Asynchronous Generator

The wind turbine generator is modeled as a squirrel cage induction machine and has a capacity of 6 MW. The parameters of the generator is shown in Table 4.3

Table 4.3: Parameters for the WT generator.

Capacity [MW]	6
Stator voltage line to line [V]	6900
Frequency [Hz]	60
Poles	6
Power factor nominal	0.9
Efficiency [%]	96.0
Stator and rotor resistance, R_1 and R_2 [pu]	0.0107
Total leakage reactance, X [pu]	0.241
Magnetizing resistance, R_m [pu]	36.60
Magnetizing reactance, X_m [pu]	4.11

4.5.3 Rotational Speed of Wind Turbine Rotor

The rotational speed of the rotor varies with the wind speed. The design wind speed for the wind turbine is set to be around 9 m/s and there should be optimal power production between +-30 % of this wind speed. To achieve this, the tip speed ratio is kept constant at its optimal value in this range of wind speeds. From Equation 2.4 it is clear that the rotational speed of the rotor must vary for this to come true. Above and below the optimal production zone for the wind speed, the rotational speed of the rotor is kept constant. This is seen in Figure 4.7.

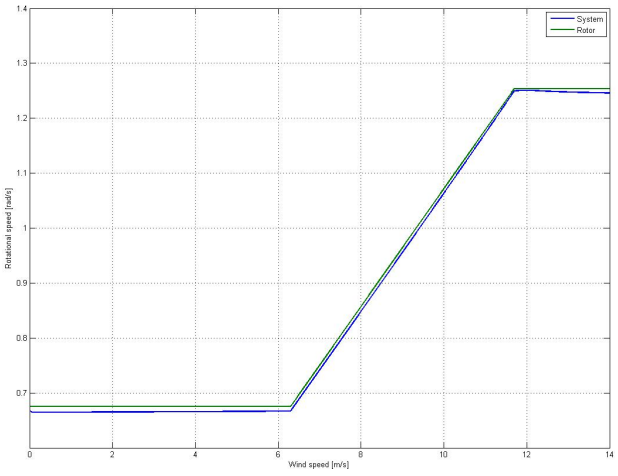

Figure 4.7: Rotational speed of WT rotor and stator magnetic field.

4.5.4 Rotational Speed of Wind Turbine Generator

It is assumed that the WT generator can run on variable frequency due to a variable frequency converter between the generator and wind turbine transformer. Because of this assumption the rotational speed of the magnetic field in the stator of the WT generator is not locked to 125.66 rad/s.[14]

The rotational speed of the WT rotor connected to the hub of the wind turbine blades is used as the rotor speed of the WT generator. Usually this rotor is connected to the rotor of the WT generator through a gear. The rotational speed of the magnetic field inside the stator of the WT generator has to be converted for the slip to be calculated correctly. This is done by the block *Convert rotational speed of magnetic field stator to rotor speed.* which is built on equation 4.1.

$$\omega_{systemWT} = \frac{\omega_{rotorWT}}{1 - slip_{nominal}} \cdot \frac{\omega_{system}}{\omega_{sync}} \tag{4.1}$$

$\omega_{systemWT}$ = Rotational speed of the magnetic field in the stator of the generator seen through gear [rad/s].

$\omega_{rotorWT}$ = Rotational speed of the rotor connected to the hub of the wind turbine blades [rad/s].

ω_{system} = Rotational speed of the magnetic field in the stator of the generator [rad/s].

ω_{sync} = Synchronous rotational speed of the generator, 125.66 [rad/s].

$slip_{nominal}$ = Slip at nominal power production of the generator. This is a negative value.

Chapter 5

Simulations with Power from Shore

Results from the Simulink model introduced in Chapter 3 is presented in this chapter. The model is based on the VSC delivering power through a transformer to the busbar. The US block will recieve power directly from the VSC transformer. The different platform load blocks are connected to the busbar. Johan Sverdrup will be directly connected and have the same voltage level as the busbar, while the other loads will be connected through transmission cable blocks. The platform load blocks contains transformers within for correct voltage level. The different blocks will calculate/measure voltage levels, currents and power.

5.1 Case 1 - Steady State with Peak Load

Case 1 steady state illustrates steady state operation, ie no variations in demanded power, and with peak loads. The simulation is run to describe system voltage levels, peak currents, total power and frequency.

Figure 5.1 illustrates the RMS voltage level over the busbar and voltage levels at Dagny and Edvard Grieg. Johan Sverdrup will have the same voltage level as the busbar because of the negligible transmission distance.

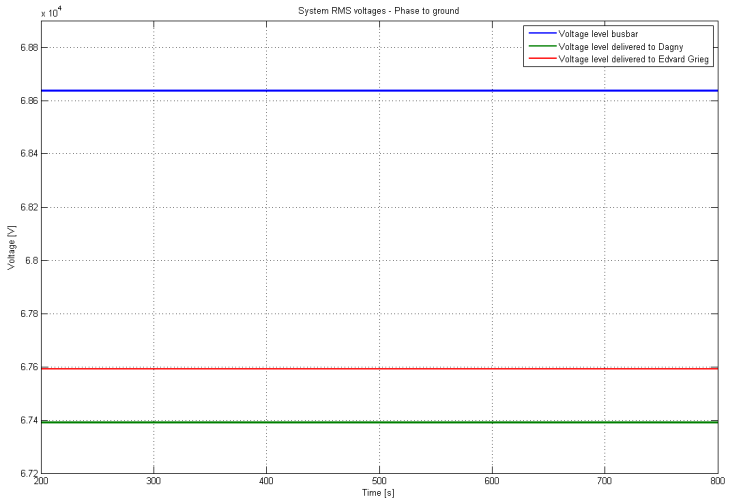

Figure 5.1: System RMS voltages during steady state with peak loads.

Figure 5.1 shows that there is a voltage drop between the VSC and the offshore installations. This is due to the DST, the transmission lines and the transformers at the offshore installations. The largest voltage drop is observed to be 1.25 kV phase to ground between DP and Dagny.

Figure 5.2 illustrates the platform RMS voltage levels for the platform motors.

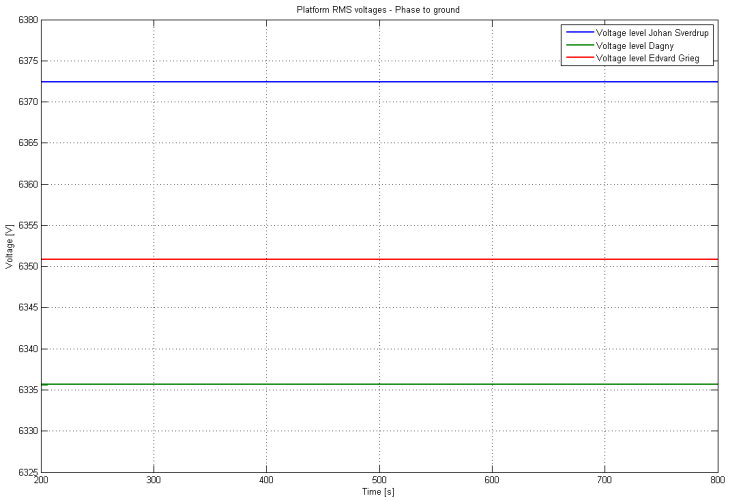

Figure 5.2: Platform RMS voltages during steady state with peak loads.

The voltage levels will vary some compared to nominal voltage level. The largest difference between actual voltage level and nominal is at Johan Sverdrup. The voltage level at Johan Sverdrup is 6372.5 V phase to ground, which is within the steady state limits of +6/-10 %.

Figure 5.3 illustrates the DS current and the load currents. The load currents are approximately the same as estimated in chapter 3.

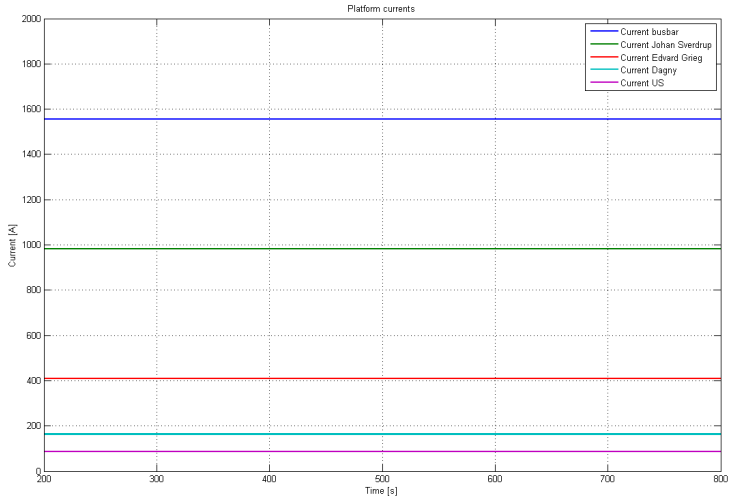

Figure 5.3: Current in DS and load currents during steady state with peak loads.

Figure 5.4 illustrates total apparent, active and reactive power consumed by the platforms during peak load.

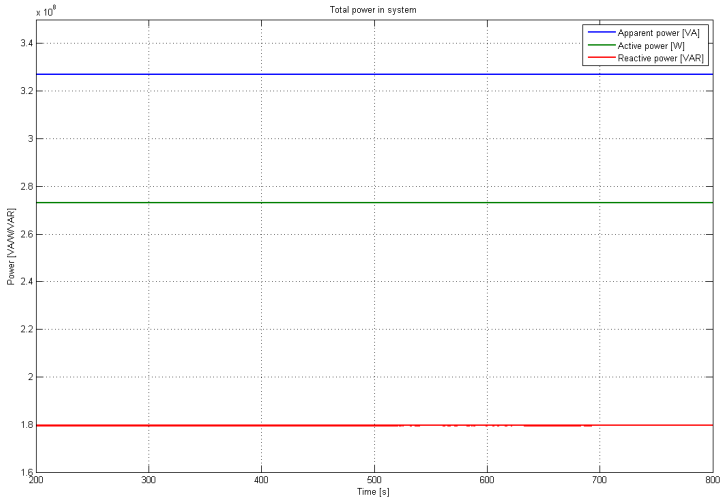

Figure 5.4: Power produced and consumed during steady state with peak loads.

The apparent power loss, due to transmission and transformers, and consumed by loads complies with estimated peak load consumption. The power factor is calculated to be approximately 0.85.

Figure 5.5 illustrates the frequency during steady state. The frequency is at 60 Hz and the system is therefore considered to be in steady state.

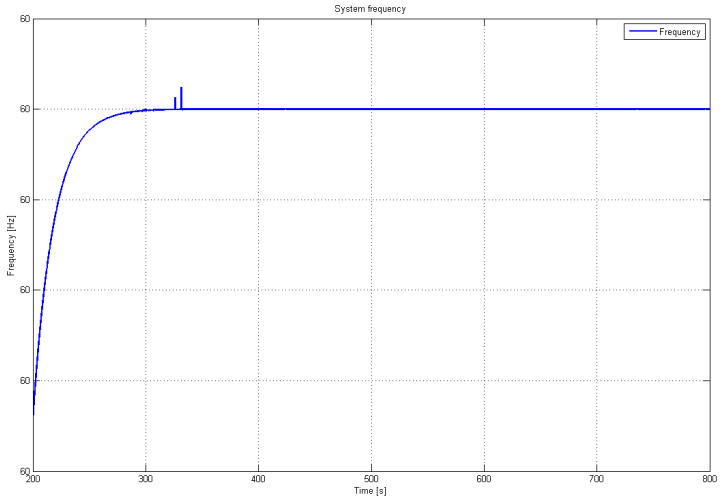

Figure 5.5: Frequency during steady state with peak loads.

5.2 Case 2 - Steady State Medium Load

This case illustrates steady state operation of estimated load conditions from 2037 and outwards presented in Figure 2.2. The motors which has been removed are three induction motors on Johan Sverdrup and one at Edvard Grieg.

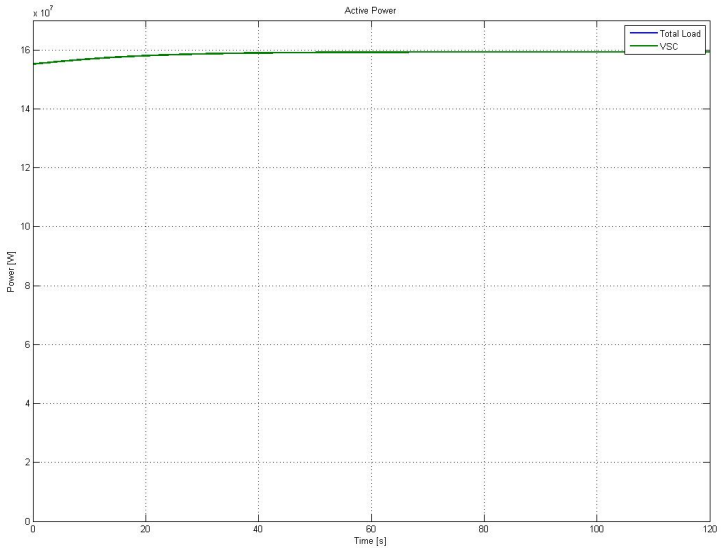

Figure 5.6: Total active power consumption of the offshore installations.

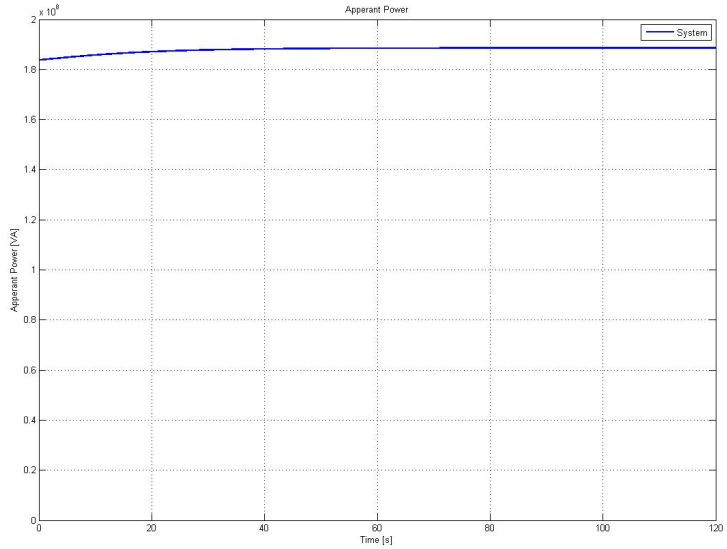

Figure 5.7: Total apperant power consumption of the offshore installations.

The total power consumption in this case is around 160 MW and the total apperant power is around 186 MVA. This gives an power factor of approximately 0.85, which is similar to the power factor in case 1.

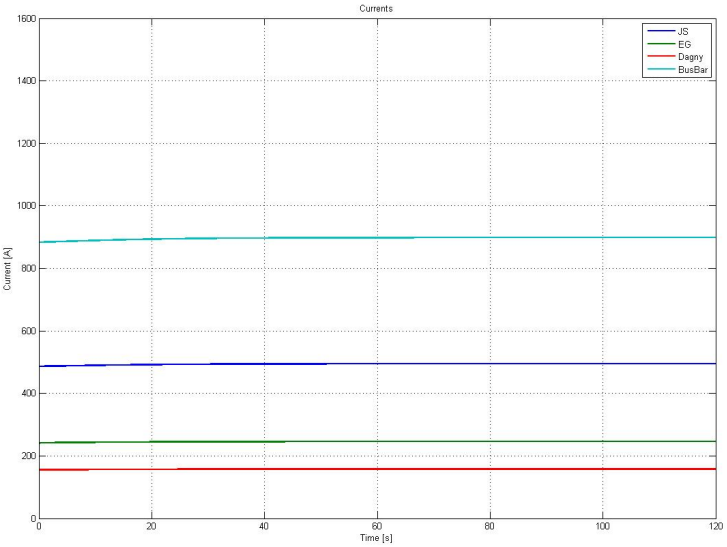

Figure 5.8: RMS currents at the 110 kV level.

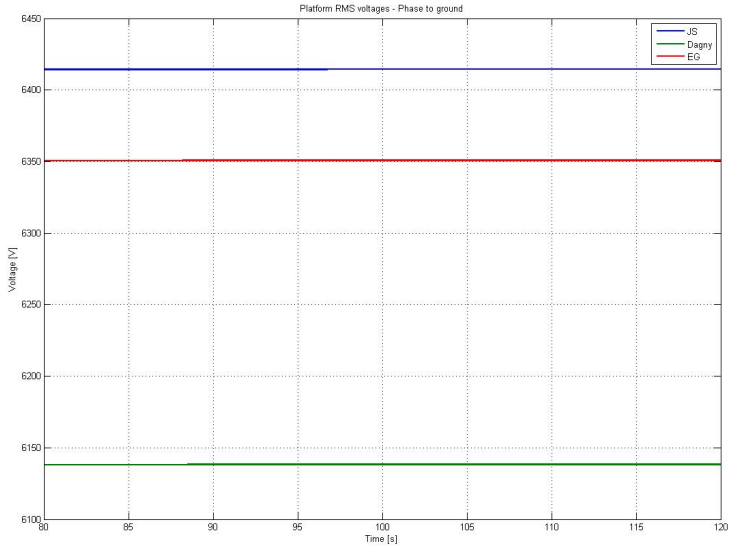

Figure 5.9: Platform voltages phase to ground at the 11 kV level.

The voltage of Dagny is 6.1 kV phase to phase. The lower steady state limit for the voltage according to Chapter 3.4 is -10 % of nominal voltage, which is 5.72 kV. The voltage of Dagny is considered well within this limit. The load currents are as expected lower for this case compared to the peak load due to the lower power demand.

5.3 Case 3 - Steady State with New Discovery and Peak Load

Case 3 steady state illustrates steady state operation with a potential new discovery and peak loads. The simulation is run to describe system voltage levels, peak currents and total power.

Figure 5.10 illustrates the RMS voltage level in the DS and voltage level after transmission recieved at the new discovery platform.

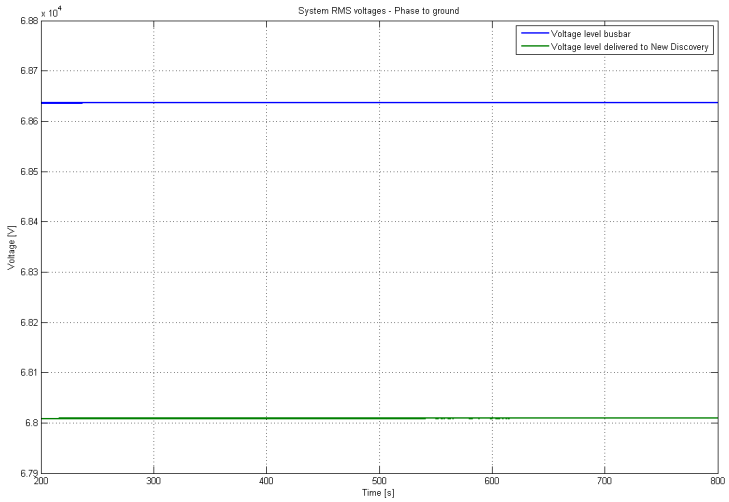

Figure 5.10: System RMS voltage during steady state with peak loads.

There will be a voltage drop of approximately 0.63 kV phase to ground between the DP and the ND platform.

Figure 5.11 illustrates the platform RMS voltage levels out from the platform transformers.

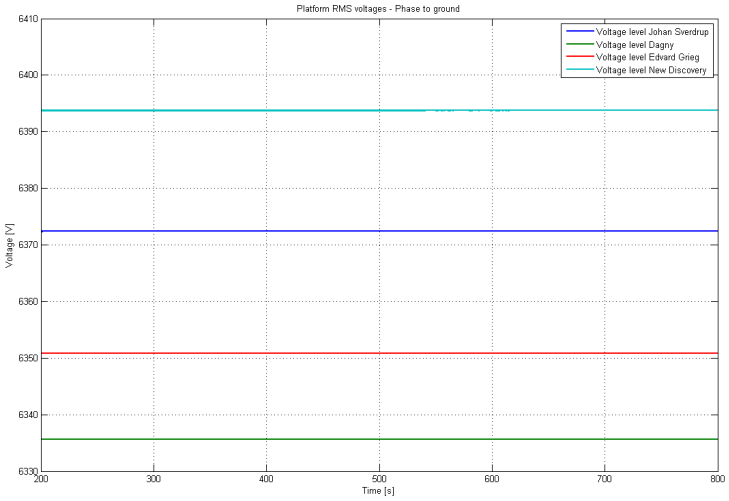

Figure 5.11: Platform RMS voltages during steady state with peak loads.

The occuring voltage at the ND platform is slightly higher then at JS. The voltage level is found to be 6394 V phase to ground, which is within steady state limits.

Figure 5.12 illustrates the DS current and the ND load current.

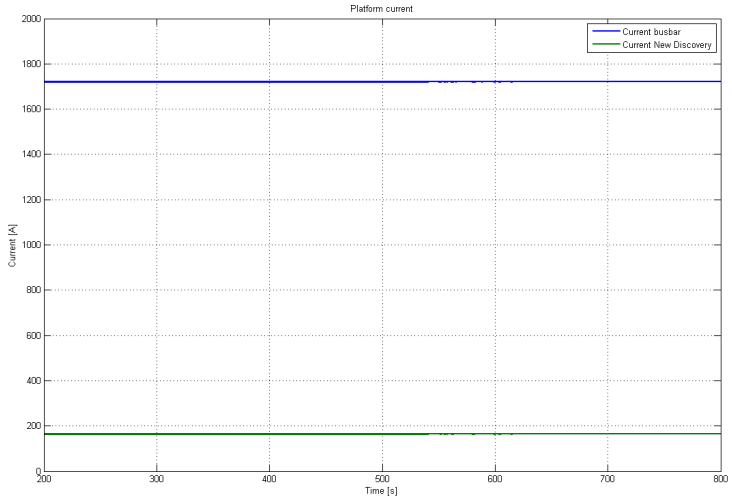

Figure 5.12: Current in DS and ND load current during steady state with peak loads.

The current in the DS have increased due to the ND load current. The ND load current is approximately the same as the Dagny load current which is because the load at ND is assumed to be approximately the same as Dagny.

Figure 5.13 illustrates total apparent, active and reactive power consumed by the platforms during peak load.

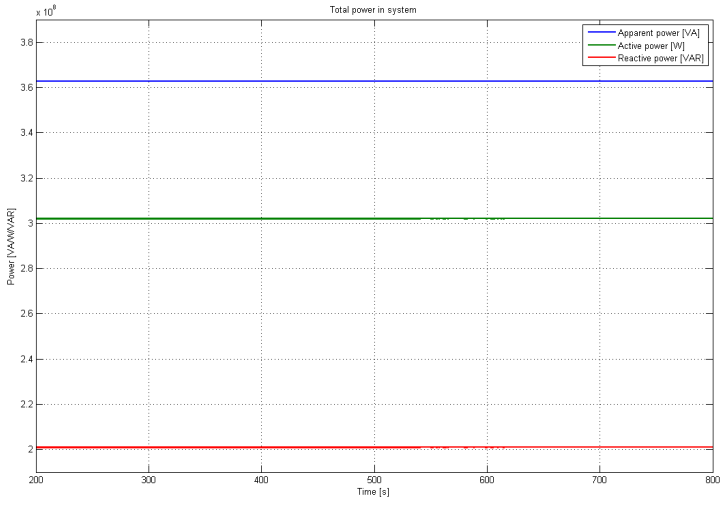

Figure 5.13: Power produced and consumed during steady state with ND and peak loads.

The apparent power lost, due to transmission and transformers, and consumed by loads complies with estimated peak load consumption with the ND platform. The power factor is calculated to still be approximately 0.85.

5.4 Short Circuit Current Contribution VSC

The short circuit is simulated by adding a impedance of 0.01 ohm and a load angle of 0.3 rad in parallell with the original load. The short circuit simulated is a balanced three phase short circuit. The short circuit occur at the 110 kV level which is the primary side of the offshore installation transformers. The current output of the VSC have been limited to 1.600 kA for the 110 kV level and it is regarded as a constant current source during the short circuit. In chapter 2.2.1 it is stated that the fault current of the VSC is limited by the thermal capacity of the power transistors (IGBT). The peak load current of the VSC is around 1.550 kA at the 110 kV level as seen in case 5.1. It would probably limit the lifetime of these power transistors if the thermal capacity was reached at the peak load. Hence the thermal capacity is probably higher and 1.600 kA is estimated. The simulation is based on a worst case where the system operates with peak load.

5.4.1 Dagny after Transmission

In this case the short circuit occur at the end of the transmission cabel to Dagny.

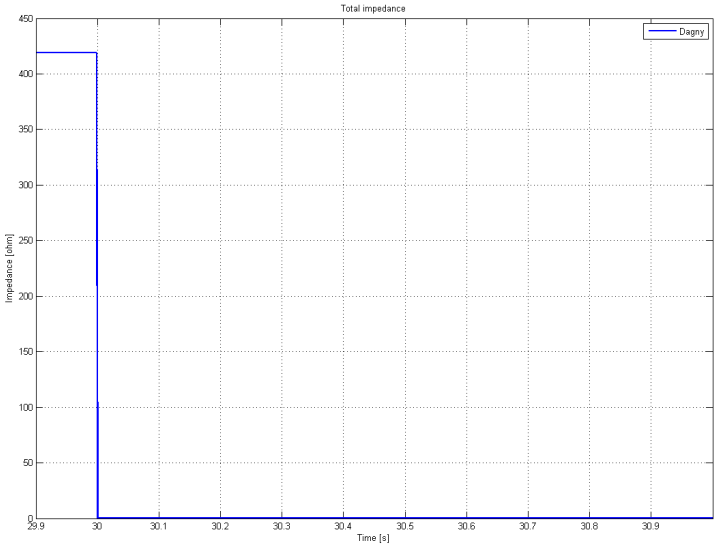

Figure 5.14: The impedance of Dagny with motor and transformer after short circuit.

When the short circuit occur the impedance of the Dagny installation fall to a fraction of its original value as seen in Figure 5.14.

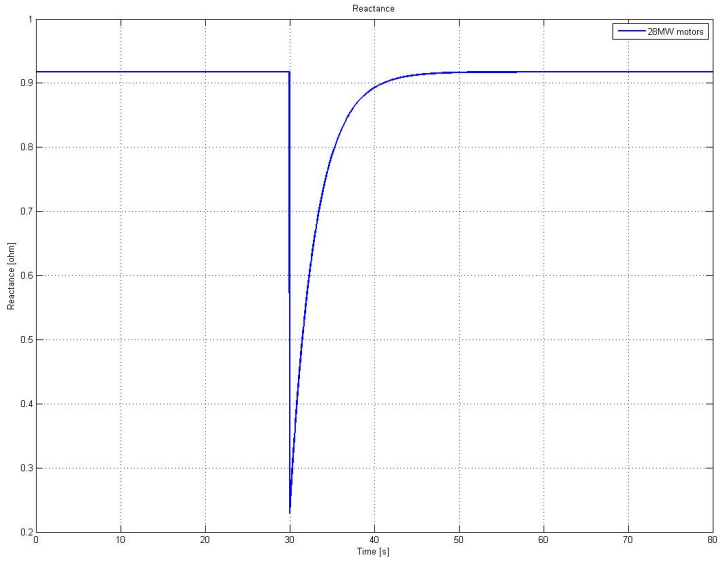

Figure 5.15: The reactance the 28 MW motors for the whole simulation period.

The reactances of the asynchronous motors fall to 25 % of their original value immediately after the short circuit. After a transient period it goes back to its original value shown in Figure 5.15 with the 28 MW motor as an example.

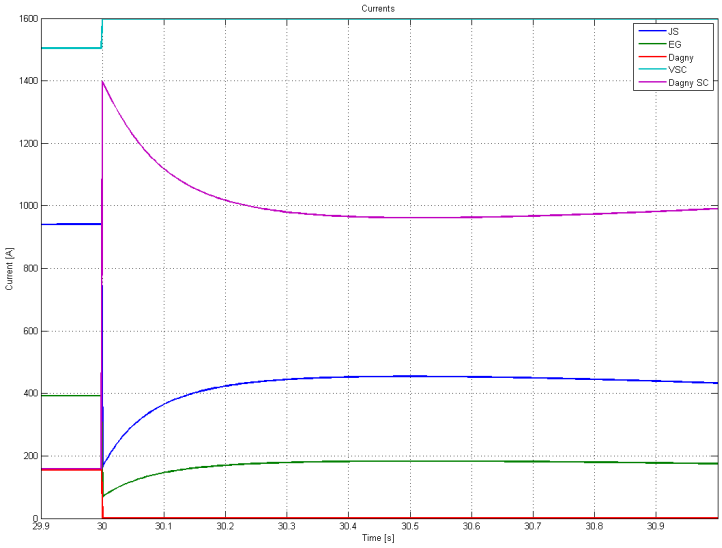

Figure 5.16: System RMS currents 1 second after the short circuit.

The RMS current peak in the transmission cabel to Dagny is around 1.400 kA around 8.23 times as large as the nominal current.

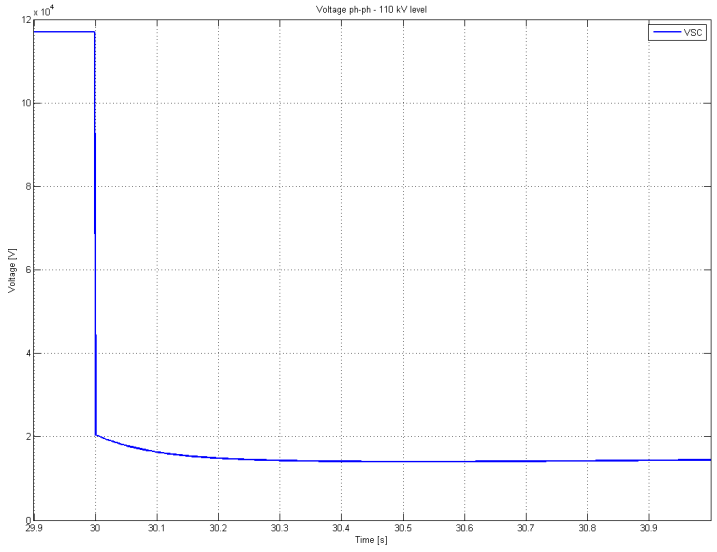

Figure 5.17: Currents in the system straight after the short circuit.

The voltage of the VSC drops to a level equal to the total system impedance multiplied with the VSC current during the short circuit. Since the AC fault is on the secondary side of three-winding transformers 1 and 2, these are seen as a load in series with the short circuit by the VSC. This is similar to the behavior of the VSC shown in Chapter 2.2.1. The voltage does not drop to near zero since the short circuit is at the end of the transmission cable to Dagny.

5.4.2 Edvard Grieg after Transmission

In this case a short circuit at the end of the transmission cable to Edvard Grieg is simulated. The results are similar to the short circuit at Dagny.

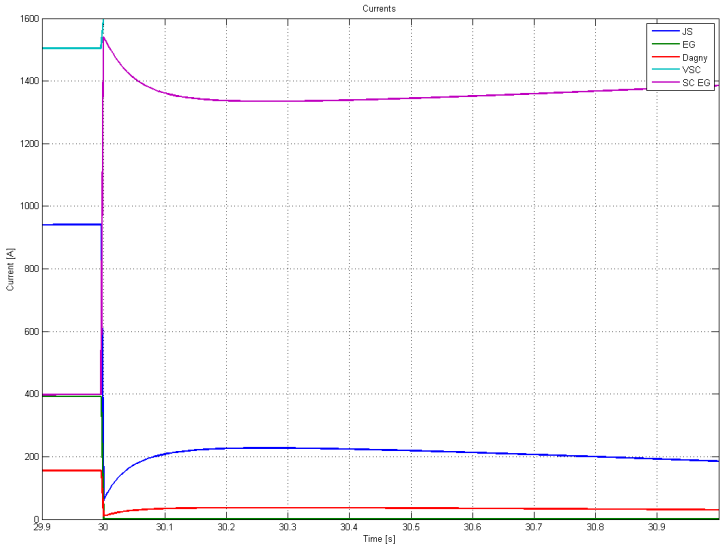

Figure 5.18: System RMS currents 1 second after the short circuit.

The RMS current peak in the transmission cabel to EG is around 1.500 kA around 3.5 times as large as the nominal current.

5.4.3 Johan Sverdrup

In this case a short circuit at the Johan Sverdrup platform is simulated. The results are similar to the other short circuit cases since the impedance of JS falls to a fraction of its original value.

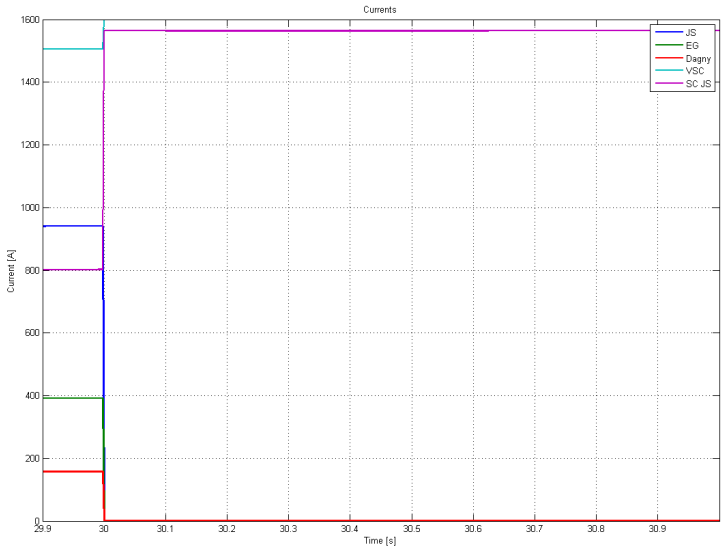

Figure 5.19: System RMS currents 1 second after the short circuit.

The RMS short circuit current is around 1.550 kA. The short circuit current does not fall as in the cases of Dagny and EG. The short circuit current is approximately 1.5 times larger then nominal value. One reason for this is the lack of a transmission impedance to JS. The impedance of the short circuit have a very low impedance compared to Dagny and EG.

This short circuit case at Johan Sverdrup illustrates how a short circuit before the transmission cabels to Dagny and EG would affect the system. The peak short circuit current could in both these cases be estimated to be around 1.550 kA RMS.

5.4.4 New Discovery

A short circuit at the end of the transmission cable to the New Discovery has been simulated.

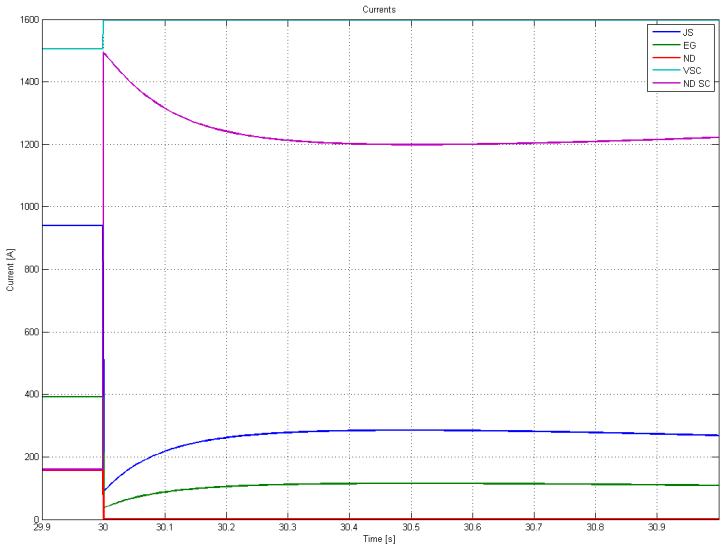

Figure 5.20: System RMS currents 1 second after the short circuit.

The result is similar to the short circuit case for Dagny seen in Figure 5.16. The RMS peak current is 1470 A, higher than Dagny since the transmission distance is 30 km to the New Discovery, while the transmission distance is 60 km to Dagny.

5.5 Short Circuit Current Contribution Offshore Installations

The short circuit simulations for the offshore installations are conducted similar to the simulations for the VSC contribution. The induction motors will behave as generators when the short circuit occur. The scenario is considered to be based on worst case since all the platform loads are modelled as inductive motors and the short circuit will occur in Johan Sverdrup transmission cable.

Figure 5.21 and 5.22 presents the simulated occuring short circuit current contribution from Johan Sverdrup. The largest phase current is approximately 3.650 kA RMS.

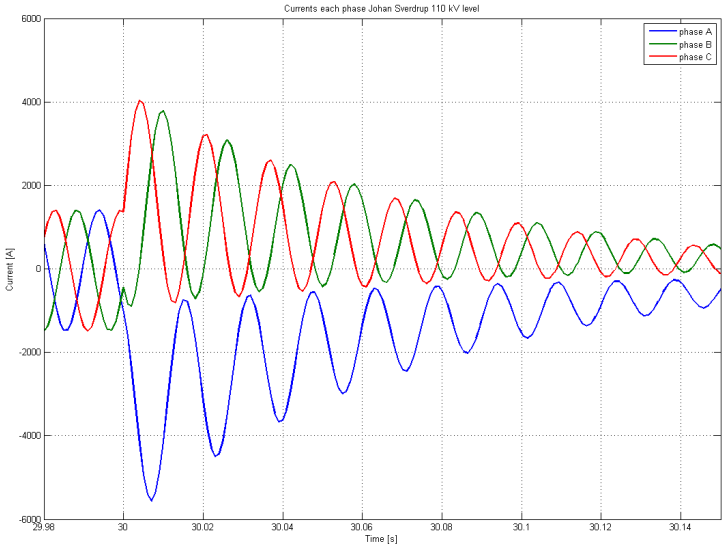

Figure 5.21: Generated current by Johan Sverdrup inductive motors during short circuit.

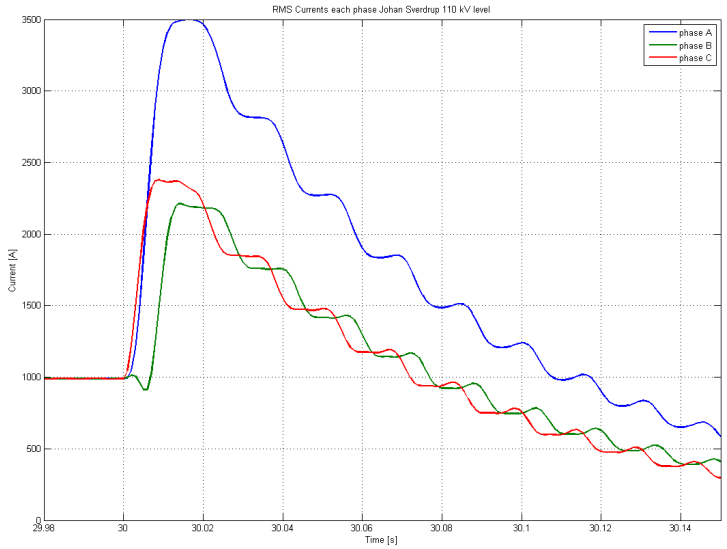

Figure 5.22: Generated RMS current by Johan Sverdrup inductive motors during short circuit.

Figure 5.23 and 5.24 presents the simulated occuring short circuit current contribution from Edvard Grieg. The largest phase current is approximately 1.450 kA RMS.

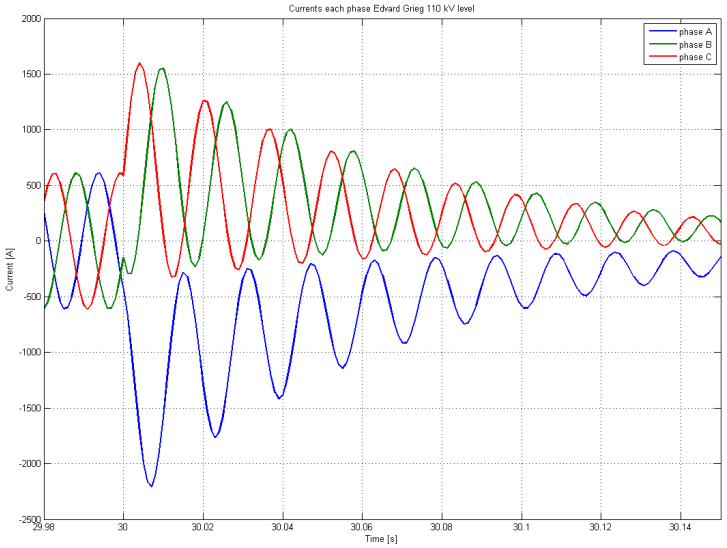

Figure 5.23: Generated current by Edvard Grieg inductive motors during short circuit.

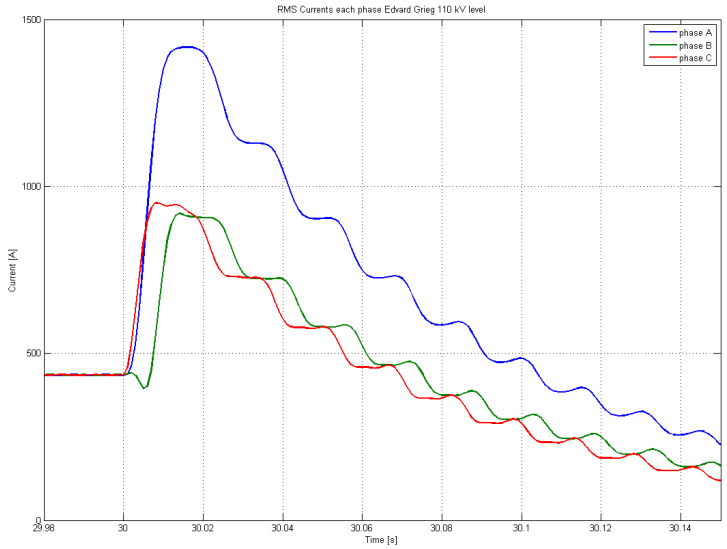

Figure 5.24: Generated RMS current by Edvard Grieg inductive motors during short circuit.

Figure 5.23 and 5.24 presents the simulated occuring short circuit current contribution from Dagny. The largest phase current is approximately 0.6 kA RMS.

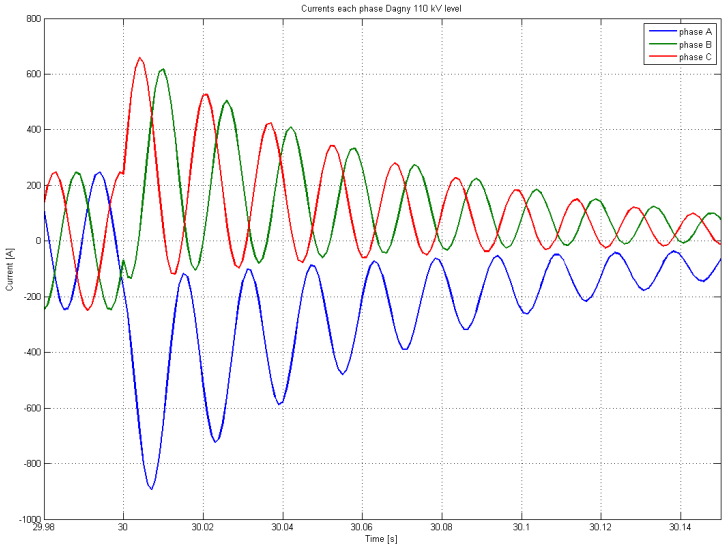

Figure 5.25: Generated current by Dagny inductive motors during short circuit.

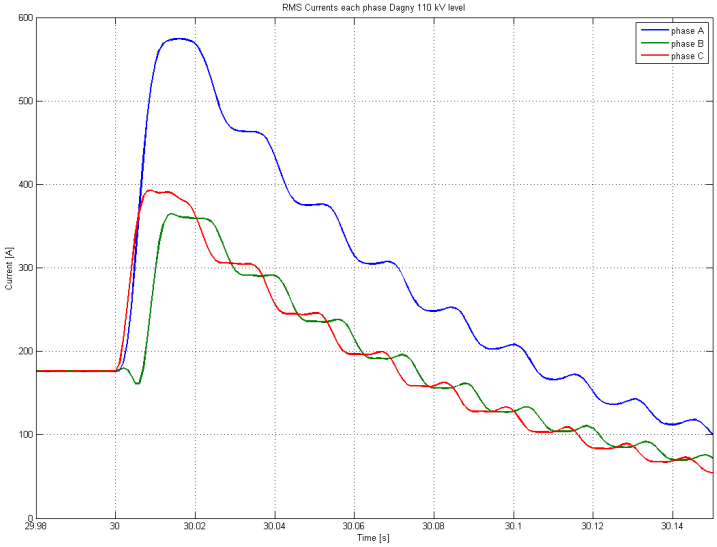

Figure 5.26: Generated RMS current by Dagny inductive motors during short circuit.

The new discovery short circuit contribution will be equal to the contribution from Dagny, ie 0.6 kA RMS. This is due to the potential new discovery platform is assumed to have equal load conditions as Dagny.

Chapter 6

Simulations with Power from Shore and Wind Power Plant

The introduced WPP block in Chapter 4 will now be added to the simulink model in order to simulate power delivered from both onshore grid (VSC) and WPP. The WPP block deliveres active power directly to the busbar, the amount of active power is dependant of both wind speed and the number of wind turbines. In order to simplify the model the US power consumption is not included in the WPP simulations.

6.1 Steady State with Wind Power Plant and Peak Load

The three cases of WPP with 13, 26 and 52 wind turbines will be simulated. The wind speed used for this simulation will be around the estimated mean wind speed introduced in Chapter 4. The simulation is run to describe system voltage levels, currents, total power and frequency.

There will be less fluctuations in the mean wind speed for a higher number of wind turbines. As a result the mean wind speed fluctuations will decrease between WPP1, WPP2 and WPP3. The wind speed curves are shown in appendix D. The variations in the wind speed causes the power produced to fluctuate. The fluctuating power produced by the WPP will cause small fluctuations to the total power, currents and voltage. The voltage levels, load currents and power will otherwise stay approximately the same as without the WPP.

Figure 6.1 and 6.2 illustrates the frequency of the system with 13 and 52 wind turbines during peak load.

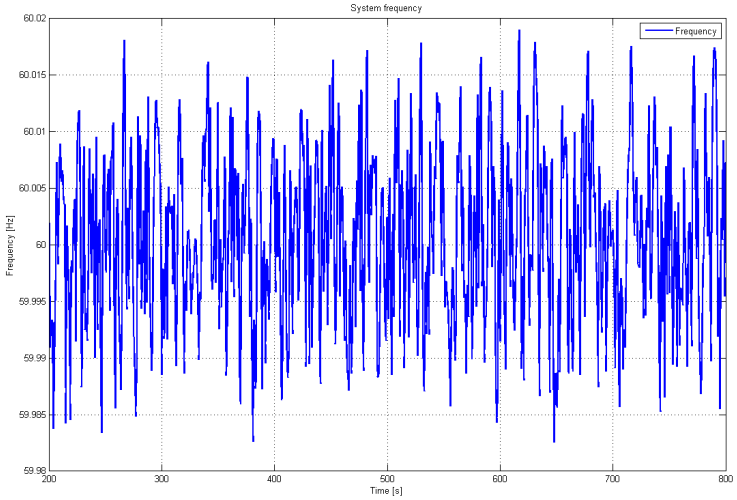

Figure 6.1: Frequency during steady state with 13 wind turbines and peak load.

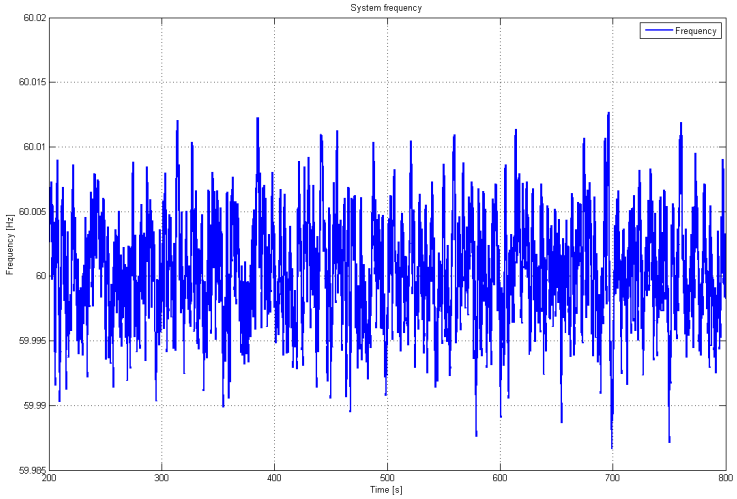

Figure 6.2: Frequency during steady state with 52 wind turbines and peak load.

The frequency in the system stays more stable by increasing the amount of wind turbines. Although the frequency is constantly fluctuating it stays within the cyclic variations limit for all cases. The frequency curve for case WPP2 with 26 wind turbines is illustrated in appendix D.

Figure 6.3 and 6.4 illustrates the total apparent, active and reactive power consumed by the platforms during peak load with 13 and 52 wind turbines.

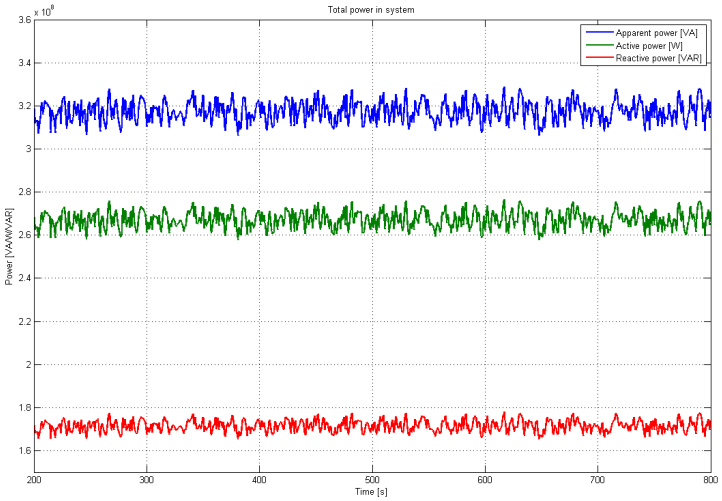

Figure 6.3: Power produced and consumed during steady state with 13 wind turbines and peak load.

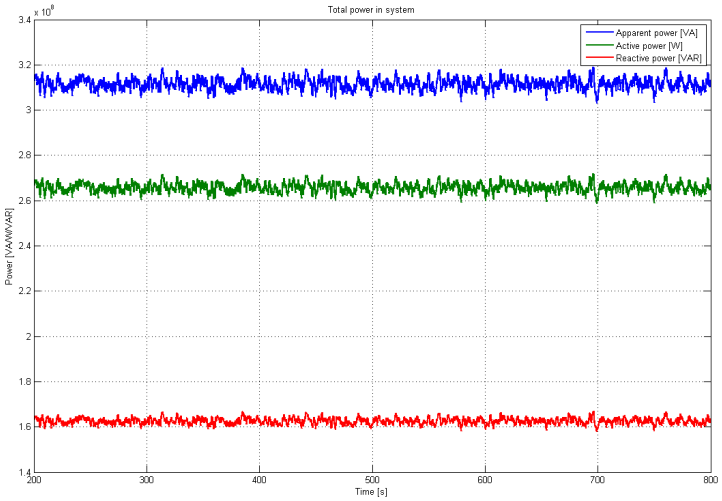

Figure 6.4: Power produced and consumed during steady state with 52 wind turbines and peak load.

The fluctuations in total power will decrease by increasing the number of turbines. The power production/consumption curve for case WPP2 with 26 wind turbines is illustrated in appendix D.

Figure 6.5 and 6.6 illustrates the total active power in the DS and the contributions from shore (VSC) and the WPP during peak load with 13 and 52 wind turbines.

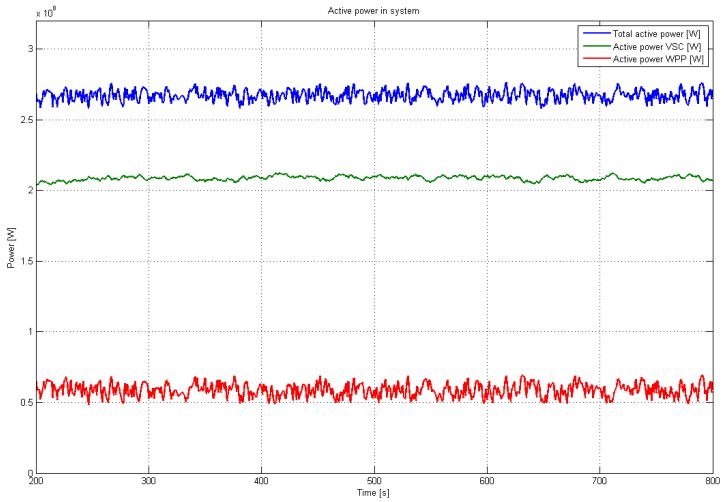

Figure 6.5: DS active power and active power delivered by WPP and VSC during steady state with 13 wind turbines and peak load.

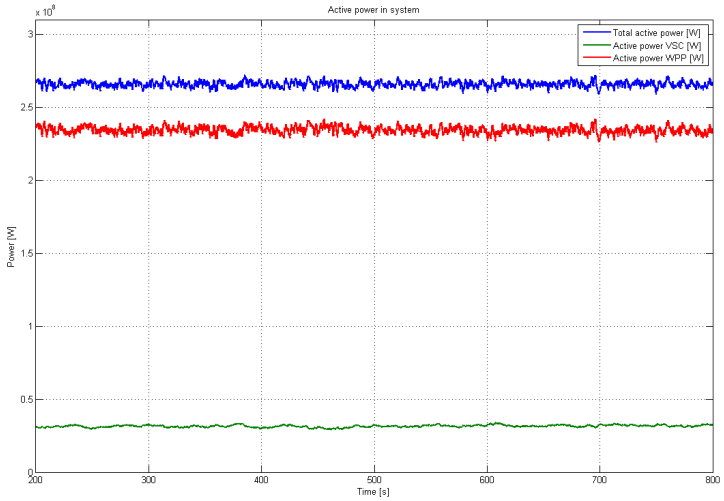

Figure 6.6: DS active power and active power delivered by WPP and VSC during steady state with 52 wind turbines and peak load.

The fluctuations will decrease by increasing the amount of wind turbines. The DS active power is at all cases only made up from the recieved active power from the VSC and WPP. Increasing the WPP active power output will decrease the active power demanded from shore (VSC). The active power production curve for case WPP2 with 26 wind turbines is illustrated in appendix D.

The DS/platform voltage levels and load currents are illustrated in appendix D. It is observed that these curves will still hold the same levels as without the WPP and the fluctuations will decrease by increasing the amount of wind turbines, which confirms the observations for the system power and active power curves.

The steady state simulation results indicate that the system frequency will fluctuate around 60 Hz. The system frequency cyclic variations are required to stay between 59.7 - 60.3 Hz. The system frequency is

observed to stay within this limit for all WPP cases, and it is also observed that the fluctuations will decrease as the number of turbines increase.

Since the steady state platform voltage levels are different, the voltages will fluctuate around their own steady state value. All platform voltage levels are observed to be within the cyclic variations limit. Furthermore, the voltage fluctuations are observed to be equal for the different platform voltage levels and decrease as the number of turbines increase. The steady state voltage level at Edvard Grieg (EG) is observed to fluctuate around the ideal value of 11 kV RMS phase to phase. The fluctuations for EG, with the case for 13 wind turbines, are observed to be between 10953 - 11045 V RMS phase to phase, which are within the required limits of 10780 - 11220 V RMS phase to phase.

6.2 Increasing Mean Wind Speed with Peak Load

This simulation will illustrate how an increasing mean wind speed will affect the power delivered to the system by the WPP, and how this affects power delivered from shore (VSC). The mean wind speed is simplified to not have variations, but will simply start at 7 m/s and increase linearly to 15 m/s. The curve for the wind speed is illustrated in appendix D.

Figure 6.7, 6.8 and 6.9 illustrates the total active power in the DS and the contributions from shore (VSC) and WPP for all three cases during peak load.

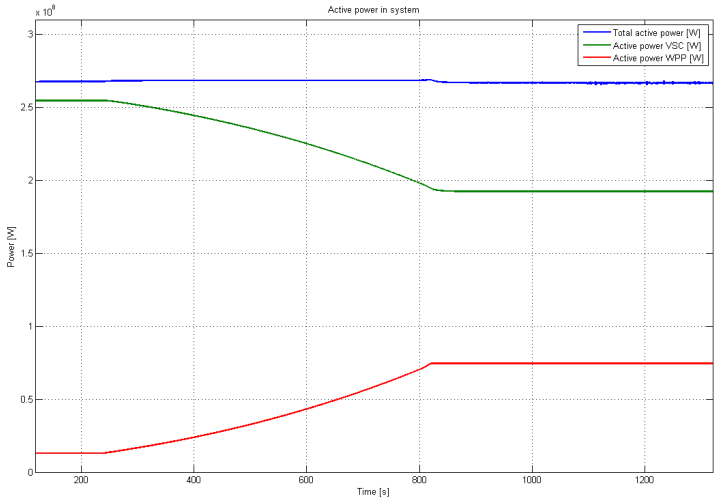

Figure 6.7: DS active power and active power delivered by WPP and VSC during increasing mean wind speed with 13 wind turbines and peak load.

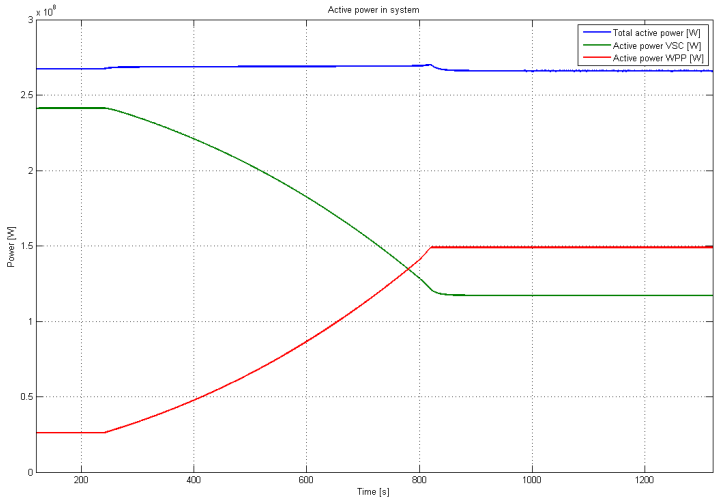

Figure 6.8: DS active power and active power delivered by WPP and VSC during increasing mean wind speed with 26 wind turbines and peak load.

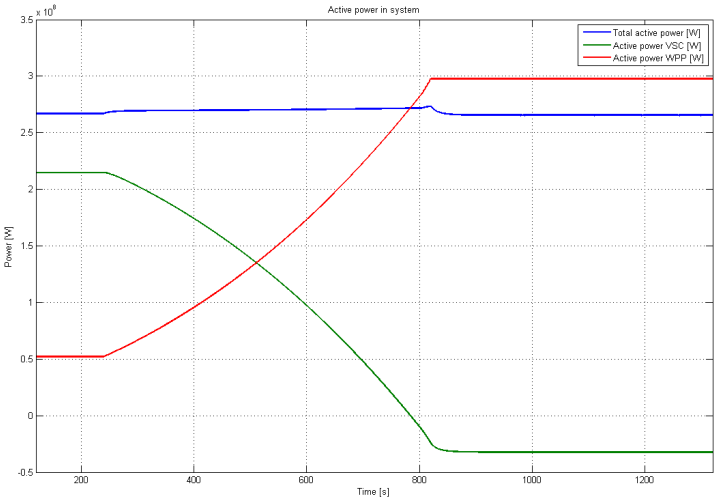

Figure 6.9: DS active power and active power delivered by WPP and VSC during increasing mean wind speed with 52 wind turbines and peak load.

As the wind speed increase the WPP active power output will increase and the VSC active power output decrease. At case WPP3 with optimal mean wind speed and 52 wind turbines the WPP will produce enough power to also supply the onshore grid.

The curves for frequency, apparent/active/reactive power, voltages and load currents are displayed in appendix D. The frequency is observed to slightly increase while the mean wind speed is increasing and stabilize at system frequency when the mean wind speed stabilize. The apparent power, voltages and load currents will slightly increase with the increasing mean wind speed and will stabilize at nominal value when the mean wind speed stabilize. The platform voltages are also observed to slightly drop when the mean wind speed starts increasing and have small peaks when the mean wind speed stabilize.

6.3 Wind Speed Reaching Critical High Point / WPP Stop in Production with Peak Load

The assumed critical high point is 25 m/s for the wind turbines. At this point the wind turbines will stop producing power and the power demanded by the offshore installations will have to be recieved from shore. For this simulation the mean wind speed have been simplified to be constant and to not have any variations. The wind speed will at first be 15 m/s which ensures full production and after running for 200 seconds the wind speed will fall to 0 m/s to simulate the wind turbines stopping production.

This simulation will illustrate how the systems variables react when the WPP goes from full production to no production. The curve for the wind speed is illustrated in appendix D.

Figure 6.10 and 6.11 illustrates the frequency of the system with 13 and 52 wind turbines during peak load and stop in WPP production.

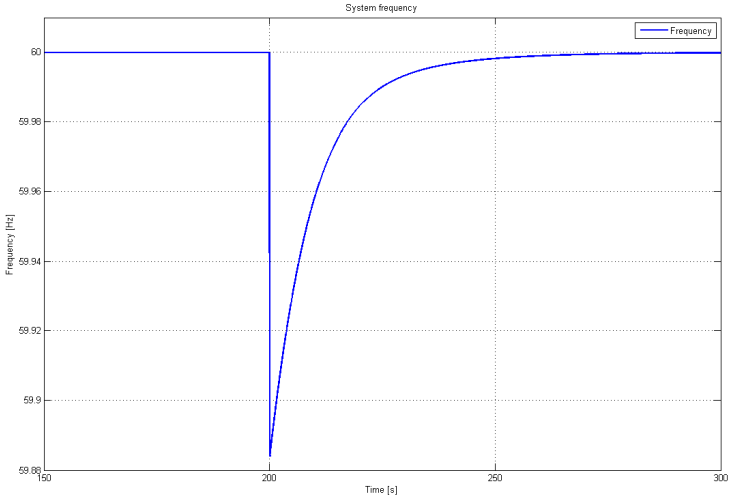

Figure 6.10: Frequency during WPP production stop with 13 wind turbines and peak loads.

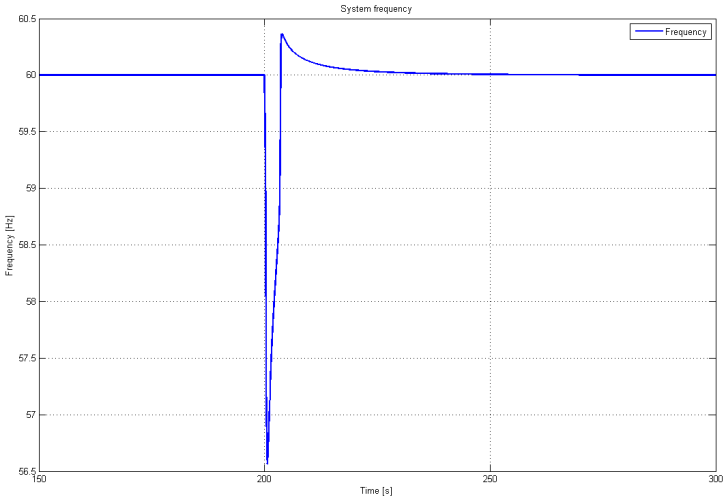

Figure 6.11: Frequency during WPP production stop with 52 wind turbines and peak loads.

The frequency will drop when the WPP stops producing. The drop will increase with an increase in wind turbines. The largest drop is observed with 52 wind turbines where the frequency will decrease to slightly above 56.5 Hz. This frequency drop is within the transient limit (+/- 12.5 %) presented in Chapter 3, but beyond the steady state limit (+/- 5 %). The frequency drop for the two other cases (WPP1/WPP2) stays within the steady state limits. The frequency curve for case WPP2 with 26 wind turbines is illustrated in appendix D. The estimated inertia of all the induction machines and the wind turbines seem to give a realistic slowness to the frequency change.

Figure 6.12 and 6.13 illustrates the total active power in the DS and the contributions from shore (VSC) and the WPP with 13 and 52 wind turbines during peak load and stop in WPP production.

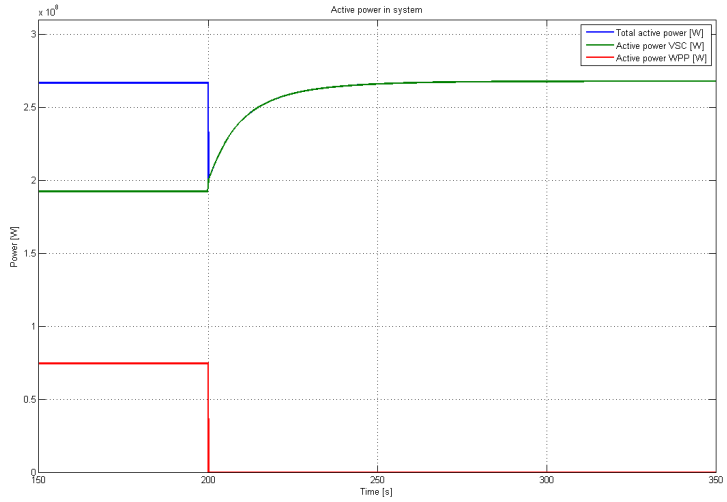

Figure 6.12: DS active power and active power delivered by WPP and VSC during WPP production stop with 52 wind turbines and peak loads.

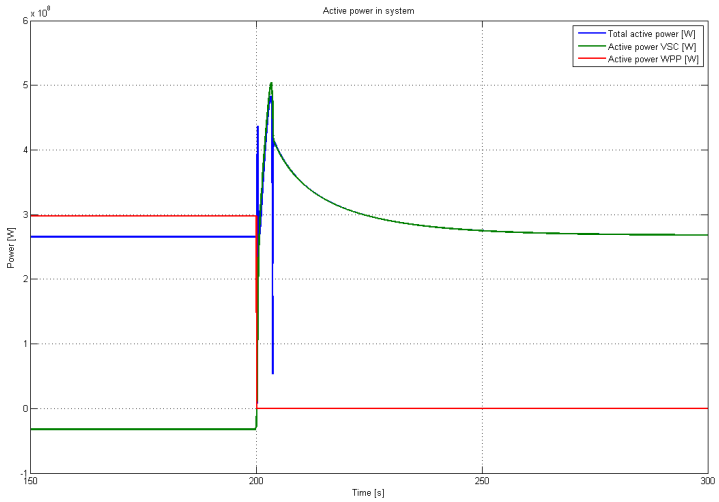

Figure 6.13: DS active power and active power delivered by WPP and VSC during WPP production stop with 52 wind turbines and peak loads.

As the WPP stop producing active power the VSC will start to take over. There will initially be a drop in the total amount of active power delivered before the VSC will be able to deliver all the required active power alone. The active power curve for case WPP2 with 26 wind turbines is illustrated in appendix D.

The curves for total apparent/active/reactive power, voltages and load currents are displayed in appendix D. The total apparent/active/reactive power and load current values will initially drop before increasing towards nominal values. The voltages will initially experience a peak in value before decreasing towards nominal value. The platform voltages for case WPP3 with 52 wind turbines can be observed to move outside of transient limits.

This case illustrates how the power from the onshore grid has to be ready to deliver the WPP capacity during a short time. In reality, the plant will not shut down instantanously, however rather ramp down the production.

Chapter 7

System Units Requirements

This chapter contains requirements for the different units in the system. The chapter aims to find accurate requirements based on specified demands, estimations introduced in Chapter 3 and 4, and simulation results presented in Chapter 5 and 6.

7.1 Transformers

In Chapter 3 the capacity for DST1 and DST2 was specified to be 175 MVA or 350 MVA in total. The capacity of the transformers are determined based on specifications in Chapter 3 and the simulation results in Chapter 5 and 6. The simulations indicate that the operating voltage level in the system will be approximately 118.9 kV phase to phase in order to ensure correct voltage levels at the platforms. The step up/down ratios of the system transformers are therefore required to be changed. The three-winding transformers should have a ratio equal to 132 / 120 kV for the primary to secondary winding. The transformer connected to the WPP will require a ratio equal to 33/120 kV.

7.1.1 VSC Transformers, DST1 and DST2

The capacity for DST1 and DST2 will be determined by the maximum power demand from shore. The estimated and simulated power demand of the whole system and the corresponding capacity requirements for the DS transformers for cases with only PFS are shown in Table 7.1. It should be noted that the estimations for maximum power demand are done without the transformer and motor losses, and therefore the simulations should be considered more accurate.

Table 7.1: DS transformers capacity requirements for only VSC cases.

	Estimated maximum power demand [MVA]	Simulated maximum power demand [MVA]	DST1/DST2 rating [MVA]	Step down voltage [kV]
Case 1	306	327	175	132/120
Case 2	181.5	186	100	132/120
Case 3	342.5	364	190	132/120

The specified capacity for the transformers will fit for case 1. In case 2 it could be considered to lower the capacity to 100 MVA for both transformers if the load conditions are considered applicable. Simulation results for case 3 shows that the capacity should be increased to 185 MVA for both transformers if Dagny, Edvard Grieg and Johan Sverdrup all operate with full load when the new discovery starts operating.

7.1.2 WPP Transformer, DST3

The capacity for DST3 will be equal to the maxmimum power production of the WPP. It is assumed that the WPP will only deliver active power. The apparent power of the DST3 will be equal to the active power delivered. It is also assumed that the capacity determined for DST1 and DST2 for case 1 will be applicable for the cases with a WPP. The estimated and simulated power production and the corresponding capacity requirements for the DS transformers for the WPP cases are shown in Table 7.2. The estimations of power production are done without the wind turbine internal losses, and therefore the simulations should be considered more accurate.

Table 7.2: DS transformers capacity requirements for WPP cases.

	Estimated maximum apparent power production [MVA]	Simulated maximum apparent power production [MVA]	DST3 capacity [MVA]	DST1/DST2 capacity [MVA]
WPP1	78	74.5	75	175
WPP2	156	149	150	175
WPP3	312	297	300	175

7.2 HVAC Transmission Cables

The transmission cables capacity are determined based on estimations of load currents introduced in Chapter 3, and simulations of voltages and load currents introduced in Chapter 5.

Simulations shows the voltage applied to all the transmission cables connected to the busbar to be approximately 118.9 kV RMS phase to phase. Hence will a rated voltage of 120.0 kV RMS phase to phase

and a highest continuous voltage of 123.0 kV RMS phase to phase be sufficient for all the transmission cables.

The estimated and simulated load currents and the corresponding capacity requirements for the transmission cables for all cases are shown in Table 7.3.

Table 7.3: Transmission cable capacity requirements with peak load.

	Estimated current [A]	Simulated current [A]	Current rating [A]	Rated RMS voltage Ph-Ph [kV]	Highest continuous voltage Ph-Ph [kV]
Dagny	163	164	170	120	123
Edvard Grieg	408	409	410	120	123
Johan Sverdrup	980	983	990	120	123
New discovery	163	163	170	120	123

The current ratings are rounded up from simulated values to get even values. Requirements to current ratings for the different transmission cables shows the need for specially designed cables for each transmission distance.

7.2.1 Short Circuit Current

The transmission cables short circuit current minimum requirements are determined based on estimations presented in Chapter 4 and simulations presented in Chapter 5. The minimum short circuit current requirements with only PFS are based on simulation results showing sub-transient short circuit current. It is assumed that when ND is operational, the total power demand offshore have decreased below load conditions for case 1. Therefore will the occuring short circuit current in NDs transmission cable be based on the VSC delivering the same amount of power as in case 1. The offshore installations short circuit current contribution, introduced in Chapter 5, are presented in Table 7.4.

Table 7.4: Offshore installations contribution short circuit current.

	I_k - Short circuit RMS current contribution [kA]
Dagny	0.600
Edvard Grieg	1.450
Johan Sverdrup	3.650
New discovery	0.600
Total - without new discovery	5.700
Total - with new discovery	6.300

The minimum short circuit current requirements with only PFS are based on the offshore installations contribution and VSC contribution and are presented in Table 7.5.

Table 7.5: Transmission cable minimum short circuit current requirements with only PFS.

Case 1 / Case 3	I_k - VSC short circuit current contribution [kA]	I_k - Offshore installations short circuit current contribution [kA]	I_k - Total sub-transient short circuit current [kA]
Dagny	1.400	5.700	7.100
Edvard Grieg	1.530	5.700	7.230
Johan Sverdrup	1.550	5.700	7.250
Dagny	1.400	6.300	7.700
Edvard Grieg	1.530	6.300	7.830
Johan Sverdrup	1.550	6.300	7.850
New discovery	1.480	6.300	7.780

The short circuit current requirements with the WPP are based on estimations for the occuring short circuit current in the DS. The sum of the short circuit current will be the contributions from shore (VSC), offshore installations and the WPP. Transmission cables short circuit current requirements for the WPP cases are presented in Table 7.6.

Table 7.6: Transmission cable minimum short circuit current requirements with WPP and without new discovery.

	I_k - Short circuit current contribution VSC and offshore installations [kA]	I - Current WPP [kA]	I_k - Sub-transient short circuit current WPP [kA]	I_k - Sub-transient short circuit current DS [kA]
WPP1	5.700	0.409	4.050	10.160
WPP2	5.700	0.819	8.090	14.610
WPP3	5.700	1.638	16.150	23.500

The short circuit currents occuring with a WPP and PFS are larger then with only PFS. This is expected and shows that the transmission cables will need to be designed to withstand higher short circuit currents with a WPP connected to the system.

7.3 Circuit Breakers

Based on the short circuit currents presented in Chapter 7.2 it is possible to estimate the capacity of the circuit breakers needed in the distribution system.

7.3.1 Power from Shore

The circuit breakers at the start of the HVAC transmission cables must be able to interrupt fault currents with the same magnitude as when the short circuit occured at Johan Sverdrup. The circuit breakers for DST1 and DST2 will have to interrupt different currents due to the voltage level on the primary and secondary side. If one of the transformers is offline its assumed the other operates at full load. The VSC is in this case assumed to restrict the short circuit current to the maximum load current of the distribution platform transformer. The fault current at the end of the transmission cables are lower than at the distribution platform due to the impedance of the transmission cables.

Table 7.7: Minimum circuit breaker capacity with only VSC as power source

	Current rating [kA]	Voltage level [kV]
DST1 and DST2 primary side	6.600	132
DST1 and DST2 secondary side	7.250	120
Transmission cable DP/JS	7.250	120
Transmission cable end at Dagny	7.100	120
Transmission cable end at Edvard Grieg	7.230	120

All the circuit breaker ratings should be set to minimum 7.250 kA.

7.3.2 Power from Shore and Wind Power Plant

With the WPP the short circuit current magnitude will be much higher immediately after the short circuit compared to only using PFS. The contribution from the WPP will quickly drop, since the voltage level in the system falls to near zero compared to the nominal voltage. This is shown for the induction motors which have the same behaviour in Chapter 5.5. When the voltage level falls the magnetic field in the stators of the wind turbines will break down and the electric power production will stop. To determine the capacity of the circuit breakers in the system with both the WPP and VSC, fault simulations should be carried out in a more appropriate software then the Simulink model presented in Chapter 3 and 4.

An interruption current level for the circuit breakers directly connected to the bus-bar has been estimated in Table 7.8. The circuit breakers are the ones before the HVAC transmission cables to Dagny and Edvard Grieg, the circuit breakers on the secondary side of DST1, DST2 and DST3, and the circuit breaker of Johan Sverdrup. Its assumed that both the WPP and the VSC supply current to the short circuit. The interruption current has been estimated by using the short circuit currents of the WPP from Chapter 3 and the load currents of the VSC from the simulation in Chapter 6.1. It is assumed the circuit breakers only have to withstand the sub-transient short circuit current, and interrupt the transient short circuit current.

Table 7.8: Estimated circuit breaker interruption currents with VSC and WPP as power sources

	I_k - Withstand current [kA]	I_k - Interruption Current [kA]
WPP1	11.760	11.090
WPP2	16.210	14.870
WPP3	25.100	22.400

It should be considered to to use a Is limiter in the system, the Is limiter will break current contribution within 1 ms. The current limiter would only allow the WPP maximum design current to pass into the DS. This would prevent the high short circuit current contributions from the WPP and decrease the requirements for the DS components in regard to short circuit currents. By introducing a current limiter to the WPP branch the circuit breaker interruption requirements will be the same as with only PFS.

7.4 Wind Power Plant

From the simulation in Chapter 6.3 it is clear that the WPP must have a planned shut down when the wind speed is around 25 m/s. This is important if the WPP has a large capacity compared to the total load of the system. The WPP should also produce its own reactive power to make sure the VSC has the capacity to supply reactive power to the offshore installations. These represent a load with a power factor of 0.85 during normal operation, but the reactive power consumed could increase during start-up of motors or if there are irregularities in the operation as showed in Chapter 5.2 and 5.3. The power output of the WPP should be controllable to match the load of the offshore installations.

Chapter 8

Discussion

This chapter contains a discussion of the Simulink model presented in Chapter 3 and 4, and the results which was obtained.

8.1 Simulink Model

The parameters for the induction machines, transformers and transmission cables are estimates. Since the offshore components are specially designed for their purpose in a real case. There is limited space on offshore installations and a high demand for avalibilty of power. Hence the components offshore are often smaller and more robust than equivalent components for onshore installations. A high robustness is necessary for achieving the extreme reliability and availability required to fulfill Norwegian regulations for offshore installations. Based on that standard stock components will not be used for this purpose, which makes it difficult to find datasheets for the components to use as examples in the model. As a result the parameters for the induction machine and transformes are based on examples from a textbook[14] and can be regarded as reasonably accurate estimations. The transmission cable parameters are from a datasheet from Nexans and can also be regarded as representative.

8.1.1 Steady State Analysis

The calculation of the currents in the system is not dynamic which means that the differential equation for the voltage across an inductor has not been used. For steady state simulation this is sufficient since the currents and voltages do not change. The purpose of the steady state simulation is to estimate load currents, power consumption of the loads and voltage levels in the different parts of the system.

8.1.2 Short Circuit Contribution VSC

A short circuit impedance of 0.01 ohms in parallel with the loads was used to simulate the short circuit. In all the cases it only represents a small fraction of the original impedance of the system. For the short circuit

cases at the end of the high-voltage AC (HVAC) transmission cable to offshore installations at Dagny, Edvard Grieg and New Discovery, this assumption would not affect the result since the transmission impedance is in the range of 5-10 ohms which limits the short circuit current. With a short circuit at Johan Sverdrup the contribution from the VSC was simulated to be 1.55 kA. In reality the short circuit impedance could lower than the simulation impedance. The result would then have been a short circuit current close to the upper limit of the VSC, which was estimated to 1.6 kA. The difference between these two values is only 0.05 kA. When the contribution from the offshore installations are added to the total short circuit current, the deviation between the simulated contribution and the upper limit contribution from the VSC does not account for much.

8.1.3 Wind Power Plant

The simulated wind speed is not based on actual measurements, but upon rough estimates, to emulate a more stable power output with a higher number of turbines in the wind power plant. Ideally one should use wind data measurement for the area and build a wind speed simulation model upon, however, wind speed measurements was not avalible. The wind power plant itself was simplified since the wind power plant is not the main problem. The model was sufficient to show how the power output changes with wind conditions and the number of turbines.

8.2 Offshore Installation Transformers

The simulations have been conducted with fixed step transformers for the offshore installations. The voltage drop in the transmission cables to the the platforms will depend on the current, so the voltage drop will change when the load conditions change. The voltage drop of the different transmission cables will also vary due to different distances from the distribution platform. All system transformers should therefore be designed with various steps in order to ensure correct operating voltage at the platforms.

8.3 Component Requirements

The medium case shows that the transformers would experience low loads from 2037. If the load in 2037 is lower than estimated it should be possible to continously run only one of the three-winding transformers and keeping the other as a standby power supply.

The short circuit rating for the transmission cables is very low compared to the 71 kA given in the datasheet from Nexans. It would therefor be safe to assume that Nexans can deliver the subsea cables needed for the transmission. Since the maximum short circuit current is relatively low compared to the example withstand rating, the cables would not be near the limit of thermal damage during a fault. It is important to note this, since the transmission cables are assumed to not be redundant.

8.4 Integration of a Wind Power Plant

8.4.1 Power Reserve

On a very cold winter day when the consumption of power is at the highest in Norway there is produced 2200 MW more then consumed. In addition there is 1200 MW in reserve. The largest WPP plant option of 312 MW would require 9 % of the sum of surplus produced power and reserve power. Due to this it could be estimated that there should be enough power reserves in the Norwegian grid to balance a 312 MW wind power plant during normal power consumption. A wind power plant in the North sea will have a higher production during the winter months than in the summer months. It could be argued that integrating a WPP would mean that the offshore installations would demand less power from shore during the winter months, when Norway's power grid experiences large demands.

8.4.2 Wind Power Plant Capacity

A 312 MW WPP could supply the total peak load of the offshore installations alone during full production. After 2031 the estimated power consumption of the offshore installations decreases, and it would be possible to regularly supply the onshore grid with power. This is probably also possible between 2023 to 2031 since 306 MW is only a peak load.

The smaller capacity wind power plants of 78 MW and 156 MW would be a supplement to the power from shore, however from 2037 a 156 MW WPP would be the main power supply.

A small capacity wind power plant as the 78 MW case could be installed to test floating wind turbine technologies and collect data of production during the winter months.

The largest WPP requires a transformer with a capacity of 300 MVA. This could be considered to be split into two transformers with a capacity of 150 MVA. This can be done in order to achieve redundancy in the supply of power from the WPP, which would be the main power supply.

8.4.3 Voltage and Frequency Fluctuations

The simulations have been conducted without any means of dampening the voltage and frequency fluctuations. Although the voltage levels are within cyclic variations limit, it should considered to implement capacitor banks or some kind of energy storage devices in the system to stabilize the fluctuations. Since the wind speeds and wind fluctuations are only based upon rough data the fluctuations may be larger and more aggressive. The energy storage devices can either be placed on the distribution platform or at the offshore installations.

8.4.4 Short Circuit Current

The short circuit current contribution from the wind power plant should be limited to avoid modifications to components. It is therefore suggested to implement a current limiter (Is-limiter) in series with the wind

power plant. The current limiter could be placed before the transformer (DST3) dedicated to the wind power plant. This should be done in order to protect the transformer and as the voltage level (33 kV RMS phase to phase) is more favorable for the current limiter. If the current limiter interrupts a short circuit it will need to be refurbished. It would therefore be advisable to have spare parts offshore as reserve to decrease the down time for the wind power plant.

Chapter 9

Conclusion

This thesis work investigates the electrical system requirements for a power distribution platform at the Utsira formation. The power distribution platform will work as a hub for distributing power between shore and the offshore installations planned around the Utsira formation. The electrical system on the distribution platform will be importent in order to efficiently distribute the power. The main aspects of the investigation are the componenets required and their specifications, system topology and the modifications required to the electrical system to integrate offshore wind power.

9.1 Conclusion

The thesis research questions, presented in Chapter 1, are solved through chapter 2-7. Results presented in Chapter 7 were discussed in Chapter 8. The following is concluded for the research questions.

RQ1 Components: What component types are needed for the distribution system?

Based on research of previous work on the electrification of Offshore installations and electrical system functionality the following components are needed:

Two voltage source converters (VSC) will receive the power from shore through HVDC cables and invert the voltage to AC. Two three-winding transformers are needed to step down the output voltage of the VSCs and supply the utility system of the distribution platform. HVAC sub-sea transmission cables will be required to supply the offshore installations Dagny, Edvard Grieg and a potential new discovery. In addition circuit breakers will be needed at each end of the transmission cables and on the secondary side of the three-winding transformers.

There will also be required to integrate a power management system (PMS). The PMS will balance the input power from the onshore grid and consumed power by the offshore installations. In order for the system to communicate between shore, the distribution platform and the offshore installations fiber cable should be laid together with the HVAC transmission cables.

RQ2 Requirements: What are the requirements for the components in the distribution system with regard to various load conditions?

A Simulink model of the distribution system was established for simulations of the steady state system currents and voltages for peak load condition, medium load condition, and balanced three phase short circuits in different parts of the distribution system. Based on the simulations the following estimated rating requirements have been found for the components:

The two three-winding transformers at the distribution platform would need a rating of 175 MVA and a primary to secondary ratio of 132 / 120 kV, and 132 / 11 kV for the primary to third ratio. The nominal phase to phase voltage across the components within the distribution system is 120 kV.

The circuit breakers at the distribution platform must have a rating of atleast 7.250 kA.

The rating of transmission cables to Dagny, Edvard Grieg and Johan Sverdrup has been estimated to 170, 410 and 990 A.

The general requirements for the components are based on Norwegian regulations from the Petroleum Safety Authority.

RQ3 System: How can the distribution system be realized based on RQ1 and RQ2?

The distribution system with only power from shore (PFS) can be realized as shown in the single line diagram presented in Appendix C. This single line diagram shows the suggested topology of the distribution system. The suggested topology for the utility system required on the distribution platform is also presented in Appendix C.

The system currents and voltages from the simulations are regarded as good estimates for the future realization of the distribution system with only power from shore. Future steady state analysis of the distribution system should look to their values presented in this thesis in order to verify if their results are within reasonable range.

RQ4 Offshore Wind Power: What adaptions to the distribution system are needed to integrate offshore wind power?

An estimation of the short circuit current contribution from the wind power plant was conducted. A wind power plant was also included in the Simulink model to test the modified distribution system for different WPP capacaties.

With a wind power plant the system components must be able to withstand a higher short circuit current and the circuit breaker ratings should be modified. To avoid this, a current limiter (Is-limiter) could be introduced, which will prohibit the short circuit current contribution from the WPP. Further a new transformer will be required within the distribution system, and the capacity must be equal to the maximum capacity of the WPP. It will also be required to introduce a new incomer in the distribution system for the WPP. The new circuit breaker should have equal ratings to the other circuit breakers placed in the distribution system.

If the floating wind turbine technology evolves, a WPP together with power from shore should be capable to supply offshore installations with power. The fast response and versatile control of the voltage source converter makes it well suitable for balancing the power of the wind power plant. The balancing would also require a maximum power reserve equal to the WPP capacity in the onshore grid.

The offshore installations at Utsira formation is planned to start production in 2016 and will be operational to 2060. These installation could either be run with gas driven turbines located on the platforms or be supplied with power from onshore. Global warming and the world's demand for gas may call for measures to supply future offshore installations with power from shore. This thesis has shown that there are

few technological restraints for the electrification of the Utsira formation with power from shore.

9.2 Recommendations

It is recommended that the design of each component is based on the selected maximum transferable power rating to gain robustness and avoid overheating in the system components.

It is also recommended to further investigate the possibility of integrating a wind power plant to the system. With a robust design for the electrical system, and by implementing solutions to decrease fluctuations in the power production, a wind power plant offshore will make a great contribution to the overall electrical system. It will be important to check the availability and reserves in the onshore grid to determine if the onshore grid is robust enough for this application.

9.3 Further Work

The following further work is recommended in order to finalize a design for the electrical system on the distribution platform.

- Perform transient simulations for different load conditions.
- Investigate harmonics in the system.
- Planning of selectivity for protection system.

It is suggested to conduct the following further work in The following tasks are recommended in order to finalize a design for the electrical system with a integrated wind power plant.

- Evaluate suitable wind turbines.
- Study power production and short circuit currents.
- Perform transient simulations for load cases.

The following tasks are recommended for finalizing the entire power from shore system.

- Investigation and design of onshore facilities and converter station.
- Investigation and design of HVDC transmission part of the system.
- Further investigation and design of HVAC transmission part of system.

Bibliography

[1] ABB Library, ”On the Short Circuit Current Contribution of HVDC Light ”, Y. Jiang-Häfner, M. Hyttinen, and B. Pääjärvi

[2] Siemens overview pdf, ”Offshore wind power projects”, *http://www.energy.siemens.com/hq/en/power-generation/renewables/wind-power/references.htm*, 2011, Siemens AG

[3] Book, ”Offshore Wind Power”, 2009, John Twidell and Gaetano Gaudiosi, Multi-Science Publishing Co. Ltd

[4] Ebook, ”Vindkart for Norge, Kartbok 4a: Produksjon i 80m høyde, fullasttimer”, 2009, Kjeller Vindteknikk, *http://www.vindteknikk.no/norges-vindressurser-kartlagt*

[5] Technical Article, “HVDC pluss – Basics and principle operation”, M. Davies, M. Dommaschk, J. Dorn, J. Lang, D. Retzmann, D. Soerangr, 2011, Siemens AG

[6] IEEE, “Modeling the Trans Bay Cable Project as Voltage-Sourced Converter with Modular Multilevel Converter Design”, 2011, Simon P. Teeuwsen

[7] Norwegian regulations PDF, ”GUIDELINES REGARDING THE FACILITIES REGULATIONS”, 2012, Petroleum Safety Authority

[8] Fact Sheet, “Hywind by Statoil, The floating wind turbine”, 2012, Statoil

[9] News Article, ”Hywind sliter med nettproblemer”, *http://www.tu.no/energi/2012/08/16/hywind-sliter-med-nettproblemer*

[10] Catalogue, ”Three-phase Induction Motors, H-compact, H-compact PLUS”, 2009, Catalog D 84.1, Siemens AG

[11] Impact study, “Plan for utbygging, anlegg og drift av Dagny og Eirin”, 2012, Unitech

[12] Standard PDF, “IEC 61892-1”, 2010, International Electrotechnical Commission

[13] Book, ”Energiproduksjon og energidistribusjon produksjon, nettsystemer og beregninger”, 2002, Steinar Svarte og Jan H. Sebergsen, Gyldendal Norsk Forlag

[14] Book, ”Electrical Machines, Drives and Power Systems”, 2006, Sixth Edition, Theodore Wildi, Pearson Prentice Hall

[15] Report, ”Analyser av offshore modellsimuleringer av vind”, 2009, Øyvind Byrkjedal, Reidar Kravik, Kjeller Vindteknikk

[16] Catalog, “Funksjonskrav i kraftsystemet 2012”, 2012, Statnett

[17] Article, “Short Circuit Behavior of Wind Turbine Generators, Reigh A. Walling, Michael L. Reichard, GE Energy

[18] Impact study, “Plan for utbygging og drift av Ivar Aasen”, 2012, Det Norske, Statoil, Bayern Gas Norge.

[19] Standard PDF, “NORSOK STANDARD Electrical systems E-001”, 2007, 5. edition, The Norwegian Oil Industry Association, Standards Norway

[20] Standard PDF, “IEC 62271-100”, 2012, 2.1. edition, International Electrotechnical Commission

[21] Catalogue, “Is - limiter - The world fastest limiting and switching device”, 2012, ABB

[22] Info page, *http://www.nve.no/no/Havvind/Havvind-forslag-til-utredningsomraader/Utsira-nord/*, NVE

[23] Impact study,”Plan for utbygging, anlegg og drift av Luno”, 2011, Lundin

[24] Press-release, *http://www.detnor.no/no/nyheter/nyhetsarkiv/1180-ivar-aasen-plattform-skal-bygges-av-smoe*, Det Norske

[25] Report, ”Elektrifiseringsvurderinger for midtre nordsjø”, 2012, add Novatech as, UNITECH Power Systems

[26] Report, ”Norway Power Project Study report ULA/GYDA/VALHALL/EKOFISK 2/4J Topside & J-tube Modification”, 2002, HALLIBURTON KBR

[27] Report, ”Statnett offshore node study”, 2011, Aker Engineering & Technology AS

[28] Book, ”Windkraftanlagen im Netzbetrieb”, 1993, Siegfried Heier, B. G. Teubner Stuttgart

[29] Report, ”Norsk effektbalanse, maksimallast vinter 2012-2013”, 2012, Statnett

Appendix A - Simulink Model

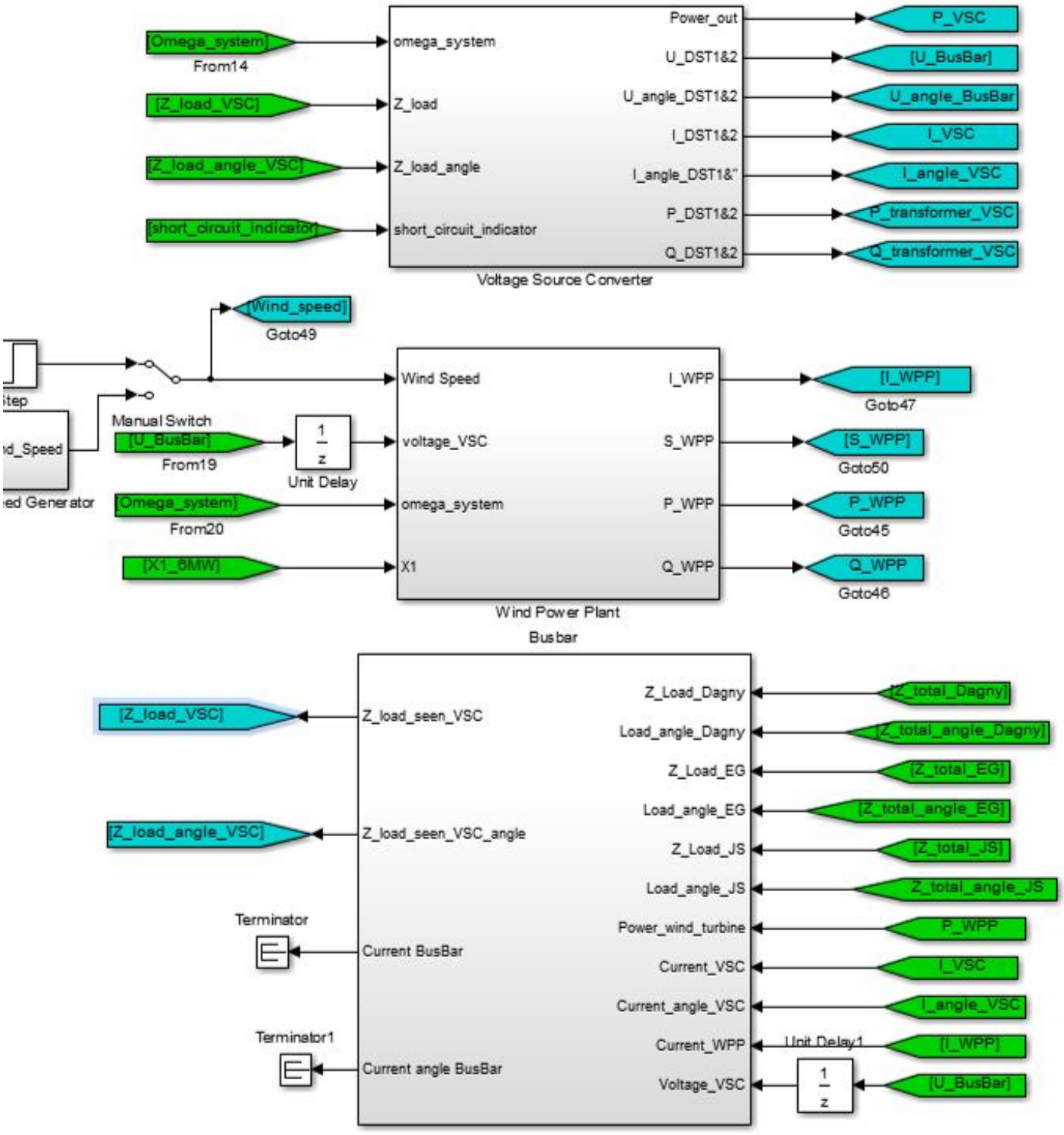

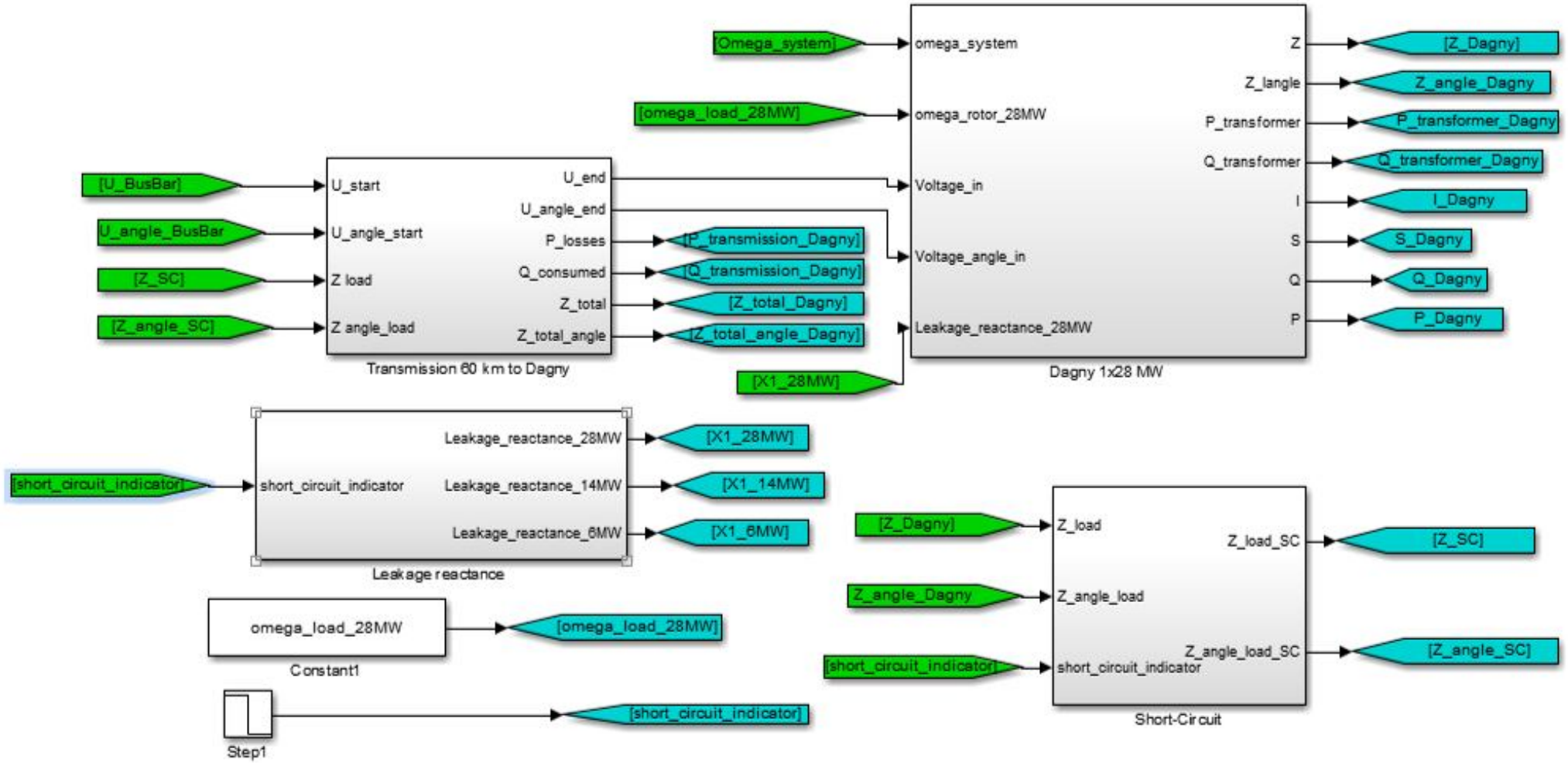

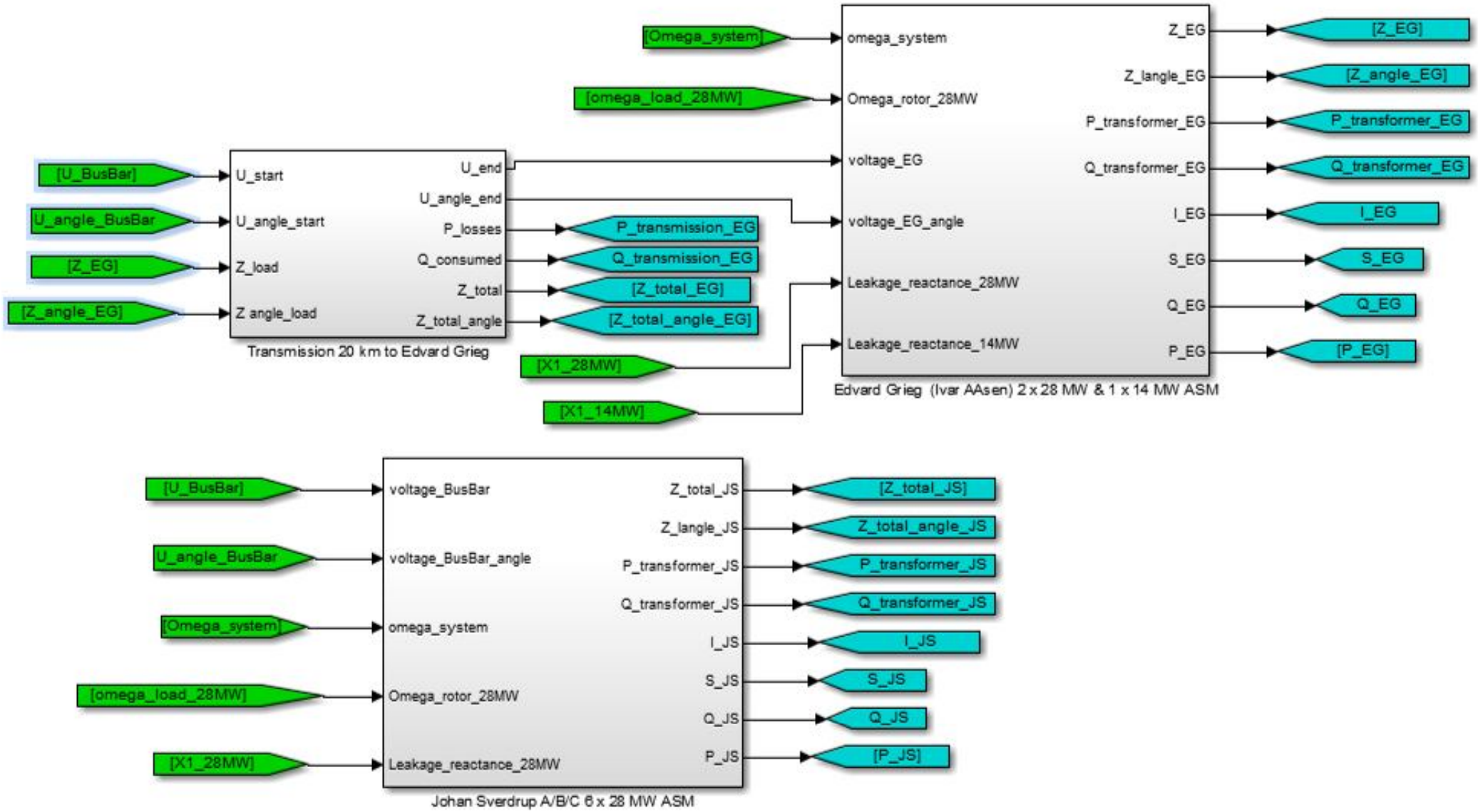

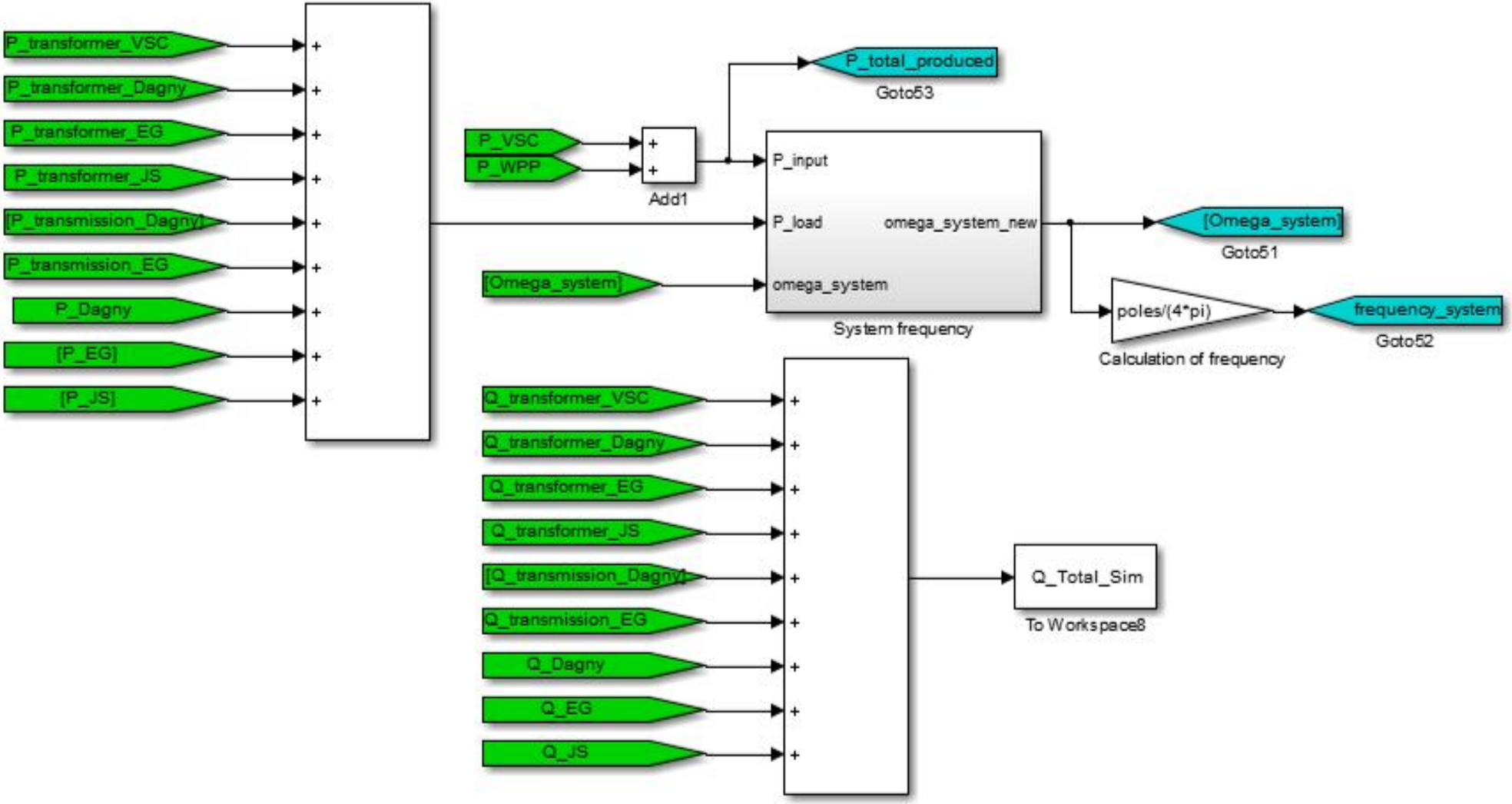

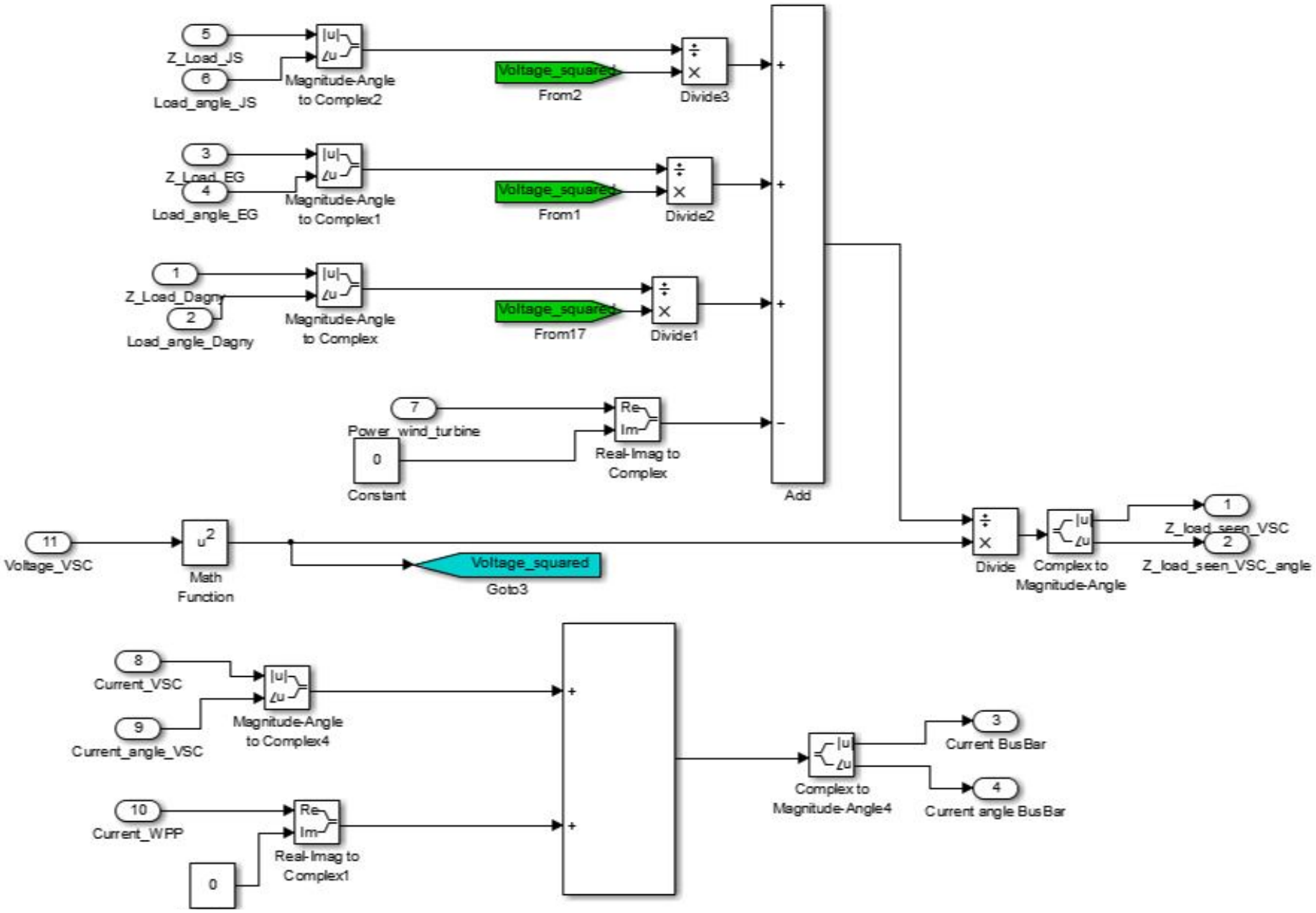

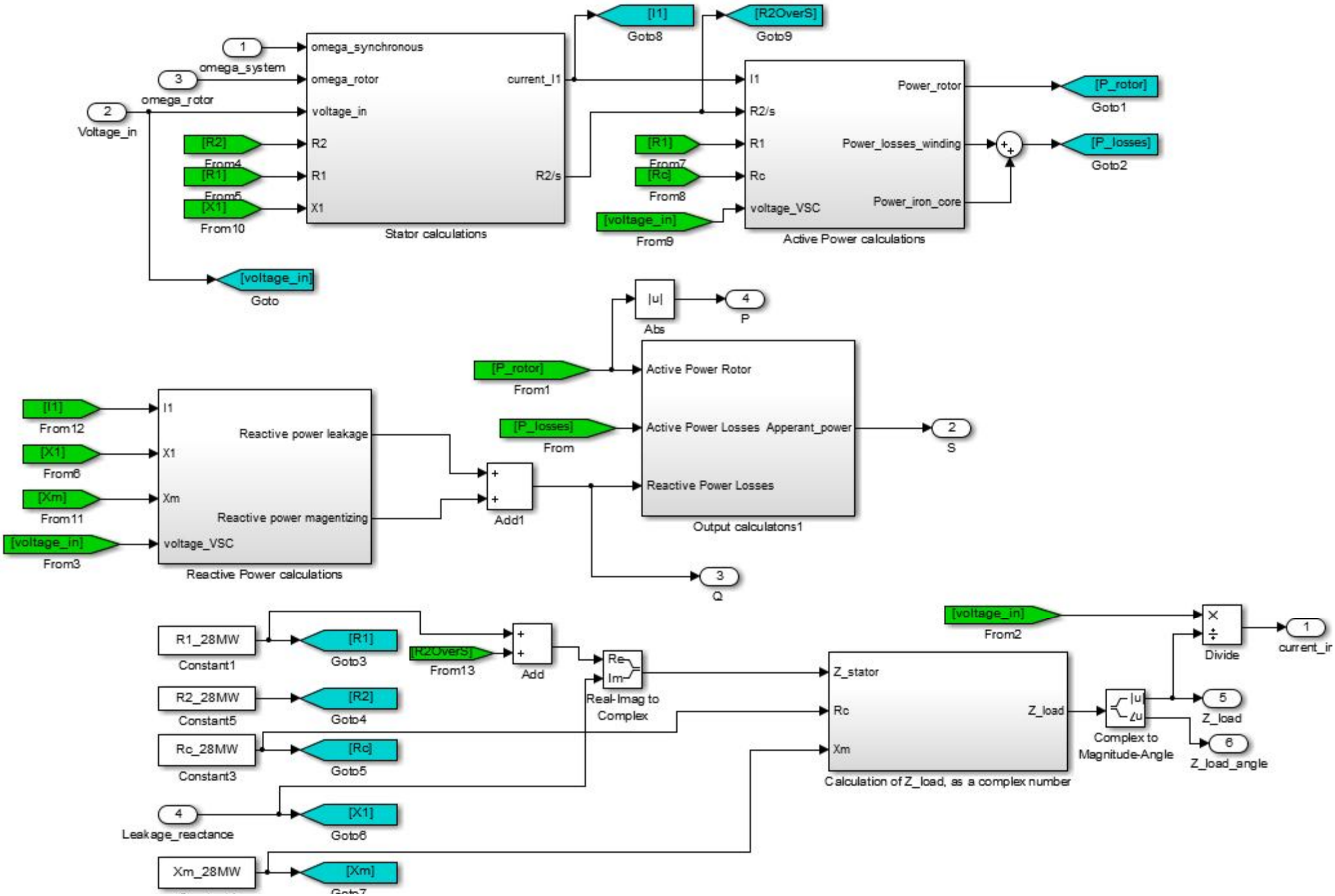

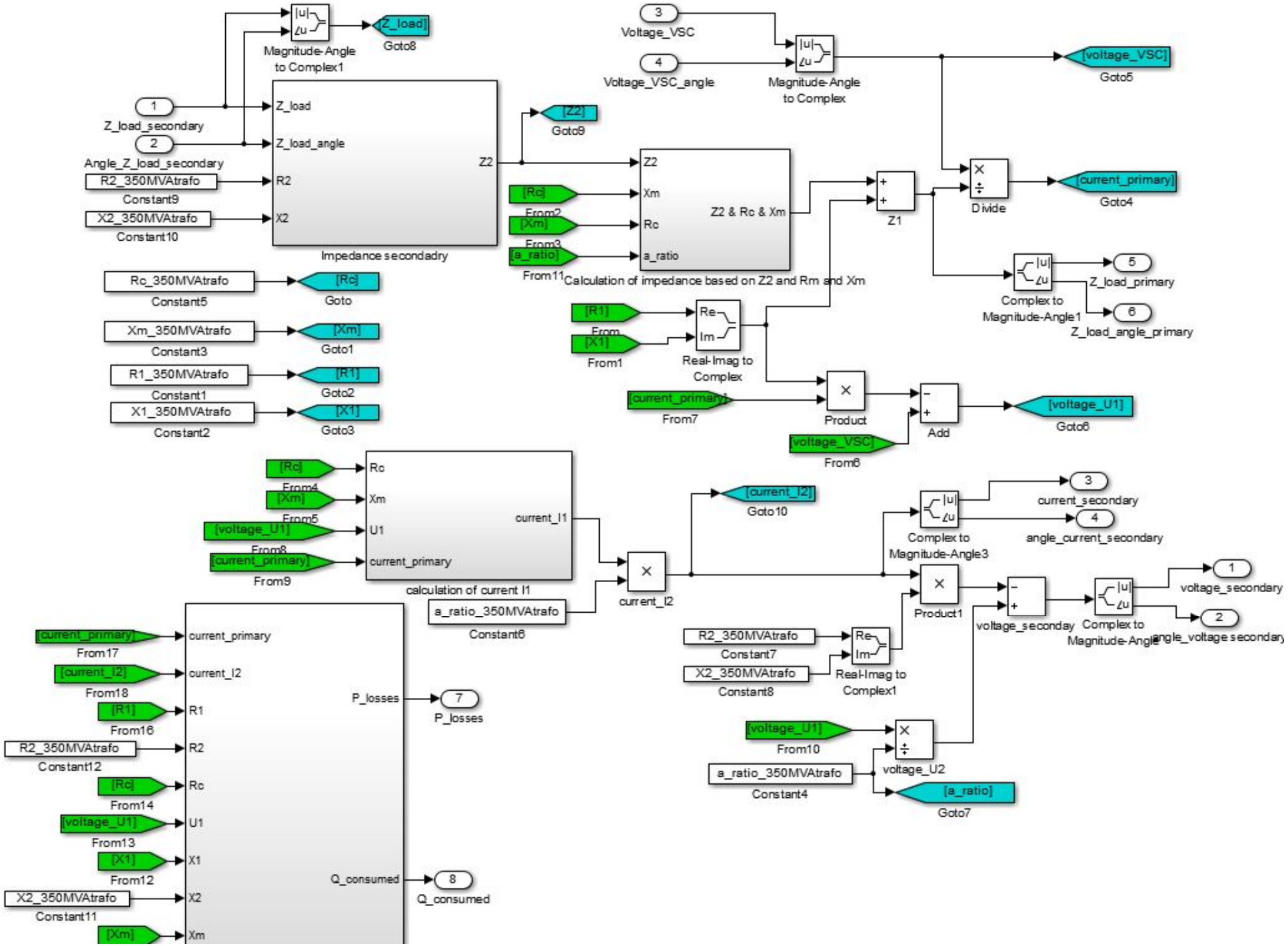

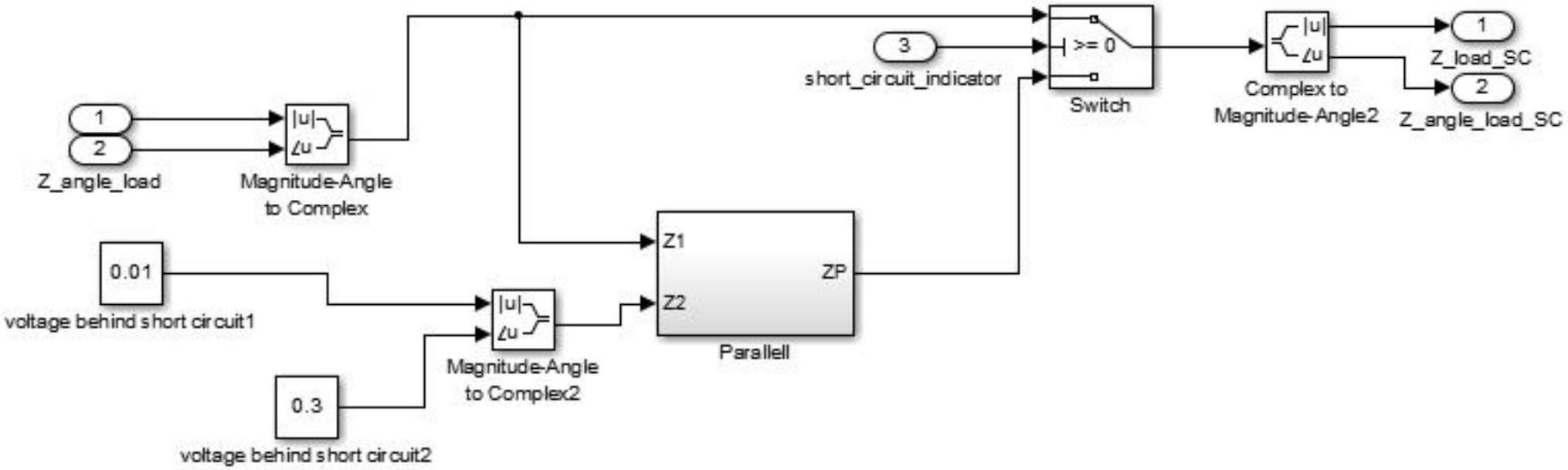

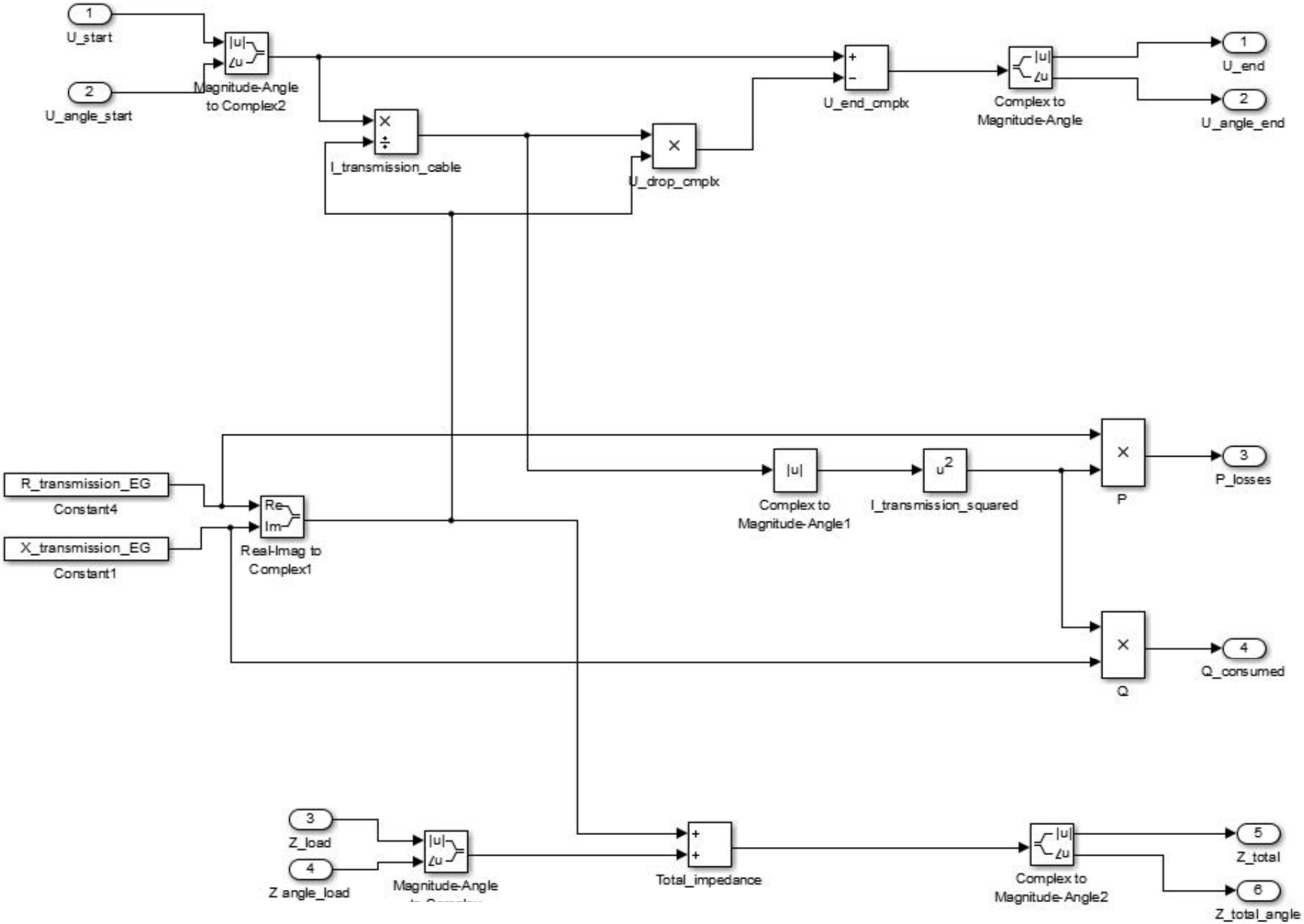

```
% Asynchron Motor 28 MW

% Nominal data
P_nominal_28MW = 28*10^6 / 3;        % Power consumption nominal load, 1 phase
U_nominal_28MW = 11000 / sqrt(3);     % Voltage over 1 phase at nominal load
cos_phi_nominal_28MW = 0.90;          % Cos phi at nominal load
I_nominal_28MW = P_nominal_28MW / (U_nominal_28MW * cos_phi_nominal_28MW); % Current↙
1 phase at nominal load
efficiency_28MW = 0.975;  % efficiency for motor at nominal load

% En røver formel for inertian, se Inertia_sheet
% formula for inertia derived from siemens motor catalogue
inertia_motor_28MW = 0.006584775*(P_nominal_28MW/1000)^1.23;

% Calculation of internal reactances and resistances
P_loss_nominal_28MW = P_nominal_28MW * ( 1 - efficiency_28MW);
Q_nominal_28MW = P_nominal_28MW*sin(acos(cos_phi_nominal_28MW))/cos_phi_nominal_28MW;

factor_Rc_28MW = 0.759;   % percentage of power loss due to iron losses
factor_Xm_28MW = 0.558;   % percentage of reactive power du to magentizing

Rc_28MW = (U_nominal_28MW)^2 / (factor_Rc_28MW * P_loss_nominal_28MW); % Core loss↙
resistance
Xm_28MW = (U_nominal_28MW)^2 / (factor_Xm_28MW * Q_nominal_28MW);  % Magnetizing↙
resistance

% Calculation of the current I_R2 ( see figure: Async_machine_drawing)
% This current is used to calculate X1, R1 and R2
I_R2_Re = I_nominal_28MW * cos_phi_nominal_28MW - U_nominal_28MW / Rc_28MW;
I_R2_Img = I_nominal_28MW * sin (acos ( cos_phi_nominal_28MW)) - U_nominal_28MW /↙
Xm_28MW;
I_R2_nominal_ASG = sqrt(I_R2_Re^2 + I_R2_Img^2);

% Stator Leakage reactance
X1_28MW = (1 - factor_Xm_28MW) * Q_nominal_28MW / (I_R2_nominal_ASG^2);

% Rotor and Stator winding resistance
R1_28MW = (1 - factor_Rc_28MW) * P_loss_nominal_28MW / (I_R2_nominal_ASG^2);
R2_28MW = R1_28MW;

% calculation of rotating speed at nominal load
P_rotor_28MW = P_nominal_28MW - P_loss_nominal_28MW;
poles_28MW = 6;
frequency_28MW = 60;
slip_nominal_28MW = (I_R2_nominal_ASG^2 * R2_28MW) / P_rotor_28MW;
omega_load_28MW = (4*pi*frequency_28MW/poles_28MW)*(1-slip_nominal_28MW);
```

```
% Asynchron Motor 14 MW

% Nominal data
P_nominal_14MW = 14*10^6 / 3;        % Power consumption nominal load, 1 phase
U_nominal_14MW = 11000 / sqrt(3);     % Voltage over 1 phase at nominal load
cos_phi_nominal_14MW = 0.89;          % Cos phi at nominal load
I_nominal_14MW = P_nominal_14MW / (U_nominal_14MW * cos_phi_nominal_14MW); % Current↙
1 phase at nominal load
efficiency_14MW = 0.965;  % efficiency for motor at nominal load

% En røver formel for inertian, se Inertia_sheet
% formula for inertia derived from siemens motor catalogue
inertia_motor_14MW = 0.006584775*(P_nominal_14MW/1000)^1.23;

% Calculation of internal reactances and resistances
P_loss_nominal_14MW = P_nominal_14MW * ( 1 - efficiency_14MW);
Q_nominal_14MW = P_nominal_14MW*sin(acos(cos_phi_nominal_14MW))/cos_phi_nominal_14MW;

factor_Rc_14MW = 0.759;   % percentage of power loss due to iron losses
factor_Xm_14MW = 0.558;   % percentage of reactive power du to magentizing

Rc_14MW = (U_nominal_14MW)^2 / (factor_Rc_14MW * P_loss_nominal_14MW); % Core loss↙
resistance
Xm_14MW = (U_nominal_14MW)^2 / (factor_Xm_14MW * Q_nominal_14MW);  % Magnetizing↙
resistance

% Calculation of the current I_R2 ( see figure: Async_machine_drawing)
% This current is used to calculate X1, R1 and R2
I_R2_Re = I_nominal_14MW * cos_phi_nominal_14MW - U_nominal_14MW / Rc_14MW;
I_R2_Img = I_nominal_14MW * sin (acos ( cos_phi_nominal_14MW)) - U_nominal_14MW /↙
Xm_14MW;
I_R2_nominal_ASG = sqrt(I_R2_Re^2 + I_R2_Img^2);

% Stator Leakage reactance
X1_14MW = (1 - factor_Xm_14MW) * Q_nominal_14MW / (I_R2_nominal_ASG^2);

% Rotor and Stator winding resistance
R1_14MW = (1 - factor_Rc_14MW) * P_loss_nominal_14MW / (I_R2_nominal_ASG^2);
R2_14MW = R1_14MW;

% calculation of rotating speed at nominal load
P_rotor_14MW = P_nominal_14MW - P_loss_nominal_14MW;
poles_14MW = 6;
frequency_14MW = 60;
slip_nominal_14MW = (I_R2_nominal_ASG^2 * R2_14MW) / P_rotor_14MW;
omega_load_14MW = (4*pi*frequency_14MW/poles_14MW)*(1-slip_nominal_14MW);
```

```
% Asynchron Gen 6MW

% Nominal data
P_nominal_ASG = 6*10^6 / 3;        % Power consumption nominal load, 1 phase
U_nominal_ASG = 6900 / sqrt(3);     % Voltage over 1 phase at nominal load
cos_phi_nominal_ASG = 0.90;          % Cos phi at nominal load
I_nominal = P_nominal_ASG / (U_nominal_ASG * cos_phi_nominal_ASG); % Current 1 phase↙
at nominal load
efficiency_ASG = 0.96;  % efficiency for motor at nominal load

% En røver formel for inertian, se Inertia_sheet
% formula for inertia derived from siemens motor catalogue
inertia_ASG = 0.006584775*(P_nominal_ASG/1000)^1.23;

% Calculation of internal reactances and resistances
P_loss_nominal_ASG = P_nominal_ASG * ( 1 - efficiency_ASG);
Q_nominal_ASG = P_nominal_ASG*sin(acos(cos_phi_nominal_ASG))/cos_phi_nominal_ASG;

factor_Rc_ASG = 0.759;   % percentage of power loss due to iron losses
factor_Xm_ASG = 0.558;   % percentage of reactive power du to magentizing

Rc_ASG = (U_nominal_ASG)^2 / (factor_Rc_ASG * P_loss_nominal_ASG); % Core loss↙
resistance
Xm_ASG = (U_nominal_ASG)^2 / (factor_Xm_ASG * Q_nominal_ASG);  % Magnetizing↙
resistance

% Calculation of the current I_R2 ( see figure: Async_machine_drawing)
% This current is used to calculate X1, R1 and R2
I_R2_Re = I_nominal * cos_phi_nominal_ASG - U_nominal_ASG / Rc_ASG;
I_R2_Img = I_nominal * sin (acos ( cos_phi_nominal_ASG)) - U_nominal_ASG / Xm_ASG;
I_R2_nominal_ASG = sqrt(I_R2_Re^2 + I_R2_Img^2);

% Stator Leakage reactance
X1_ASG = (1 - factor_Xm_ASG) * Q_nominal_ASG / (I_R2_nominal_ASG^2);



% Rotor and Stator winding resistance
R1_ASG = (1 - factor_Rc_ASG) * P_loss_nominal_ASG / (I_R2_nominal_ASG^2);
R2_ASG = R1_ASG;

% calculation of rotating speed at nominal load
P_rotor_ASG = P_nominal_ASG - P_loss_nominal_ASG;
poles_ASG = 6;
frequency_ASG = 60;
slip_nominal_ASG = -(I_R2_nominal_ASG^2 * R2_ASG) / P_rotor_ASG;
```

```
U_primary_350MVAtrafo = 132000 / sqrt(3);
U_secondary_350MVAtrafo = 110000 / sqrt(3);

S_nominal = 350*10^6 / 3; % divid the apperant power by each phase

% Base impedance used to calculate resistances and reactances
% Calculated from primary side
Z_base = (U_primary_350MVAtrafo)^2 / S_nominal;

% ratio inside transformer
a_ratio_350MVAtrafo = U_primary_350MVAtrafo / U_secondary_350MVAtrafo;

% all resistances and reactances
% first number is PU value
R1_350MVAtrafo = 0.006 * Z_base;
R2_350MVAtrafo = R1_350MVAtrafo / a_ratio_350MVAtrafo^2;
X1_350MVAtrafo = 0.04 * Z_base;
X2_350MVAtrafo = X1_350MVAtrafo / a_ratio_350MVAtrafo^2;
Rc_350MVAtrafo = 500 * Z_base;
Xm_350MVAtrafo = 200 * Z_base;
```

```
U_secondary_190MVAtrafo = 11000 / sqrt(3);
U_primary_190MVAtrafo = 110000 / sqrt(3);

S_nominal = 190*10^6 / 3; % divid the apperant power by each phase

% Base impedance used to calculate resistances and reactances
% Calculated from primary side
Z_base = (U_primary_190MVAtrafo)^2 / S_nominal;

% ratio inside transformer
a_ratio_190MVAtrafo = U_primary_190MVAtrafo / U_secondary_190MVAtrafo;

% all resistances and reactances
% first number is PU value
R1_190MVAtrafo = 0.006 * Z_base;
R2_190MVAtrafo = R1_190MVAtrafo / a_ratio_190MVAtrafo^2;
X1_190MVAtrafo = 0.07 * Z_base;
X2_190MVAtrafo = X1_190MVAtrafo / a_ratio_190MVAtrafo^2;
Rc_190MVAtrafo = 500 * Z_base;
Xm_190MVAtrafo = 200 * Z_base;
```

```
U_secondary_75MVAtrafo = 11000 / sqrt(3);
U_primary_75MVAtrafo = 110000 / sqrt(3);

S_nominal = 75*10^6 / 3; % divid the apperant power by each phase

% Base impedance used to calculate resistances and reactances
% Calculated from primary side
Z_base = (U_primary_75MVAtrafo)^2 / S_nominal;

% ratio inside transformer
a_ratio_75MVAtrafo = U_primary_75MVAtrafo / U_secondary_75MVAtrafo;

% all resistances and reactances
% first number is PU value
R1_75MVAtrafo = 0.002 * Z_base;
R2_75MVAtrafo = R1_75MVAtrafo / a_ratio_75MVAtrafo^2;
X1_75MVAtrafo = 0.06 * Z_base;
X2_75MVAtrafo = X1_75MVAtrafo / a_ratio_75MVAtrafo^2;
Rc_75MVAtrafo = 150 * Z_base;
Xm_75MVAtrafo = 70 * Z_base;
```

```
U_secondary_30MVAtrafo = 11000 / sqrt(3);
U_primary_30MVAtrafo = 110000 / sqrt(3);

S_nominal = 30*10^6 / 3; % divid the apperant power by each phase

% Base impedance used to calculate resistances and reactances
% Calculated from primary side
Z_base = (U_primary_30MVAtrafo)^2 / S_nominal;

% ratio inside transformer
a_ratio_30MVAtrafo = U_primary_30MVAtrafo / U_secondary_30MVAtrafo;

% all resistances and reactances
% first number is PU value
R1_30MVAtrafo = 0.002 * Z_base;
R2_30MVAtrafo = R1_30MVAtrafo / a_ratio_30MVAtrafo^2;
X1_30MVAtrafo = 0.06 * Z_base;
X2_30MVAtrafo = X1_30MVAtrafo / a_ratio_30MVAtrafo^2;
Rc_30MVAtrafo = 150 * Z_base;
Xm_30MVAtrafo = 70 * Z_base;
```

```
Z_transmission = (0.073) + (1i*0.12); %per km

X_transmission_dag = imag(Z_transmission)*60;
R_transmission_dag = real(Z_transmission)*60;

X_transmission_EG = imag(Z_transmission)*20;
R_transmission_EG = real(Z_transmission)*20;

X_transmission_ND = imag(Z_transmission)*30;
R_transmission_ND = real(Z_transmission)*30;
```

```
% Wind turbine info

%power coefficients
C1 = 0.5;
C3 = 0.022;
C4 = 5.6;
rotor_radius = 70;      % Radius wind turbine

lambda_ideal = 7.5;     % ideal lambda of wind turbines
wind_speed_design = 9;  % Optimal production -+30 % of design wind speed
rho = 1.225;            % Air density

inertia_rotor = 400;
Power_WT_max = 6*10^6;

inertia_Wind_Turbines = number_of_turbines * inertia_rotor;
```

```
WindSpeed_Initial = 5;
WindSpeed_SampleTime = 13/number_of_turbines;

%increase in m/s over 100 seconds
WindSpeed_Change = 1 / 200; %
WindSpeed_Max = 7;
WindSpeed_Min = 5;

%time for start in increase
WindSpeed_Change_StartTime = 800;

P_wind_gen = 0.4;
I_wind_gen = 10;

WindSpeed_Variance = 10 / number_of_turbines;
```

Appendix B - Datasheets

Design data for TKRA 123 kV 3x1x500 mm² KQ

Conductor	Diameter of conductor Round stranded compressed copper conductor of 61 wires filled with a semiconducting compound	26.5 mm
Conductor screen	Extruded layer of semiconducting crosslinked polyethylene	
Insulation	Nominal thickness Diameter over insulation Extruded layer of insulating crosslinked polyethylene (XLPE)	15.0 mm 59.5 mm
Insulation screen	Extruded layer of semiconducting crosslinked polyethylene	
Longitudinal water-block	Semiconducting water-swellable tape	
Lead sheath	Nominal thickness The sheathing material is lead alloy	2.0 mm
Inner sheath	Nominal thickness Extruded sheath of semiconducting polyethylene	1.9 mm
Laying up	The cores are laid up. Polypropylene yarn fillers are located in the interstices between the cores.	
Binder tape	Two layers of binder tape	
Armour bedding	Polypropylene yarn and bitumen	
Armour	Shape of armour wires Dimension of armour wires Number of armour wires, approx. One layer of galvanized steel wires	Round 4.2 mm ⌀ 118
Outer serving	Two layers of polypropylene yarn and bitumen	
Diameter	Diameter of cable, approx.	177 mm
Weight	Total weight of cable, approx.	56 kg/m

Mechanical data for TKRA 123 kV 3x1x500 mm² KQ

Bending radius	Minimum permissible bending radius during laying: - spooling - coiling	 2.7 m 5.4 m
Pulling tension	Maximum permissible pulling tension	75 kN

Electrical data for TKRA 123 kV 3x1x500 mm² KQ

Current rating	Current rating in seabed	635 A
Conductor temperature	Max. permissible conductor temperature	90 °C
Ambient conditions	Max. ambient temperature for the cable in seabed at burial depth Max. burial depth Thermal resistivity of seabed Load factor	25 °C 1.0 m 1.0 K.m/W 100 %
Frequency	Frequency	50 Hz
Short circuit current	Permissible thermal short circuit current: - in the conductor for 1 second - in the lead sheaths for 1 second	 71 kA 3x10 kA
Rated voltage	Rated RMS system voltage (U) Rated RMS voltage between conductor and screen (U_o)	120 kV 64 kV
Highest voltage	Highest continuous RMS system voltage (U_m)	123 kV
Basic insulation level	Lightning impulse withstand voltage (1.2/50 µsec.)	550 kV
Electrical stress	Maximum electrical stress in insulation at 120 kV	6.7 kV/mm
Conductor resistance	Max. DC resistance at 20 °C AC resistance at 90 °C	0.0366 Ω/km 0.0493 Ω/km
Cable impedance	Cable impedance at 600 A	0.073 + j0.12 Ω/km
Capacitance	Capacitance between conductor and screen	0.20 µF/km
Charging current	Charging current at 120 kV	4.3 A/km
Loss angle	Maximum value at ambient temperature and rated voltage	0.001
Losses	Losses at 120 kV and 600 A: - conductor losses - dielectric losses - sheath losses - armour loss Total losses per cable	 3x17.8 W/m 3x0.3 W/m 3x2.2 W/m 19.0 W/m 79.9 W/m

GE
Marine

LM2500+ Marine Gas Turbine

GE's LM2500+ gas turbine is based on the industry standard-setting GE LM2500 marine gas turbine. Its main features are increased power (20%) compared to the LM2500, the same high availability and reliability, and an even higher efficiency (lower SFC) than the LM2500. As in the case of the LM2500, the LM2500+'s simple modular design with its split compressor casing, in-place blade and vane replacement, in-place hot section maintenance and external fuel nozzles provides for easy maintenance.

Comparing the Design of the LM2500+ to the LM2500

The primary difference between the two engines is the addition of one stage of compressor blades forward of the LM2500's first stage blading which results in approximately a 20% airflow increase at full power. This "zero" stage is a wide-chord, single-piece bladed disk or blisk. The LM2500+'s stage one blades have been redesigned without mid-span dampers. The LM2500+'s 19-stage compressor has an increased pressure ratio to 23.1:1 from 18:1 of the LM2500.

Aft of the LM2500+'s compressor is the fully annular combustor with externally mounted fuel nozzles; a two-stage air-cooled high pressure turbine which drives the compressor and the accessory drive gearbox; and a six-stage aerodynamically coupled, low pressure power turbine which is driven by the gas generator's high energy exhaust gas flow. The increase in power warranted several design changes in the existing LM2500 power turbine. The overall flow function was increased 11% to account for the higher airflow. Stage 1 and Stage 6 blades are optimized for aerodynamic efficiency to keep the power turbine at its previously high level of efficiency. The power turbine rotor has been strengthened for the higher torque and potential energy of the LM2500+.

Pre-wired, pre-piped and factory-tested for easy installation, the LM2500+ module weighs just 50,600 pounds (23,000 kg) with shock mounts and 48,090 pounds (21,859 kg) without. It requires only 338 x 108 x 120 cubic inches of ship space (28.2 x 9 x 10 feet) (7.16 x 2.74 x 3.05 m). The inlet duct flow area is 57 square feet (5.35 sq m) and the exhaust flow area is 36 square feet (3.3 sq m).

Performance

Output	40,500 shp (30,200 kW)
SFC	.354 lb/shp-hr
Heat rate	6,522 Btu/shp-hr
	8,746 Btu/kWs-hr
	9,227 kJ/kWs-hr
Exhaust gas flow	189 lb/sec (85.9 kg/sec)
Exhaust gas temperature	965°F (518°C)
Power turbine speed	3600 rpm

Average performance, 60 Hz, 59°F, sea level, 60% relative humidity, no inlet/exhaust losses

Max Power vs. Ambient Temperature

(losses: inlet/exhaust 4/6 inches water)

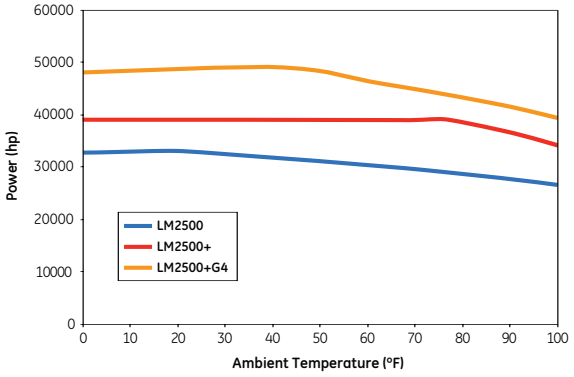

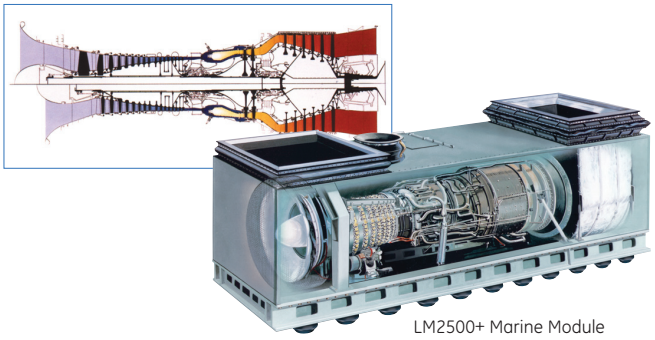

LM2500+ Marine Module

LM2500+ Marine Gas Turbine

LM2500+ Marine Gas Turbine - Genset

The LM2500+ marine gas turbine can be coupled with an electric generator making an LM2500+ marine gas turbine-generator set. The LM2500+ gensets are ideal for military applications for which electric drive is the propulsion system of choice. The Japanese Asuka is already using the similar LM2500 in an electric drive propulsion system. More than 17 cruise ships are in service or under construction that use GE's LM2500 and LM2500+ gas turbine gensets as the total propulsion and on-board energy system. GE furnishes the complete LM2500+ gas turbine-generator set using a generator from a generator manufacturer acceptable to the customer.

Dimensions*

Base plate width		123 in (3.12 m)
Base plate length		566 in (14.38 m)
Enclosure height		157 in (3.99 m)
Base plate weight		208,000 lbs (94,545 kg)
Duct flow areas	Inlet	57 sq ft (5.3 sq. m)
	Exhaust	36 sq ft (3.3 sq. m)

Performance*

Output	29,000 kW
Heat rate	8,856 Btu/kW-hr
Thermal efficiency	38%

Average performance, 60 Hz, 59°F, sea level, 60% relative humidity, 4 in. water inlet loss, 6 in. water exhaust loss

Specific Qualifications

The LM2500+ gas turbine propulsion system (turbine, base and enclosure and lube oil storage and conditioning assembly) is undergoing evaluation and acceptance testing for the U.S. Navy. It will be tested for shock, vibration, EMI and electrical bonding plus airborne and structure-borne noise to meet U.S. requirements for surface combatant vessels. The first military application of the LM2500+ will be on the Navy's LHD 8 assault ship. Each LM2500+ production unit is tested by GE and is available for customer witness. The LM2500+ marine gas turbine has been granted type approval by ABS, DNV and RINA.

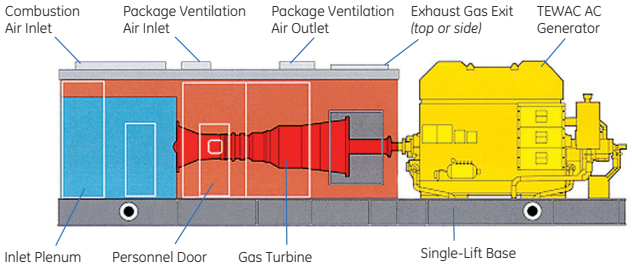

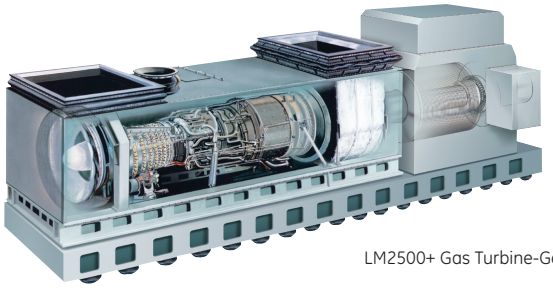

LM2500+ Gas Turbine-Generator Set

Contact us at www.ge.com/marine

*Exact dimensions, weight and performance vary with the specific generator selected. Other product sheets are available on the LM500, LM1600, LM2500, LM2500+G4 and LM6000.

AE-28203G (08/06)

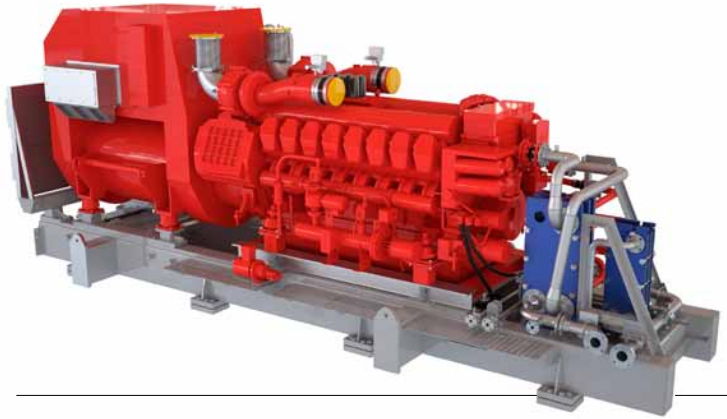

Available options

- Start system to NFPA 20, electric or pneumatic with optional hydraulic black start
- Diesel fuel oil system for 12, 18 or 24 hours
- Combustion air and exhaust gas systems – several options including water-cooled exhaust
- HVAC – can also be delivered for pressurization in zone 2 areas
- Anti-surge device with air release and vacuum breaker valve with optional minimum flow and/or test facilities
- Local control panels, PLC based with communication to fire and gas system
- Electrical distribution panel with optional isolation cabinet for installation in hazardous areas
- Fire and gas detection within container
- Fire extinguishing systems
- AFFF system including tanks, pumps and control systems, with power supply from fire pump engine

Framo Electric Fire Water Pumps

TECHNICAL DATA

PERFORMANCE DOMAIN

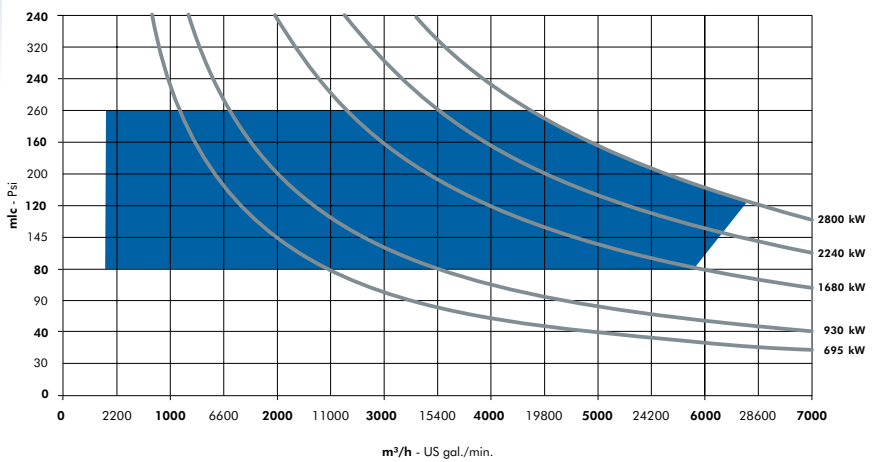

DIESEL ELECTRIC FWP

DIESEL ENGINE RATING	695 kW	930 kW	1680 kW	2240 kW	2800 kW
Skid dimensions (LxWxH) [m]	5,0 x 2,2 x 3,2	5,4 x 2,2 x 3,2	5,6 x 2,2 x 3,2	6,2 x 2,2 x 3,2	7,4 x 2,2 x 3,2
Skid weight (Dry ex. fuel tank) [kg]	10300	11900	1740	19000	27200
Module dimensions (LxWxH) [m]	7,0 x 4,2 x 4,0	7,3 x 4,2 x 4,0	7,6 x 4,5 x 4,0	8,1 x 4,5 x 4,0	9,8 x 4,8 x 4,2
Module weight (Dry) [kg]	33100	35400	47100	51300	67000

SUBMERGED LIFT PUMP

PUMP TYPE	SE225	SE280	SE315	SE355	SE400	SE450
Required caisson diameter*	26"	30"	34"	40"	50"	54"
Pipestack diameter min/max	10"/14"	10"/18"	14"/18"	18"/24"	20"/32"	24"/32"
Max. power (50 Hz/60 Hz) [kW]	400/400	800/1000	1000/1200	2100/2500	2200/2800	2900/3600
Voltage (min/max) [kV]	0,40/0,69	0,40/4.16	0,40/6,6	0,40/11,0	3,3/11,0	3,3/11,0
Weight pump/motor unit [kg]	1500	2100	5400	6400	7400	10200
Weight per 6m pipestack [kg] (min dia./max dia.)	394/500	394/591	500/591	591/792	740/1150	792/1150
Weight top-bend and top plate [kg] (min dia/max dia)	350/360	490/511	365/601	701/845	755/960	995/1070

*) Include space for anti-fouling hose

Appendix C - Electrical Drawings

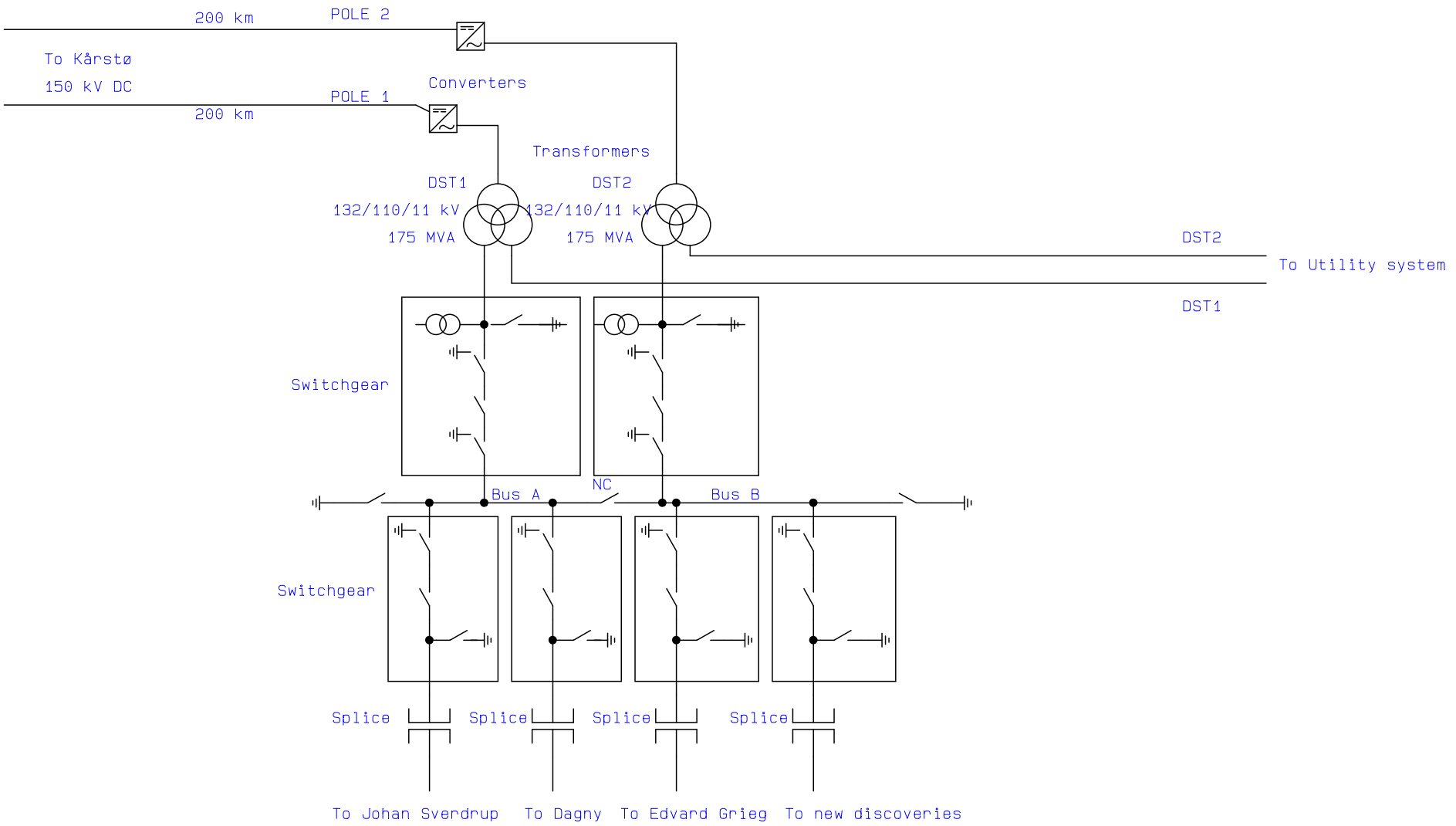

PC|SCHEMATIC Automation

Project title: Distribution system		**Project no.:**	**Project rev.:**	**Page** 1
Customer:		DCC:		Scale: 1:2
Page title:		Drawing no.:	Page rev.:	Previous page:
Filename: Distribution system		Constructor (project/page)	Last printed: 01.05.2013	Next page:
Page ref.:		Appr. (date/sign.)	Last correction: 01.05.2013	Number of pages: 1

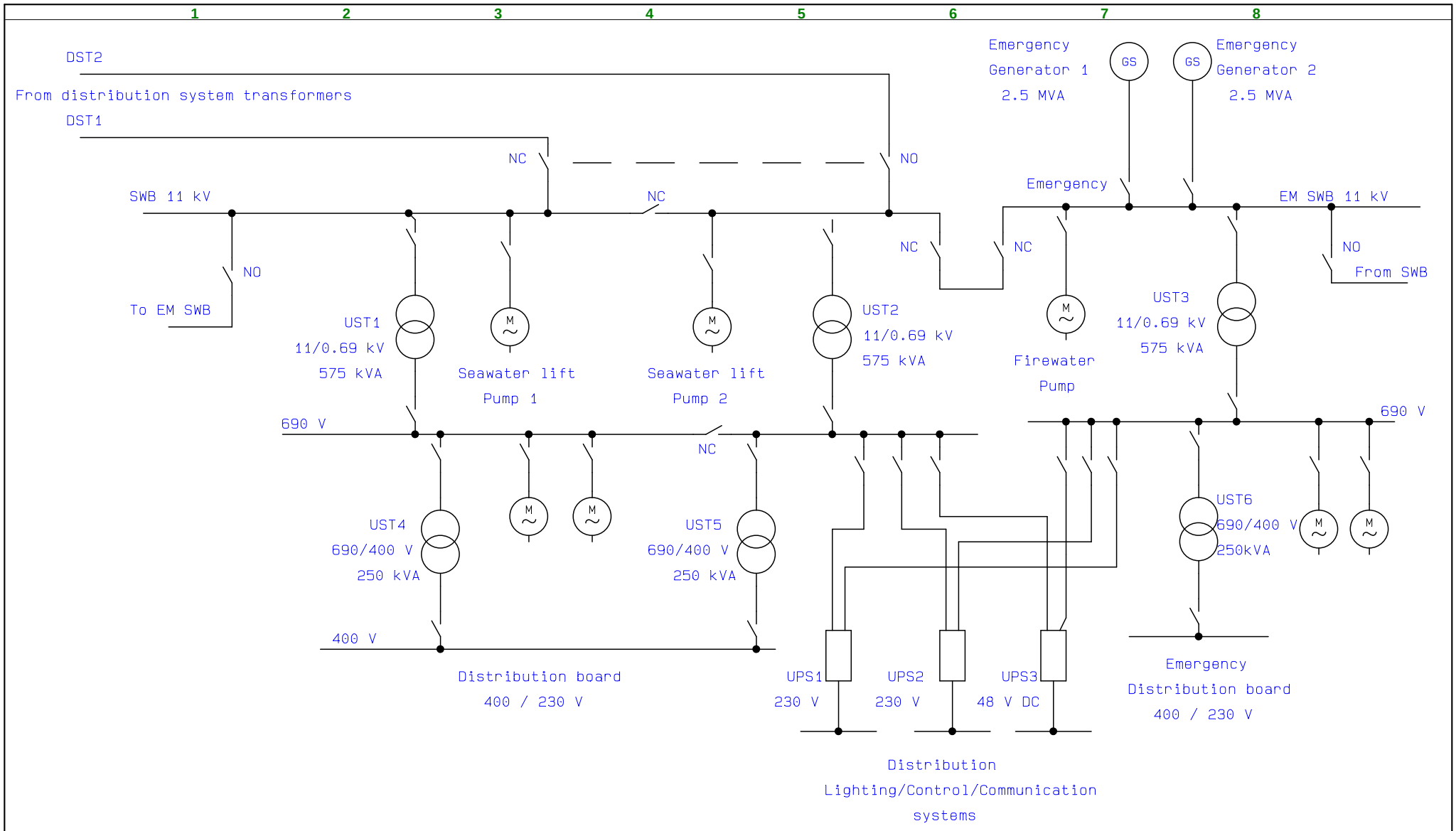

PC|SCHEMATIC Automation

Project title:		**Project no.:**	**Project rev.:**	**Page** 1
Customer:		DCC:		Scale: 1:2
Page title:	Utility Circuit	Drawing no.:	Page rev.:	Previous page:
Filename:	Utility system_new2	Constructor (project/page)	Last printed: 21.05.2013	Next page:
Page ref.:		Appr. (date/sign.)	Last correction: 21.05.2013	Number of pages: 1

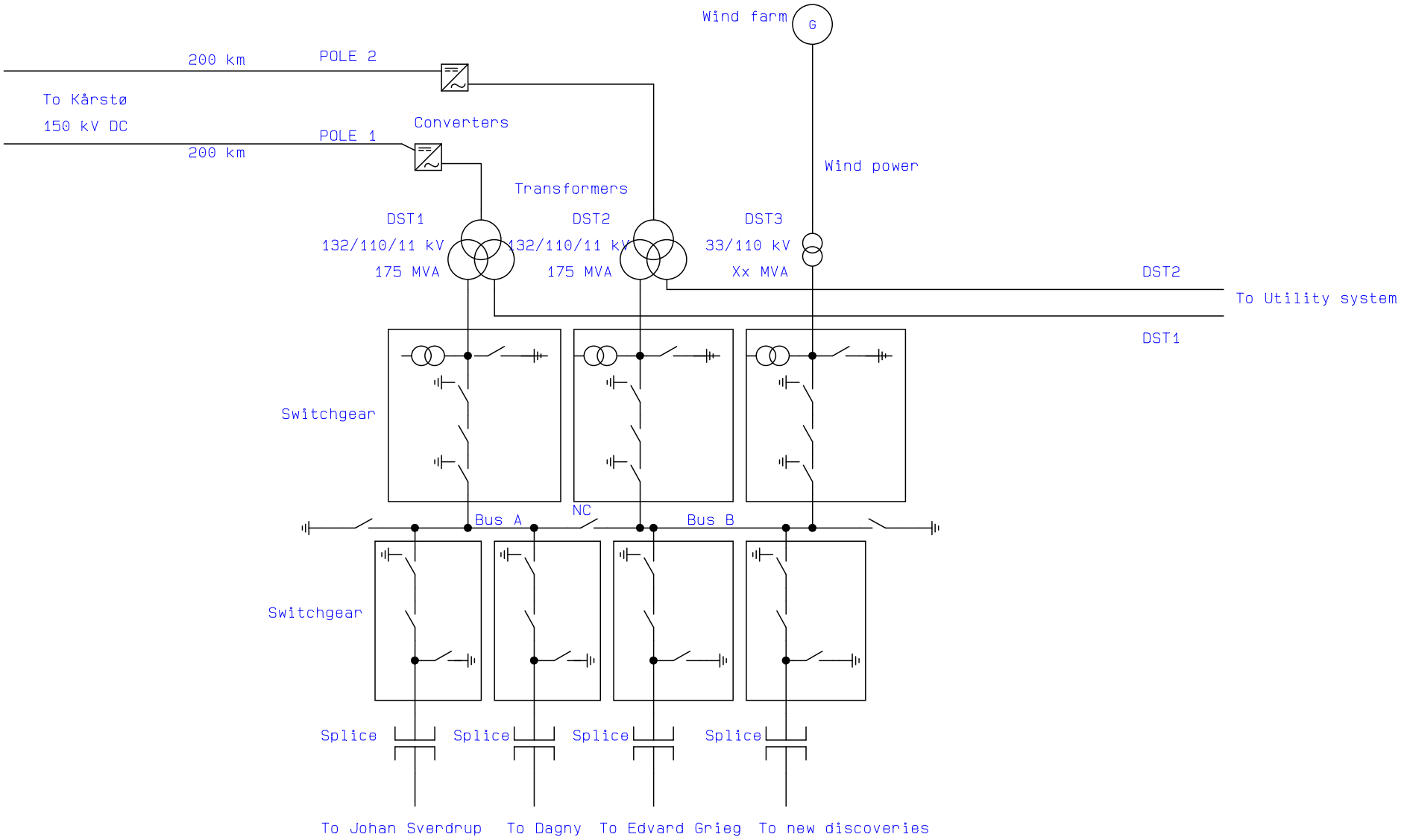

PC|SCHEMATIC Automation

Project title: Distribution system		**Project no.:**	**Project rev.:**	**Page** 1
Customer:		DCC:		Scale: 1:2
Page title:		Drawing no.:	Page rev.:	Previous page:
Filename:	Distribution system with wind power1	Constructor (project/page)	Last printed: 01.05.2013	Next page:
Page ref.:		Appr. (date/sign.)	Last correction: 01.05.2013	Number of pages: 1

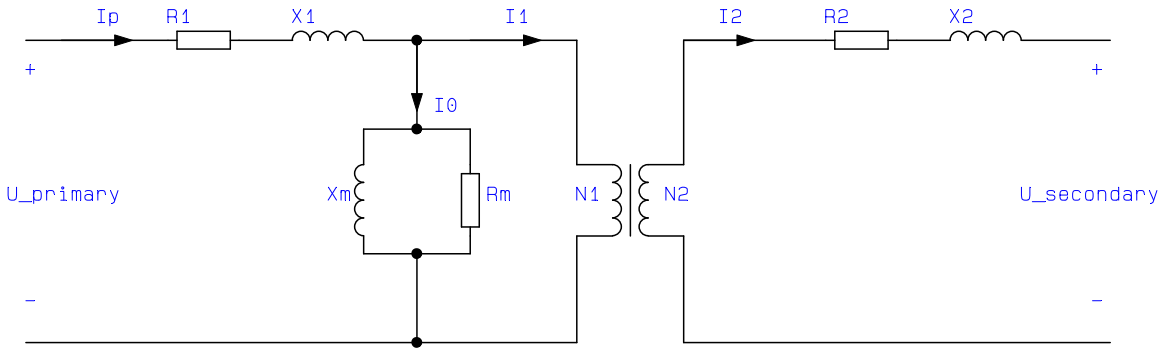

PC|SCHEMATIC Automation

Project title: Transformer		**Project no.:**	**Project rev.:**	**Page** 1
Customer:		DCC:		Scale: 1:1
Page title:		Drawing no.:	Page rev.:	Previous page:
Filename: Transformer		Constructor (project/page)	Last printed: 30.04.2013	Next page:
Page ref.:		Appr. (date/sign.)	Last correction: 30.04.2013	Number of pages: 1

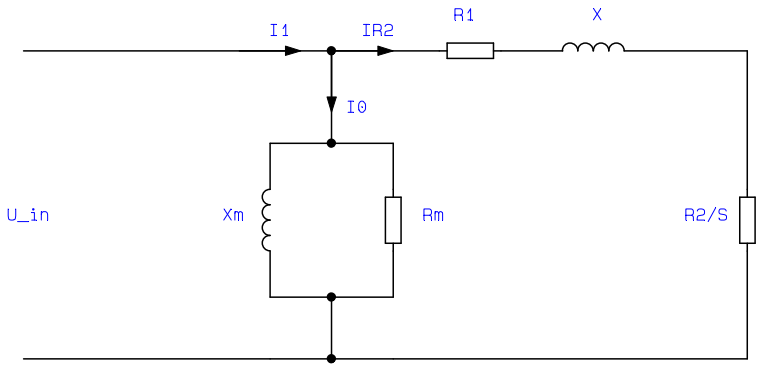

PC|SCHEMATIC Automation

	Project title: Asynchronous Motor/Generator	**Project title: Asynchronous Motor/Generator**	**Project rev.:**	**Page** 1
	Customer:	DCC:		Scale: 1:1
	Page title:	Drawing no.:	Page rev.:	Previous page:
	Filename: Asynchronous	Constructor (project/page)	Last printed: 30.04.2013	Next page:
	Page ref.:	Appr. (date/sign.)	Last correction: 30.04.2013	Number of pages: 1

Appendix D - Simulation Results

Steady State with Wind Power Park Simulation curves

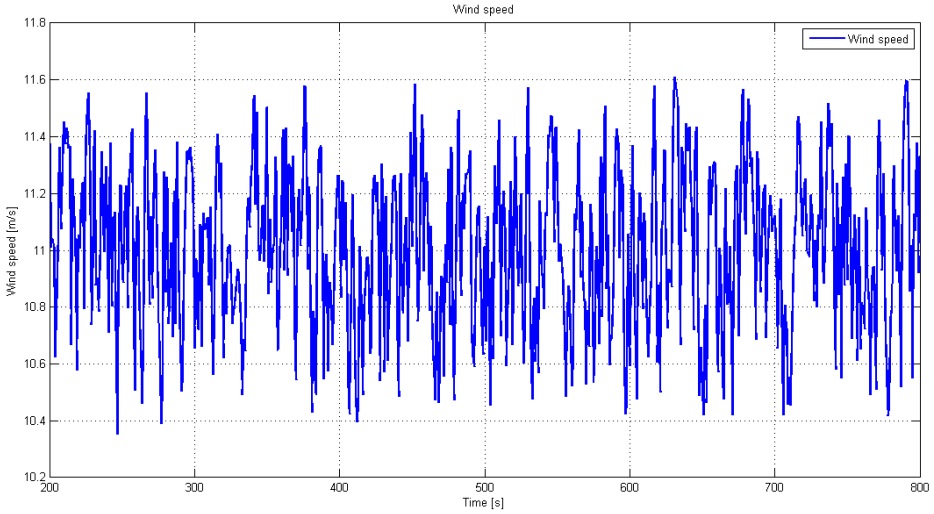

Figure 9.1: Wind speed variation with 13 wind turbines

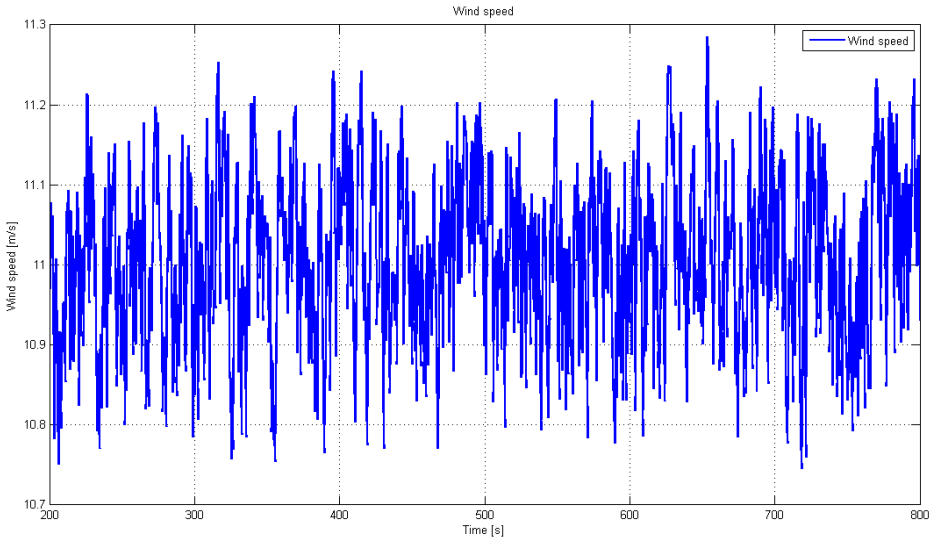

Figure 9.2: Wind speed variation with 26 wind turbines

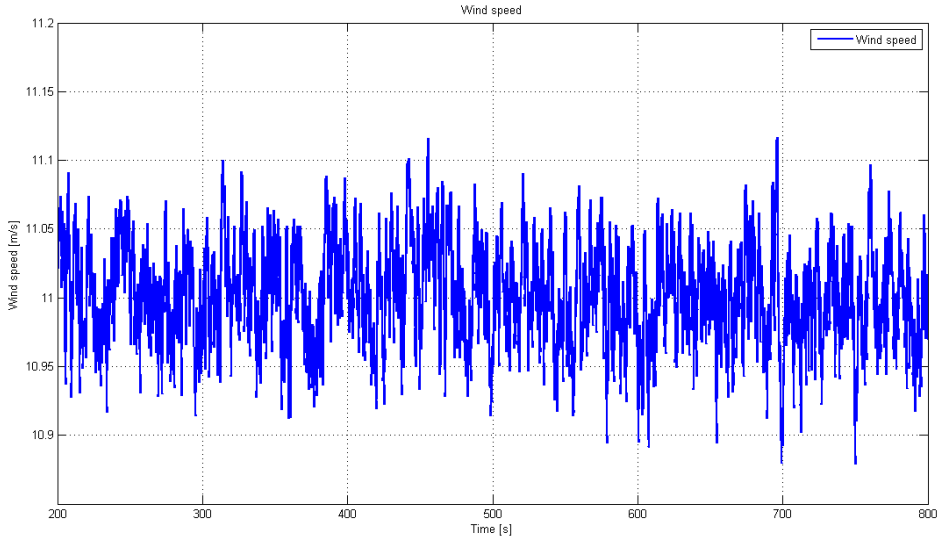

Figure 9.3: Wind speed variation with 52 wind turbines

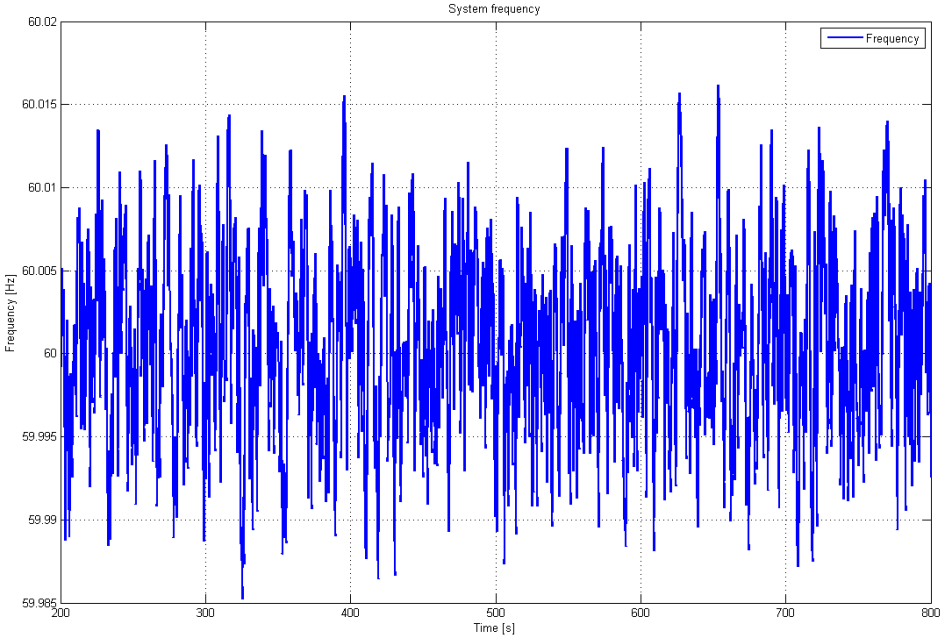

Figure 9.4: Frequency during steady state with 26 wind turbines and peak loads

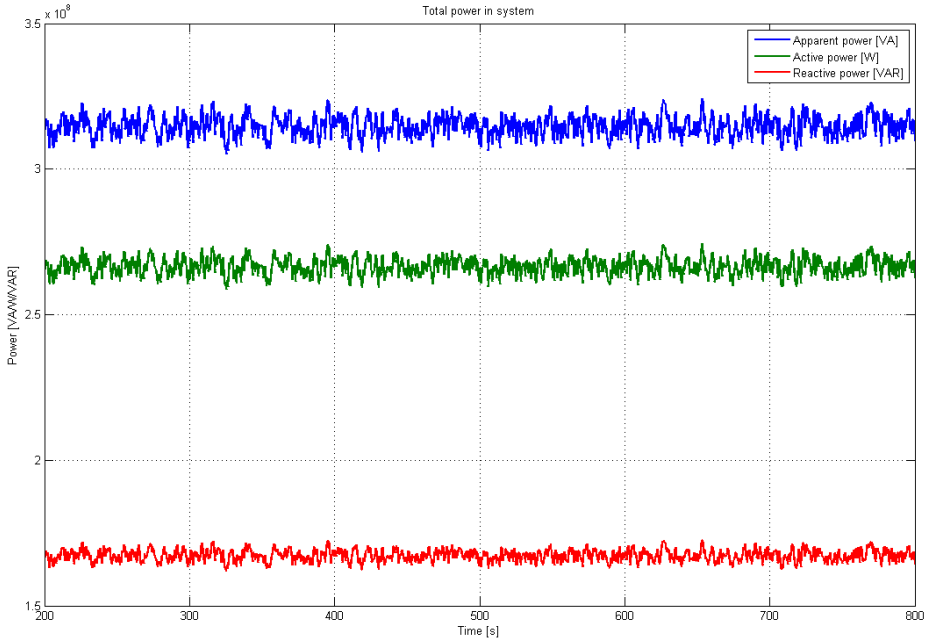

Figure 9.5: Power produced and consumed during steady state with 26 wind turbines and peak loads

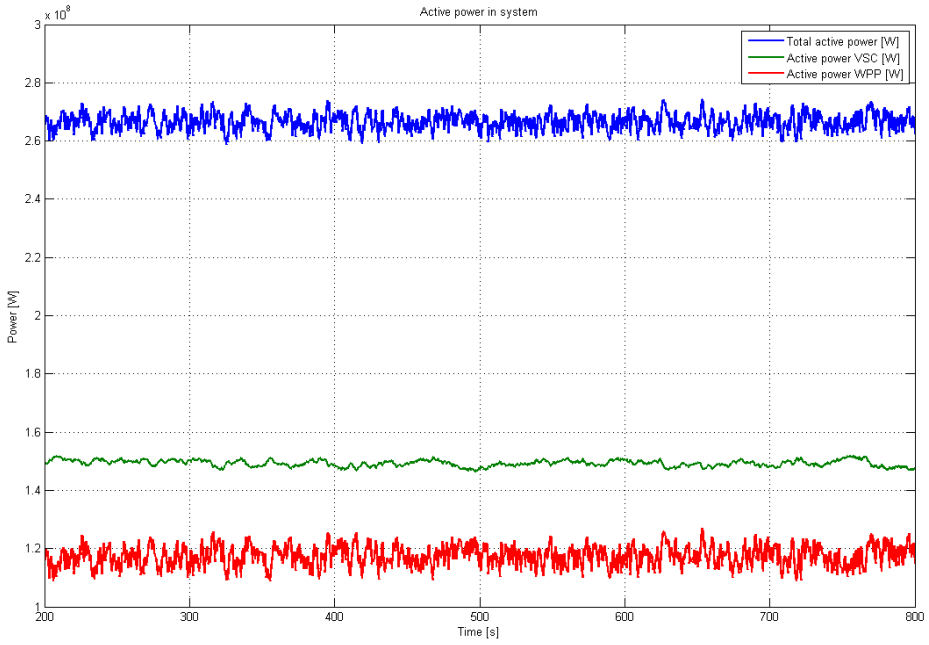

Figure 9.6: DS active power and active power delivered by WPP and VSC during steady state with 26 wind turbines and peak loads

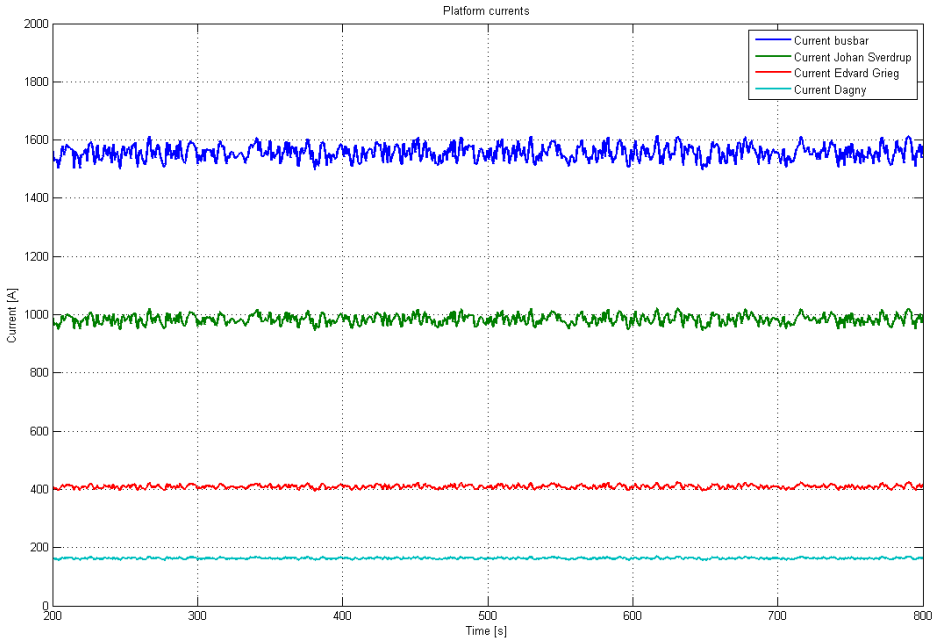

Figure 9.7: Current in DS and load currents during steady state with 13 wind turbines and peak loads

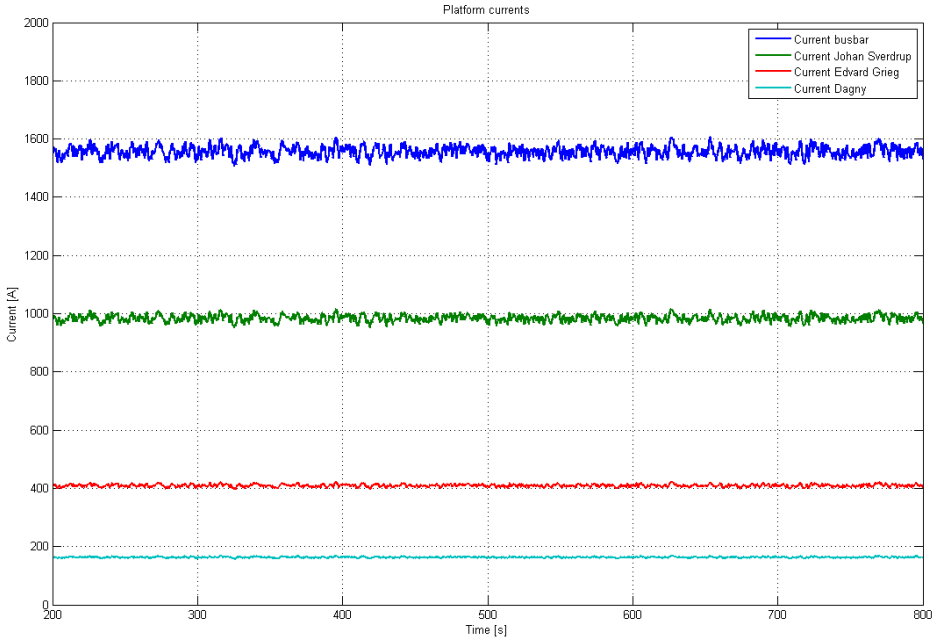

Figure 9.8: Current in DS and load currents during steady state with 26 wind turbines and peak loads

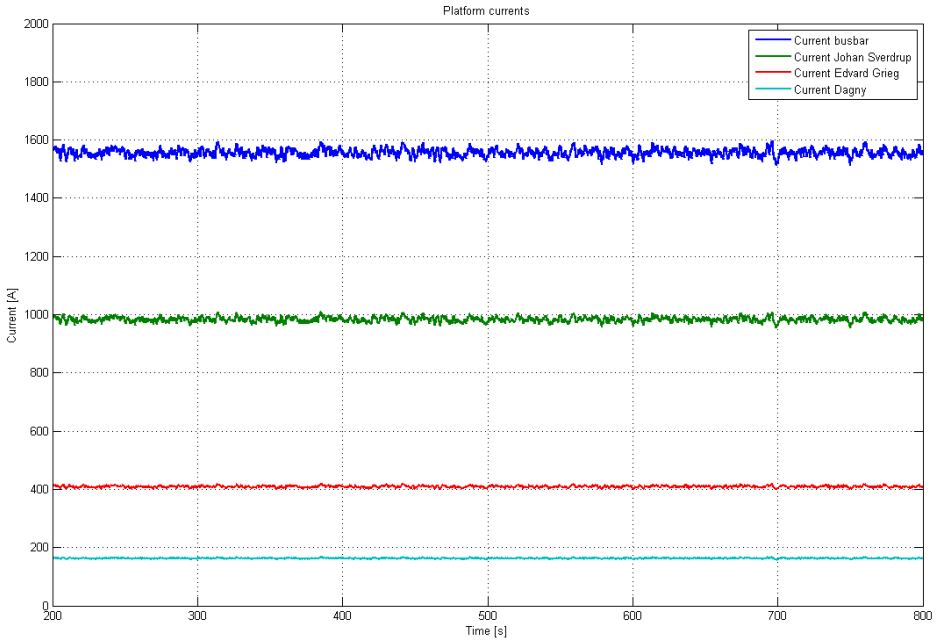

Figure 9.9: Current in DS and load currents during steady state with 52 wind turbines and peak loads

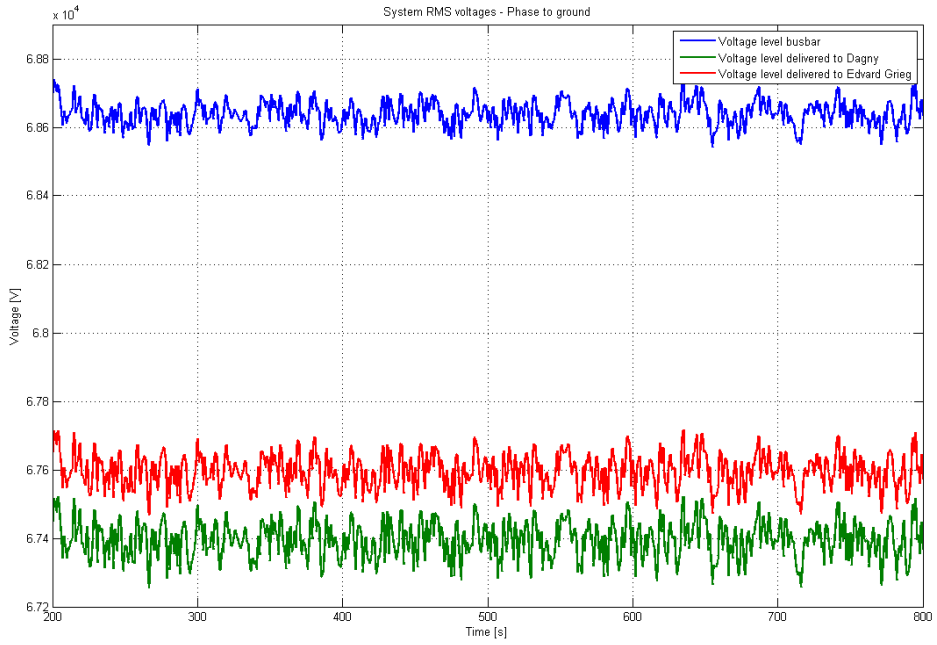

Figure 9.10: System RMS voltages during steady state with 13 wind turbines and peak loads

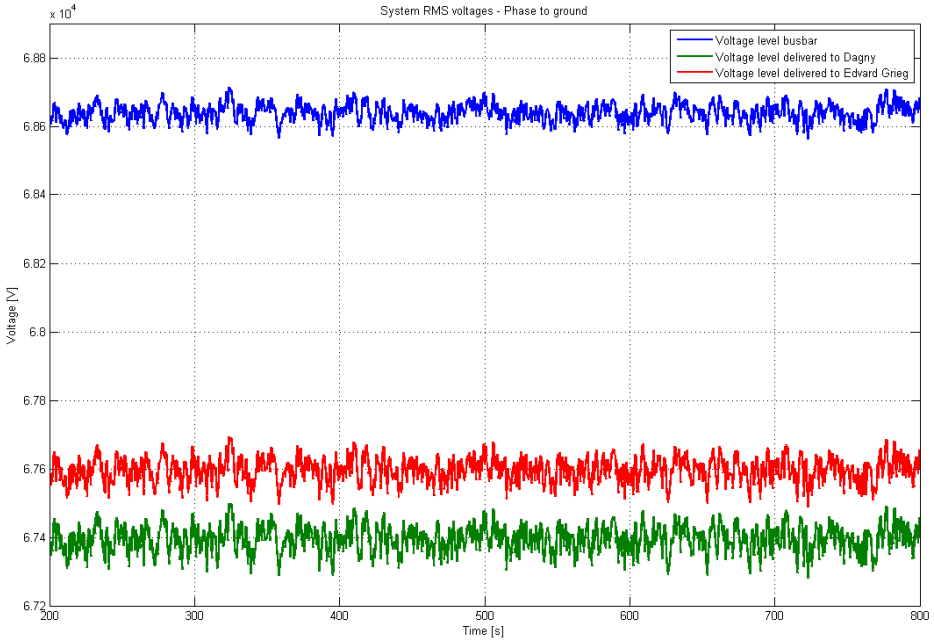

Figure 9.11: System RMS voltages during steady state with 26 wind turbines and peak loads

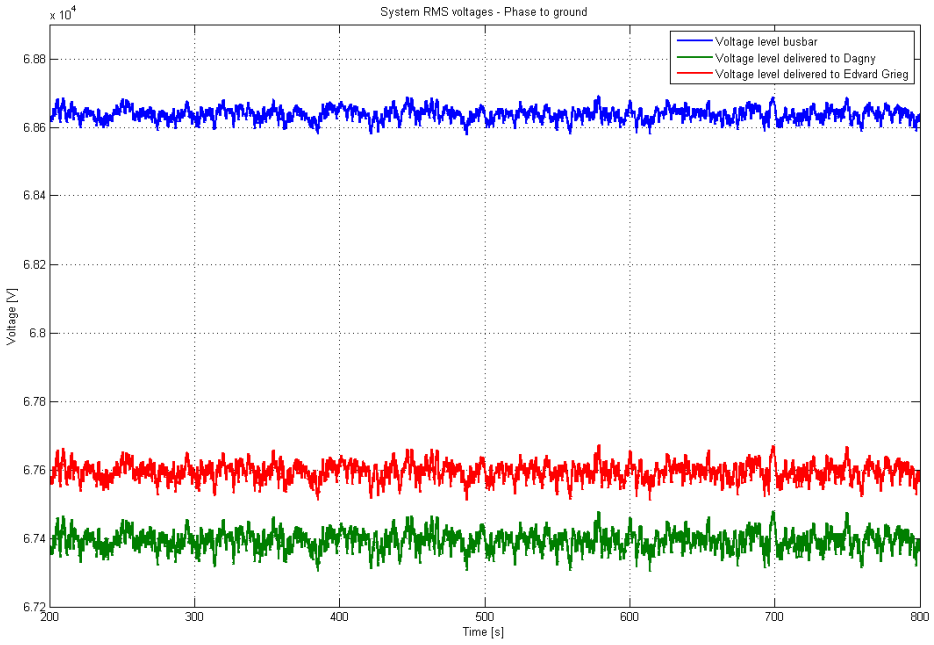

Figure 9.12: System RMS voltages during steady state with 52 wind turbines and peak loads

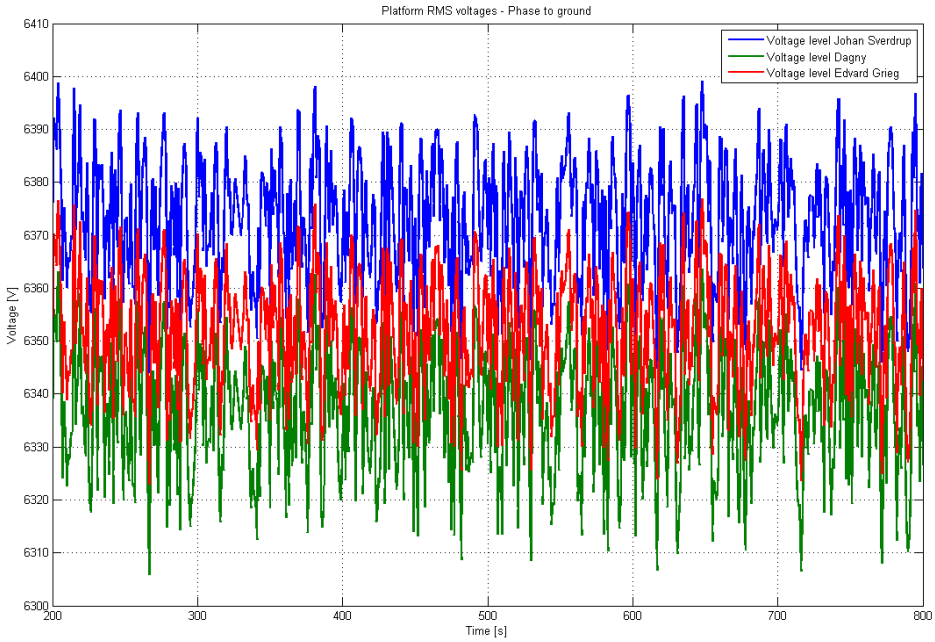

Figure 9.13: Platform RMS voltages during steady state with 13 wind turbines and peak loads

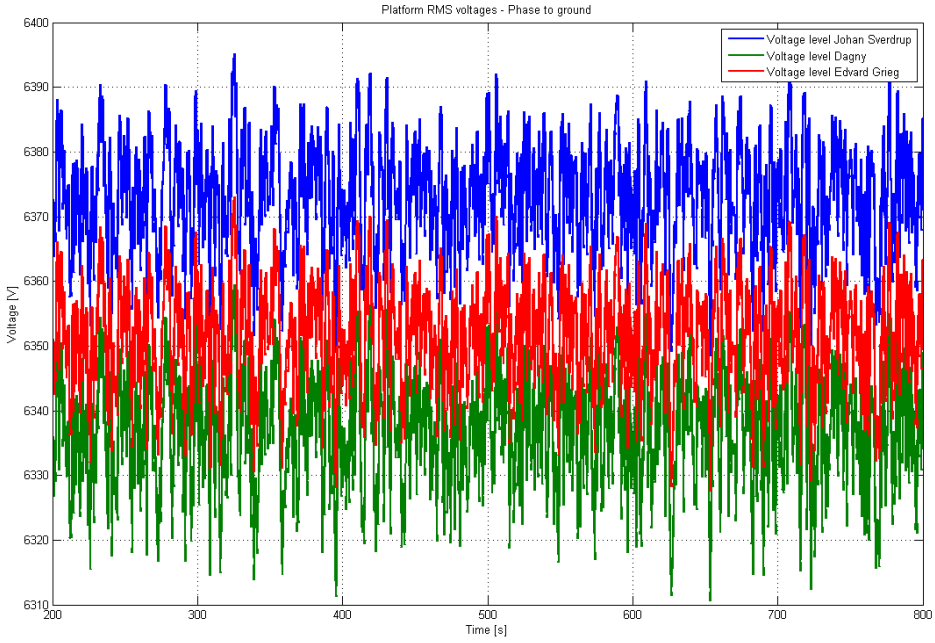

Figure 9.14: Platform RMS voltages during steady state with 26 wind turbines and peak loads

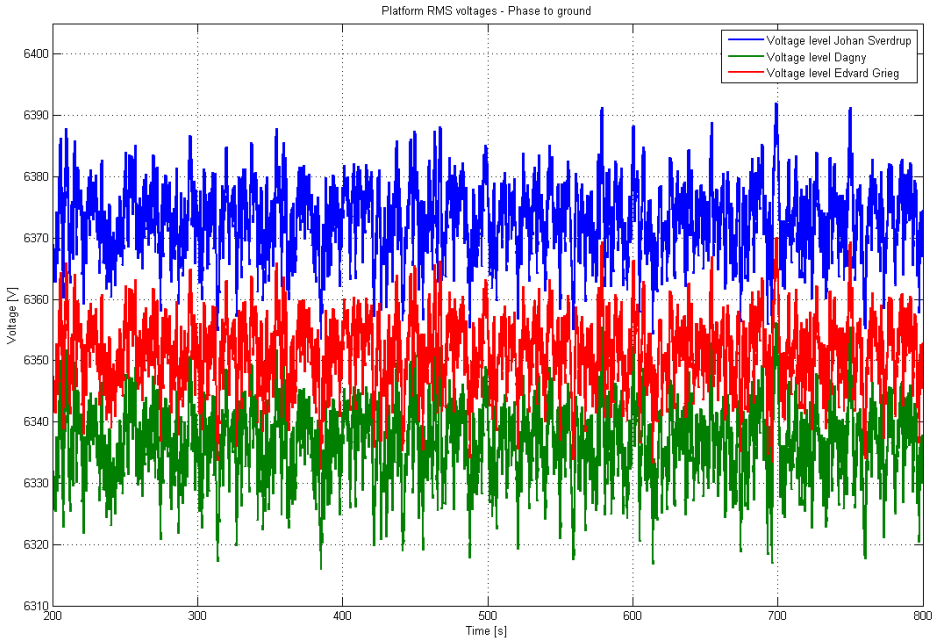

Figure 9.15: Platform RMS voltages during steady state with 52 wind turbines and peak loads

Increasing Mean Wind Speed with Peak Load

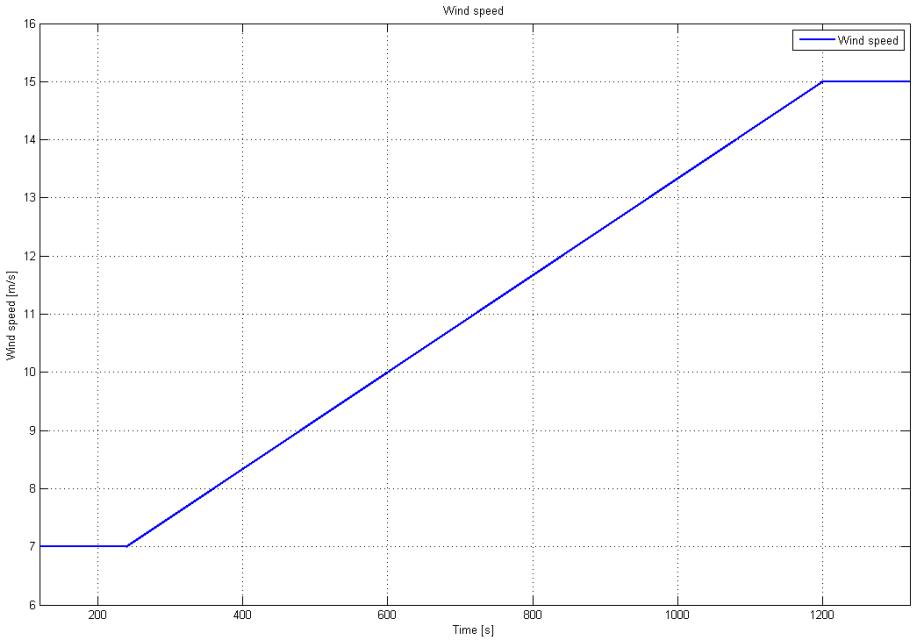

Figure 9.16: Wind speed during increase in WPP production for all three cases.

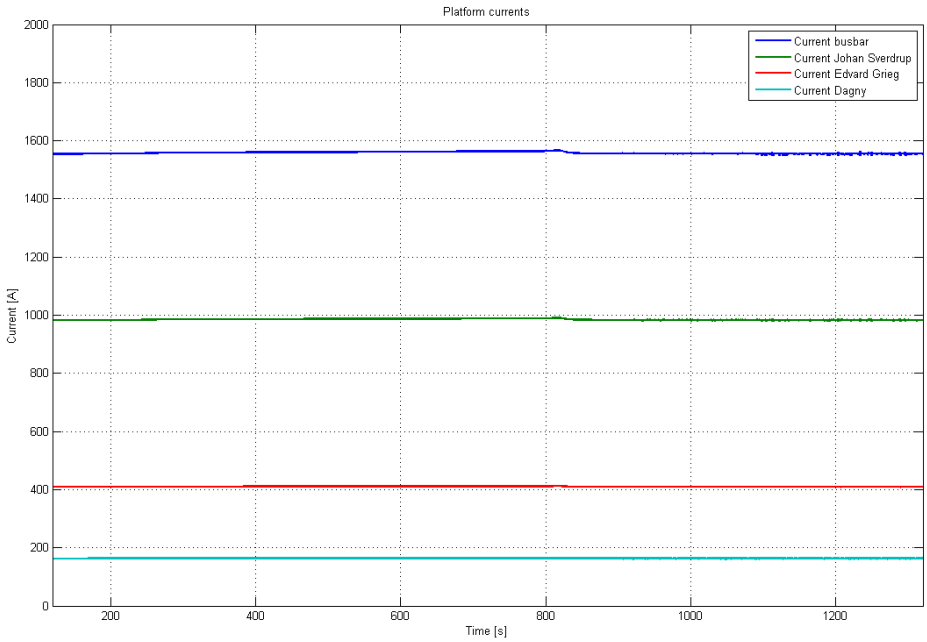

Figure 9.17: Current in DS and load currents during increasing wind speed with 13 wind turbines and peak loads.

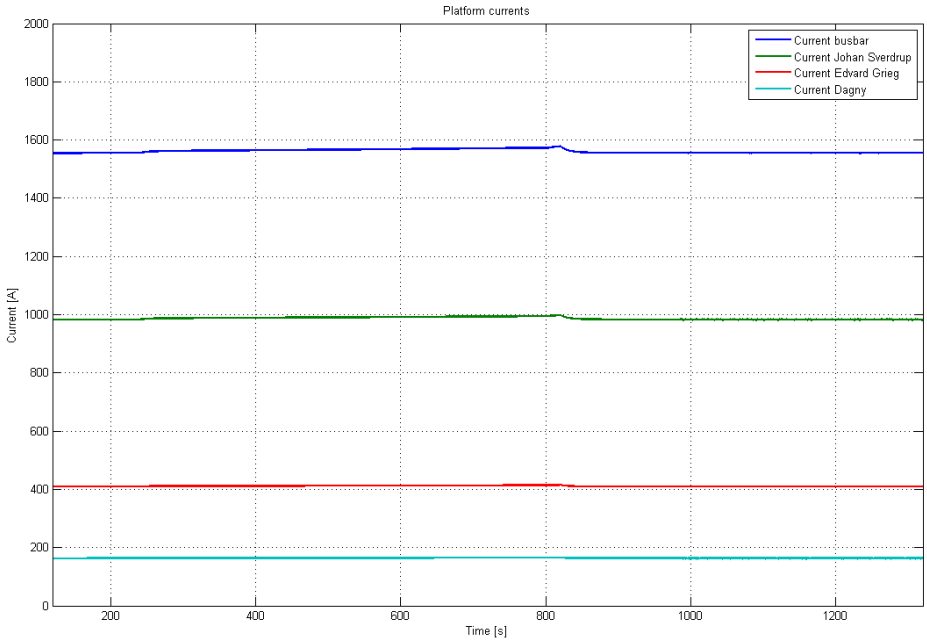

Figure 9.18: Current in DS and load currents during increasing wind speed with 26 wind turbines and peak loads.

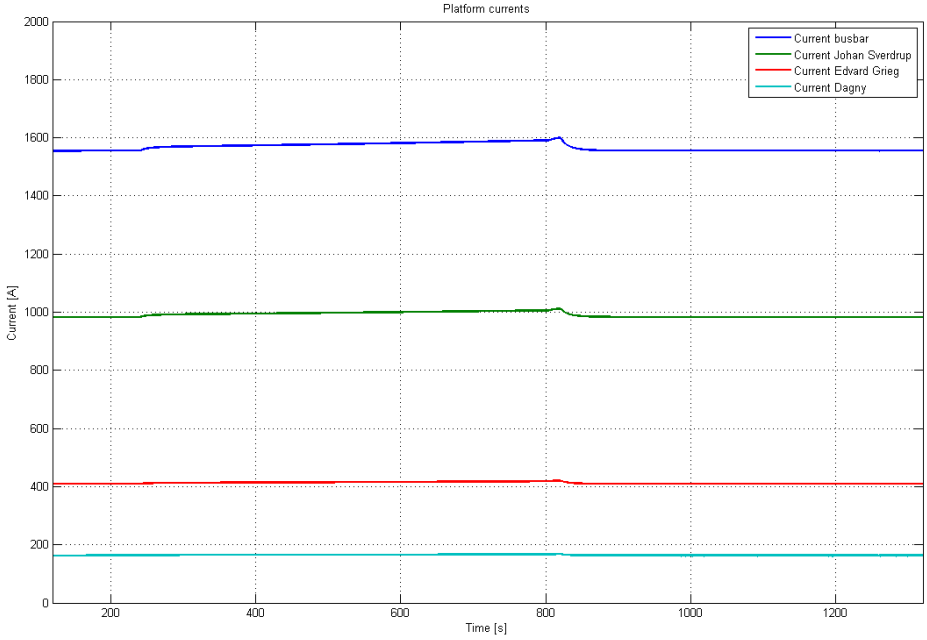

Figure 9.19: Current in DS and load currents during increasing wind speed with 52 wind turbines and peak loads.

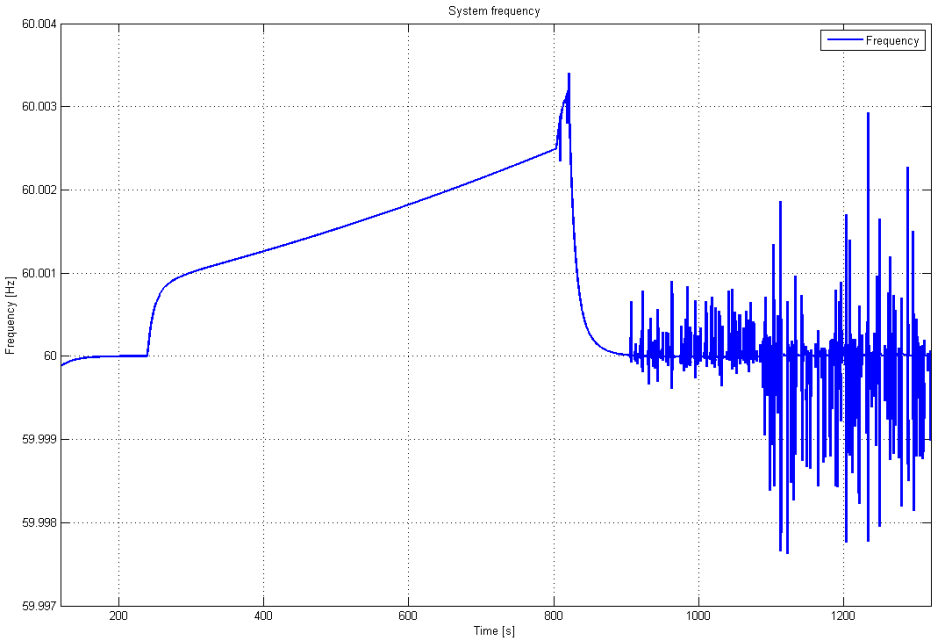

Figure 9.20: Frequency during increasing wind speed with 13 wind turbines and peak loads.

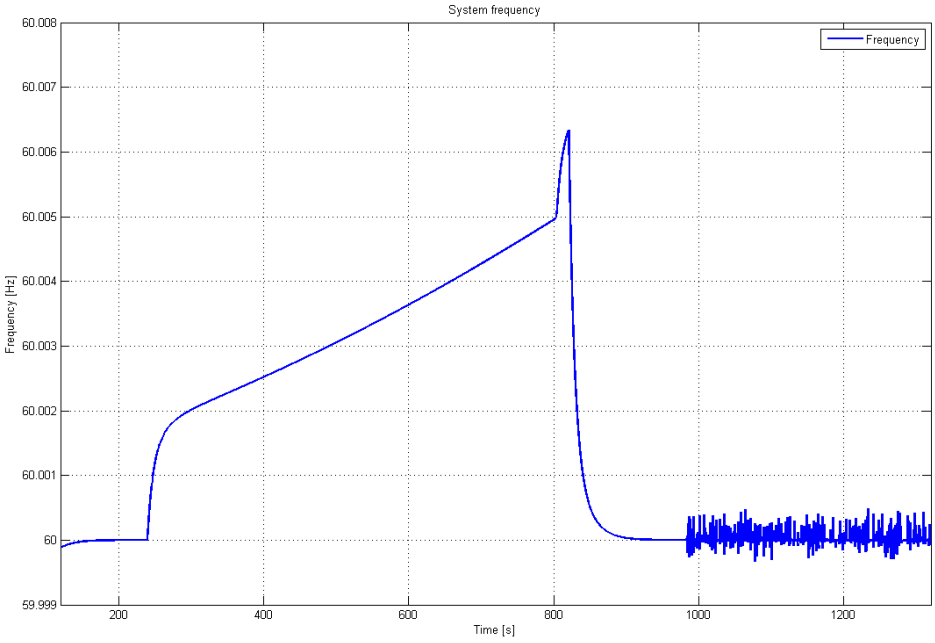

Figure 9.21: Frequency during increasing wind speed with 26 wind turbines and peak loads.

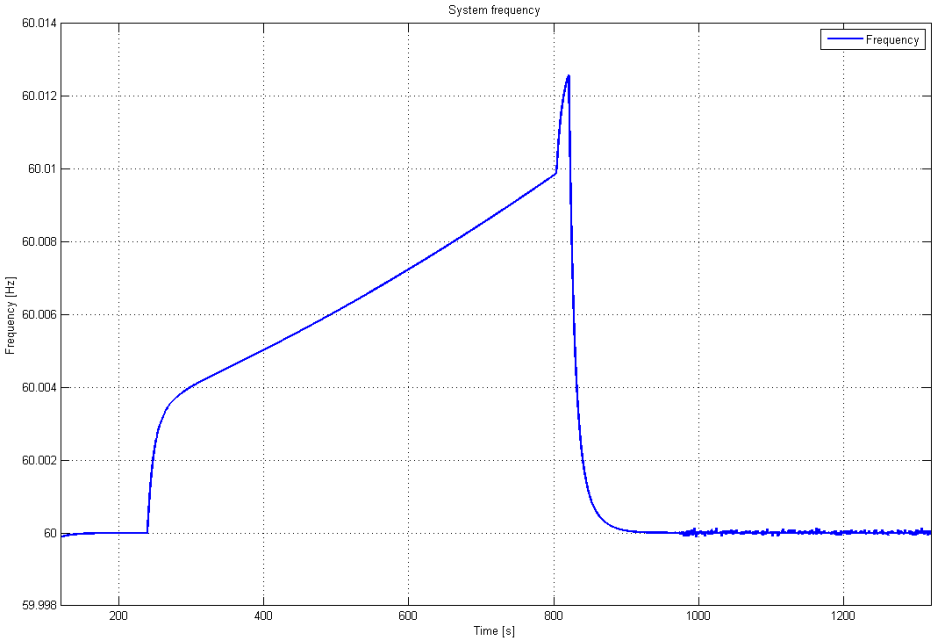

Figure 9.22: Frequency during increasing wind speed with 52 wind turbines and peak loads.

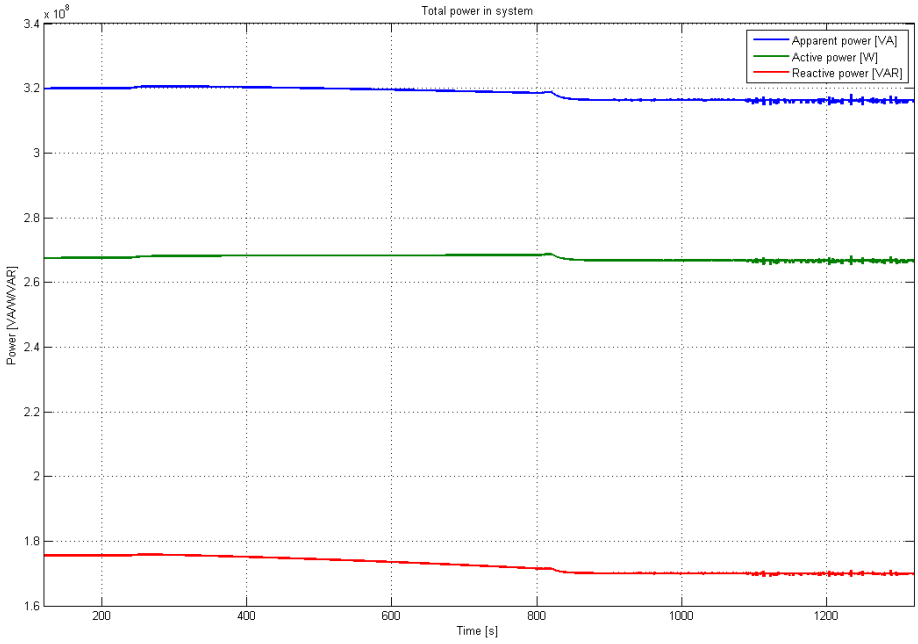

Figure 9.23: Power produced and consumed during increasing wind speed with 13 wind turbines and peak loads.

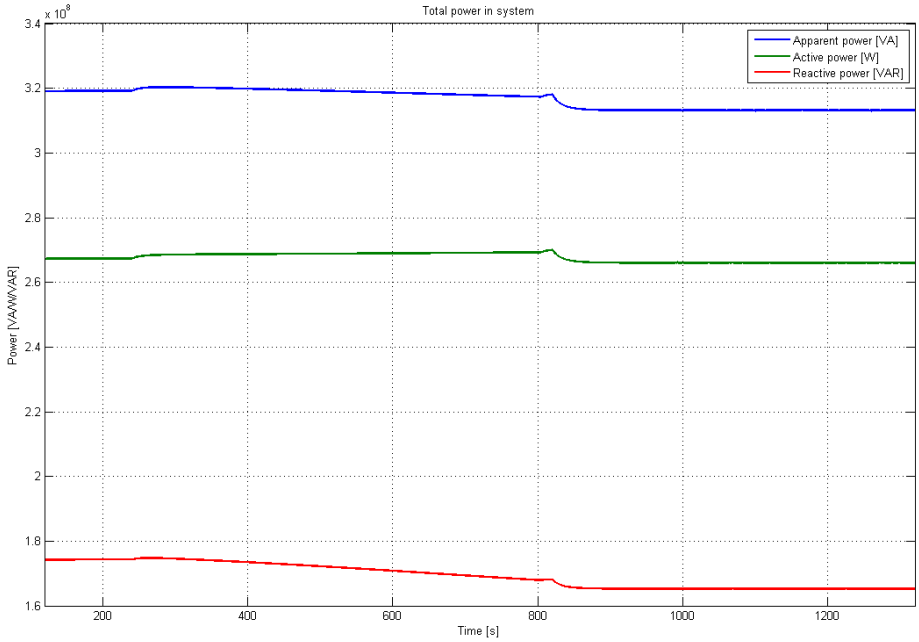

Figure 9.24: Power produced and consumed during increasing wind speed with 26 wind turbines and peak loads.

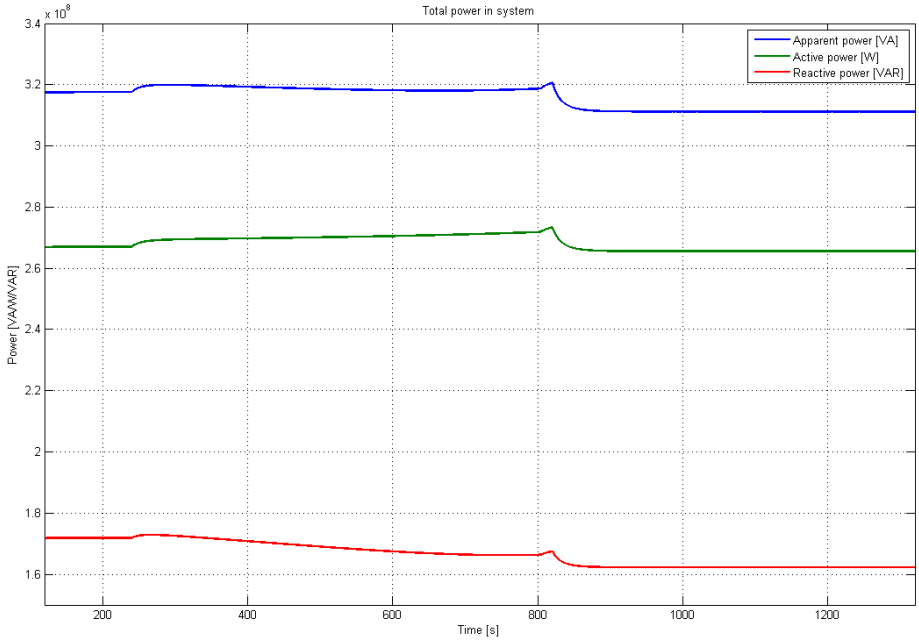

Figure 9.25: Power produced and consumed during increasing wind speed with 52 wind turbines and peak loads.

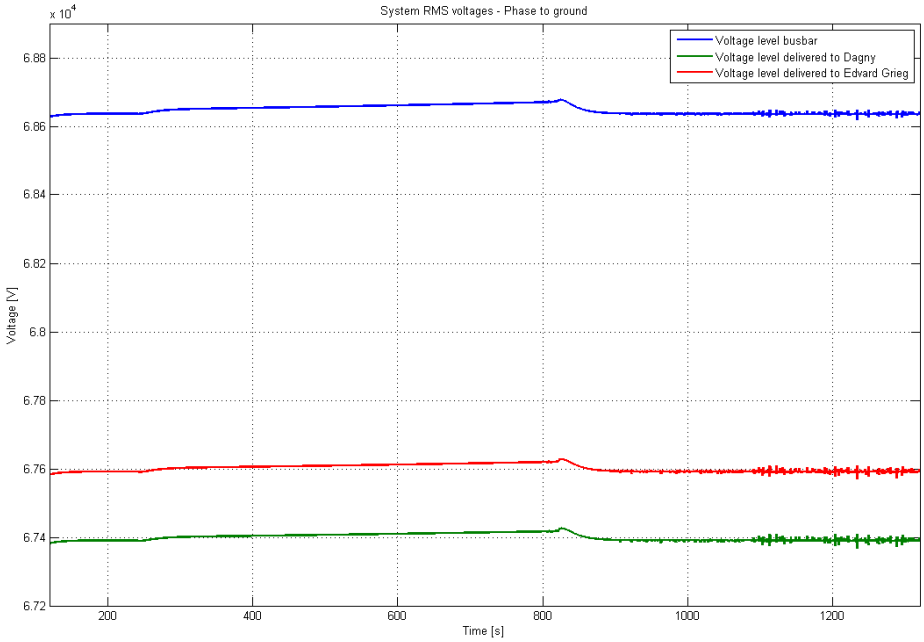

Figure 9.26: System RMS voltages during increasing wind speed with 13 wind turbines and peak loads.

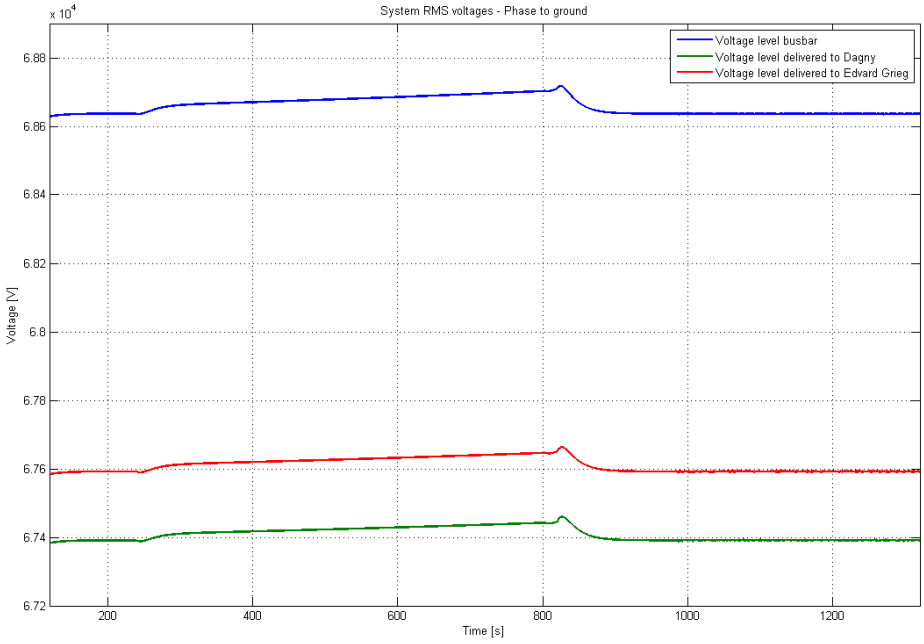

Figure 9.27: System RMS voltages during increasing wind speed with 26 wind turbines and peak loads.

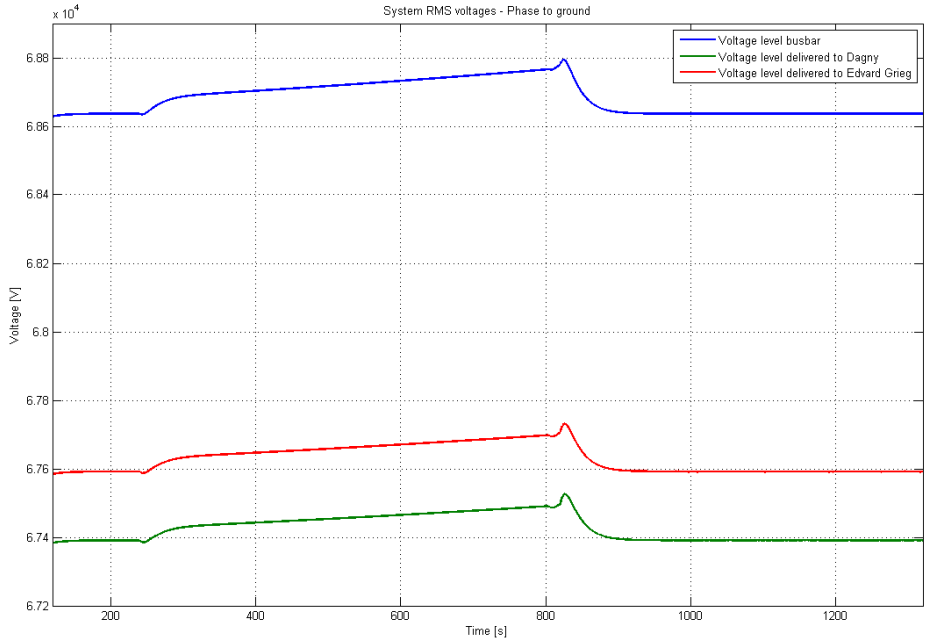

Figure 9.28: System RMS voltages during increasing wind speed with 52 wind turbines and peak loads.

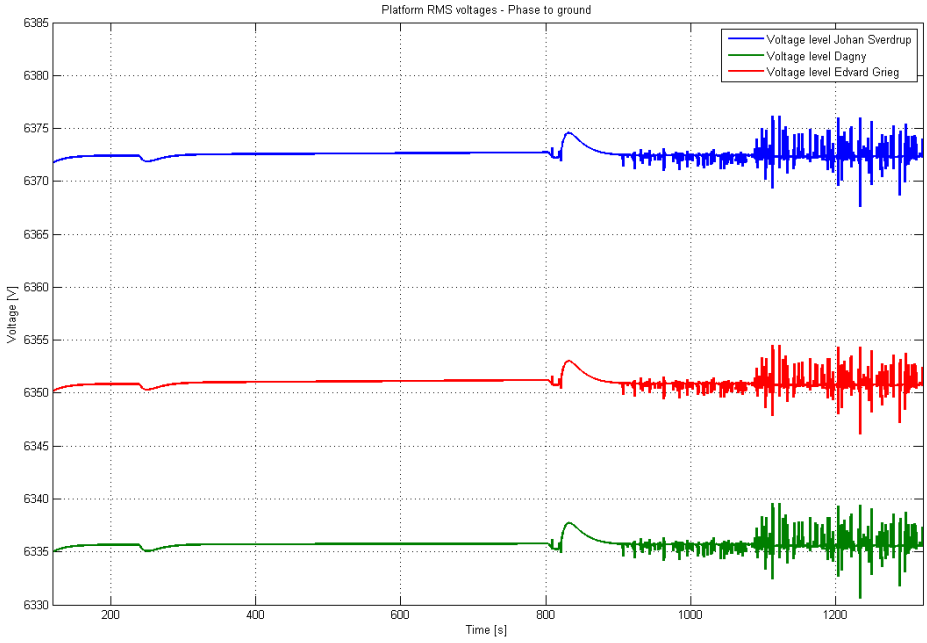

Figure 9.29: Platform RMS voltages during increasing wind speed with 13 wind turbines and peak loads.

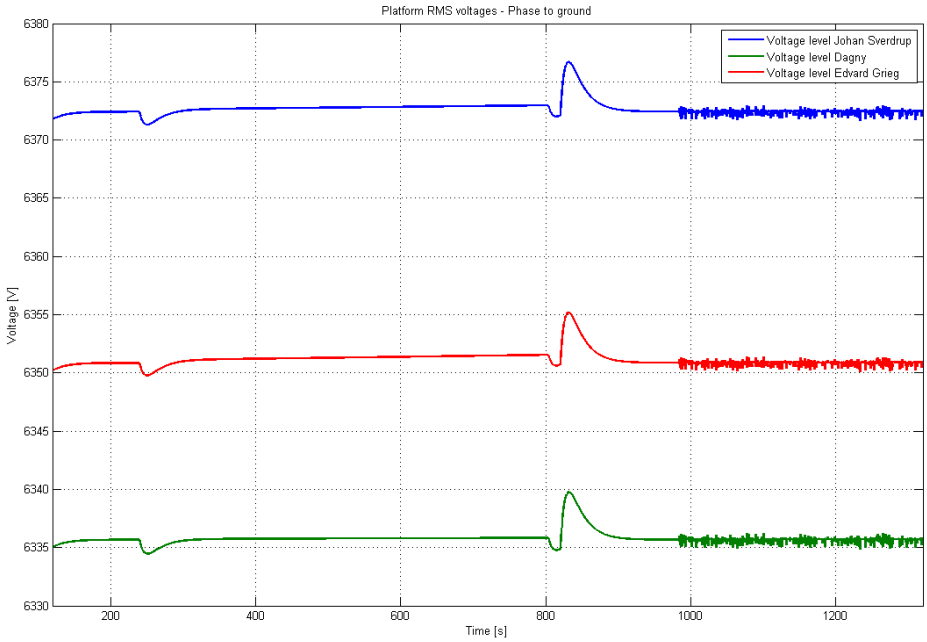

Figure 9.30: Platform RMS voltages during increasing wind speed with 26 wind turbines and peak loads.

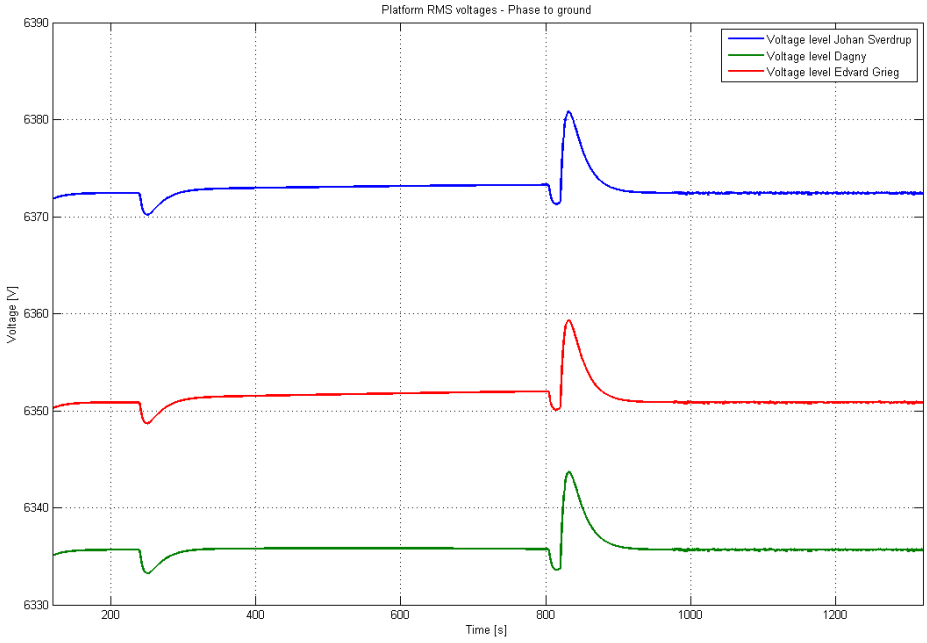

Figure 9.31: Platform RMS voltages during increasing wind speed with 52 wind turbines and peak loads.

Wind Speed Reaching Critical High Point / WPP stop in production with Peak Load

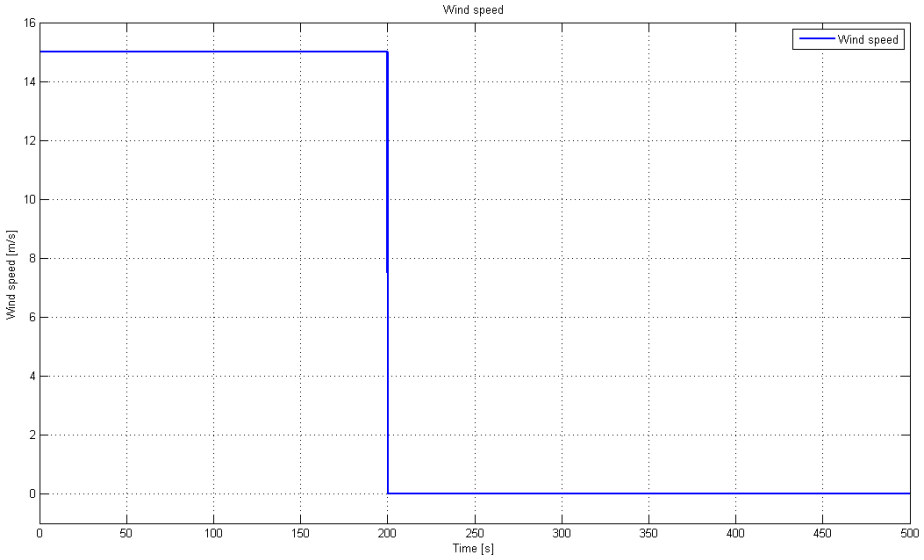

Figure 9.32: Wind speed during WPP production stop for all three cases.

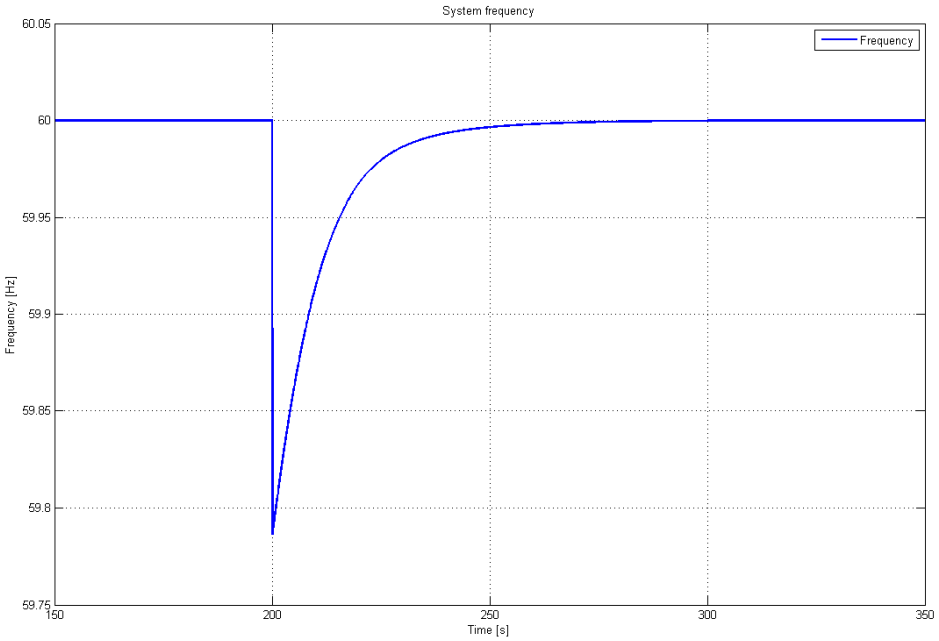

Figure 9.33: Frequency during WPP production stop with 26 wind turbines and peak loads.

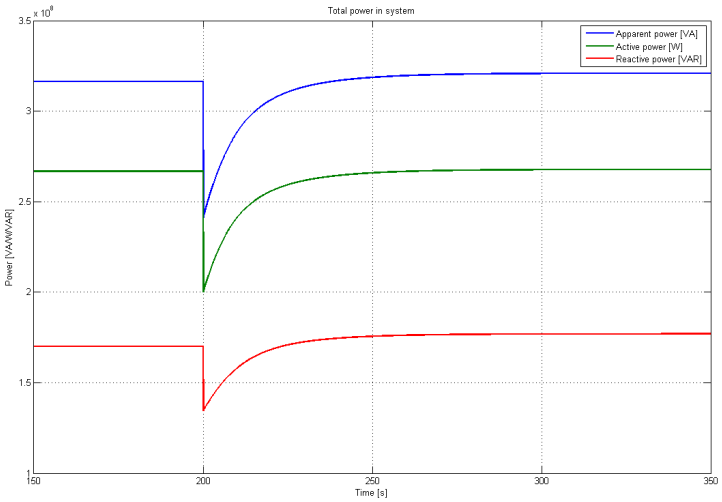

Figure 9.34: Power produced and consumed during WPP production stop with 13 wind turbines and peak loads.

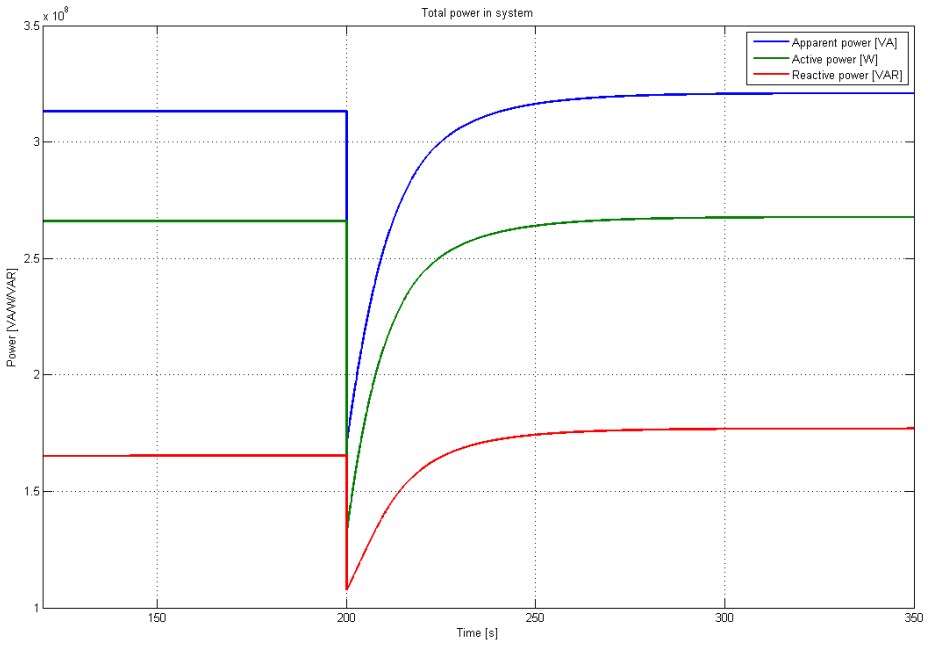

Figure 9.35: Power produced and consumed during WPP production stop with 26 wind turbines and peak loads.

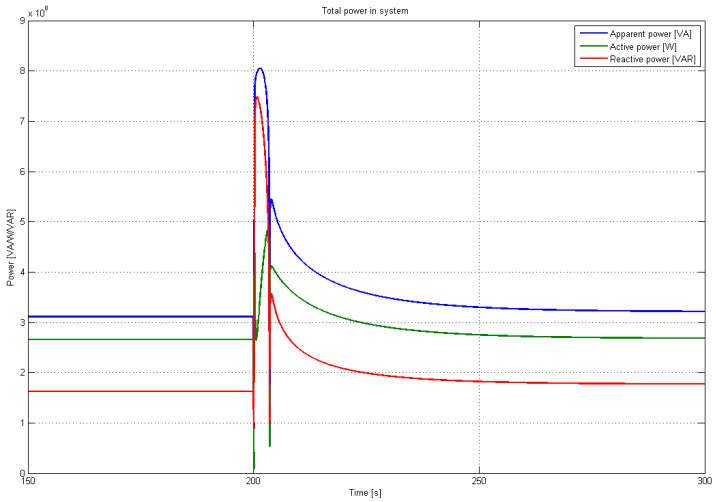

Figure 9.36: Power produced and consumed during WPP production stop with 52 wind turbines and peak loads.

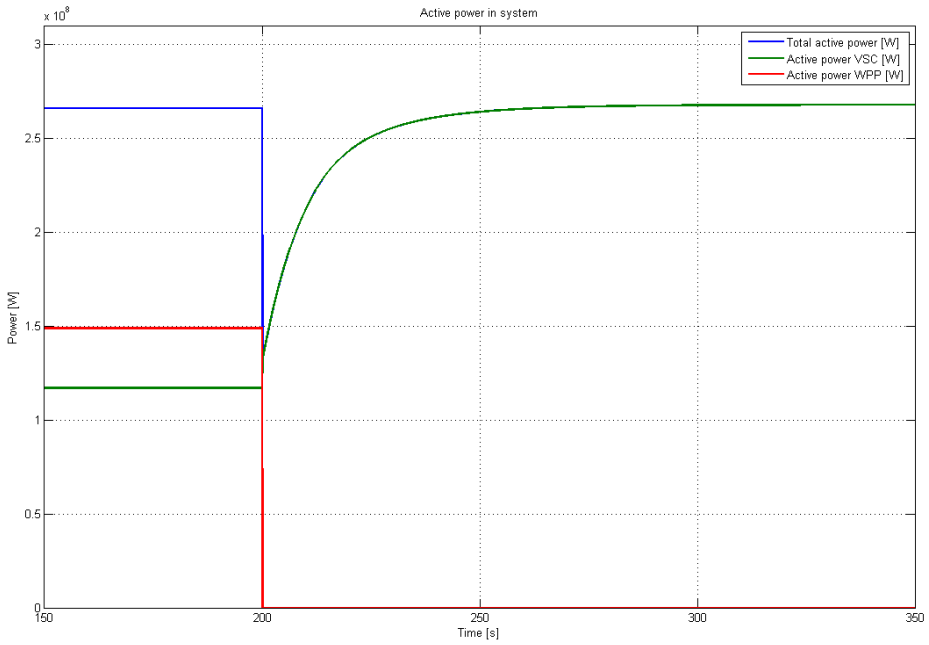

Figure 9.37: DS active power and active power delivered by WPP and VSC during WPP production stop with 26 wind turbines and peak loads.

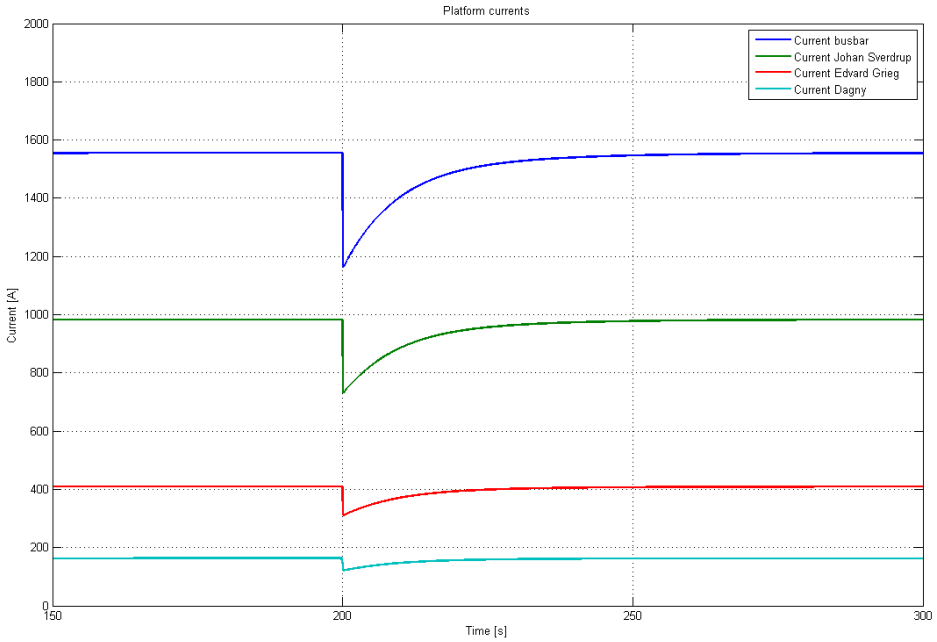

Figure 9.38: Current in DS and load currents during WPP production stop with 13 wind turbines and peak loads.

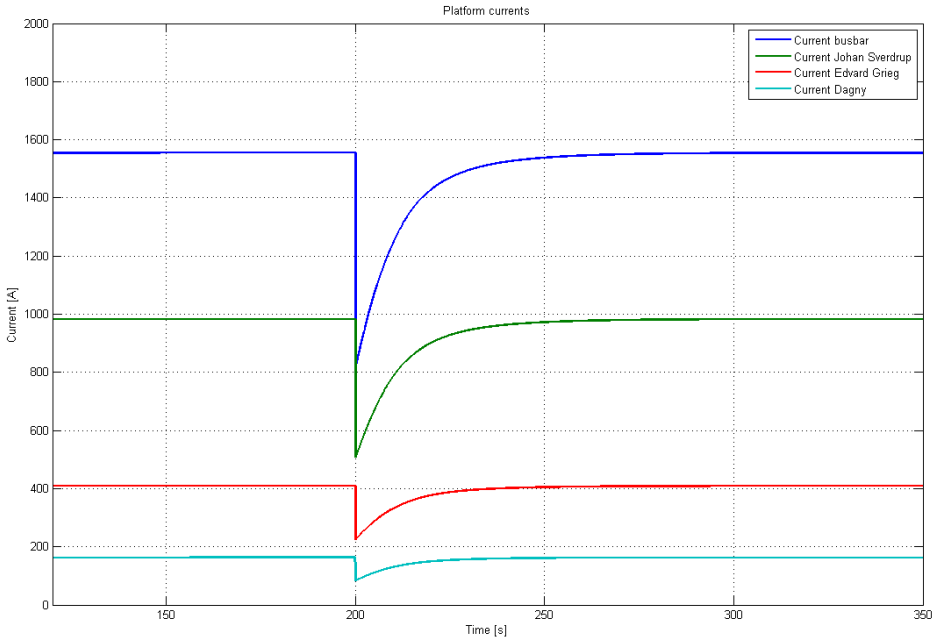

Figure 9.39: Current in DS and load currents during WPP production stop with 26 wind turbines and peak loads.

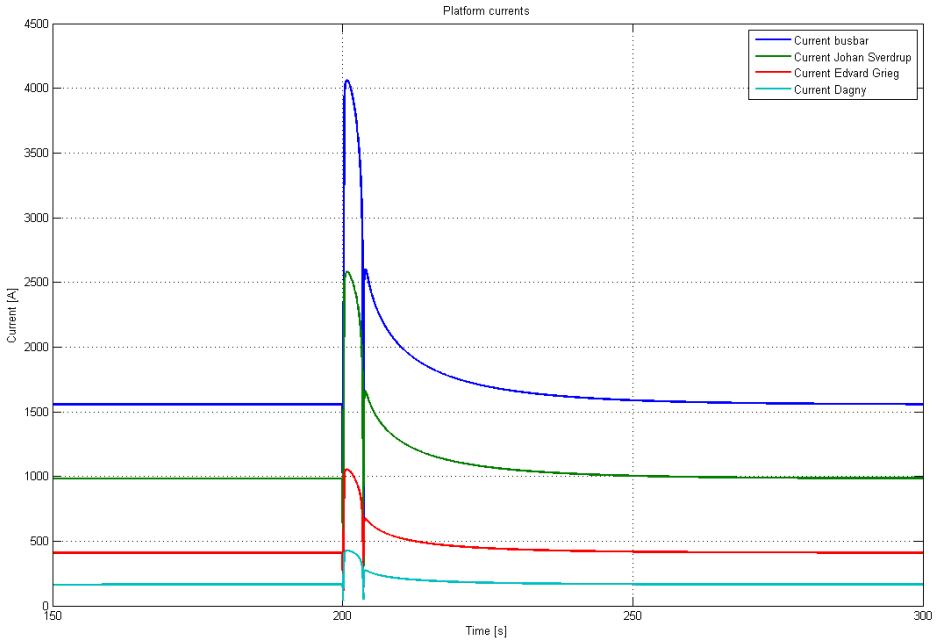

Figure 9.40: Current in DS and load currents during WPP production stop with 52 wind turbines and peak loads.

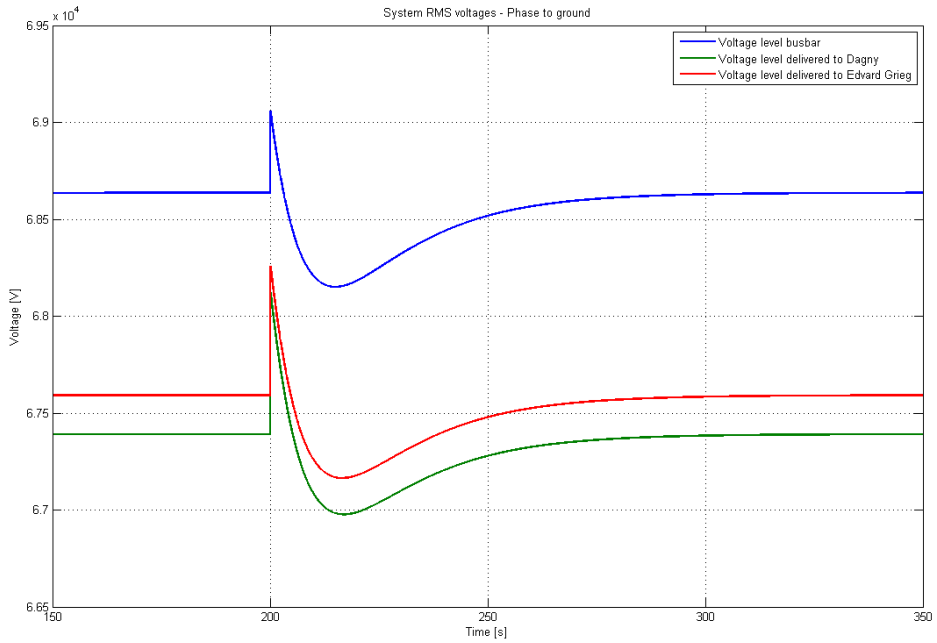

Figure 9.41: System RMS voltages during WPP production stop with 13 wind turbines and peak loads.

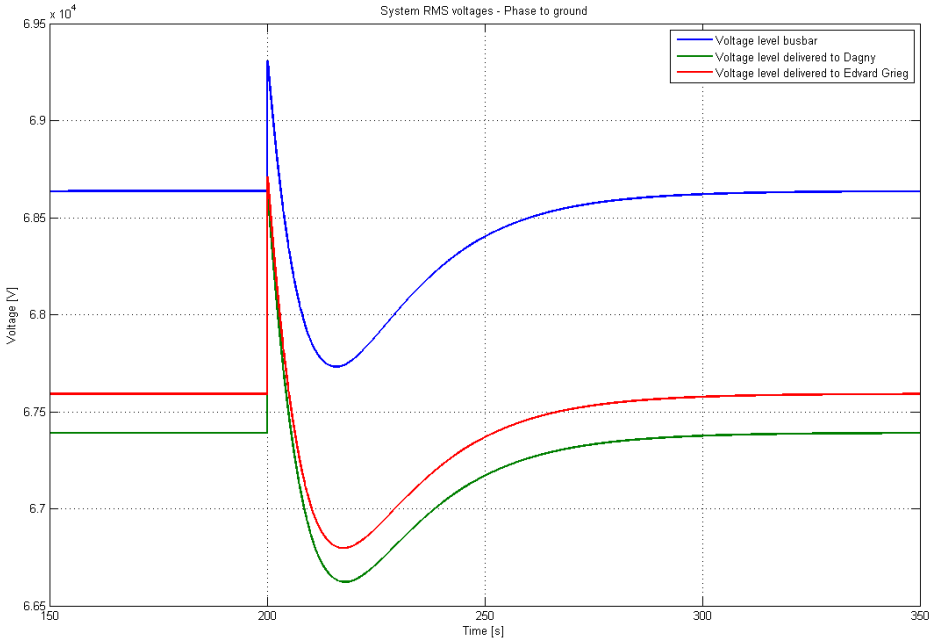

Figure 9.42: System RMS voltages during WPP production stop with 26 wind turbines and peak loads.

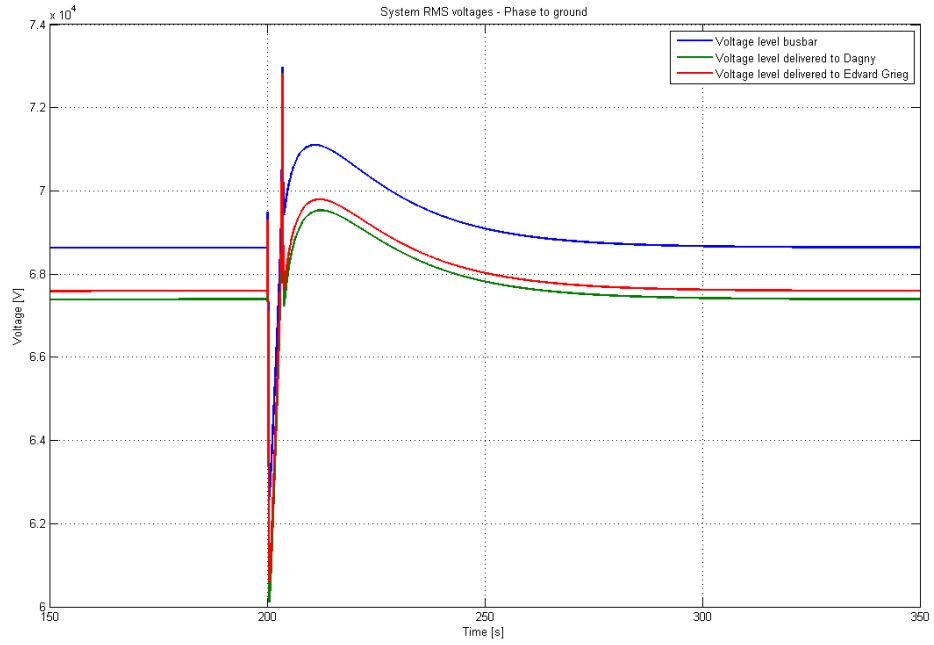

Figure 9.43: System RMS voltages during WPP production stop with 52 wind turbines and peak loads.

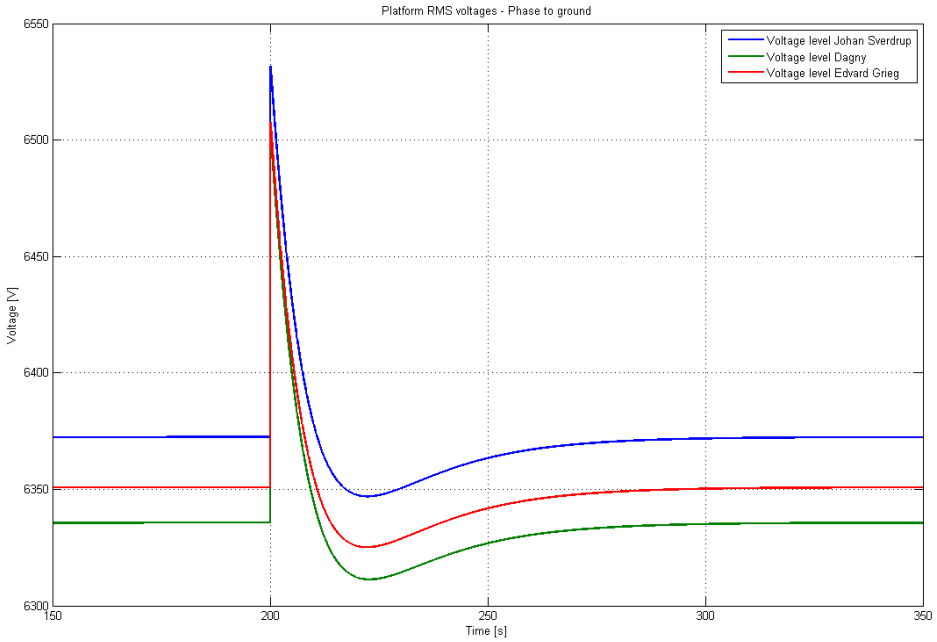

Figure 9.44: Platform RMS voltages during WPP production stop with 13 wind turbines and peak loads.

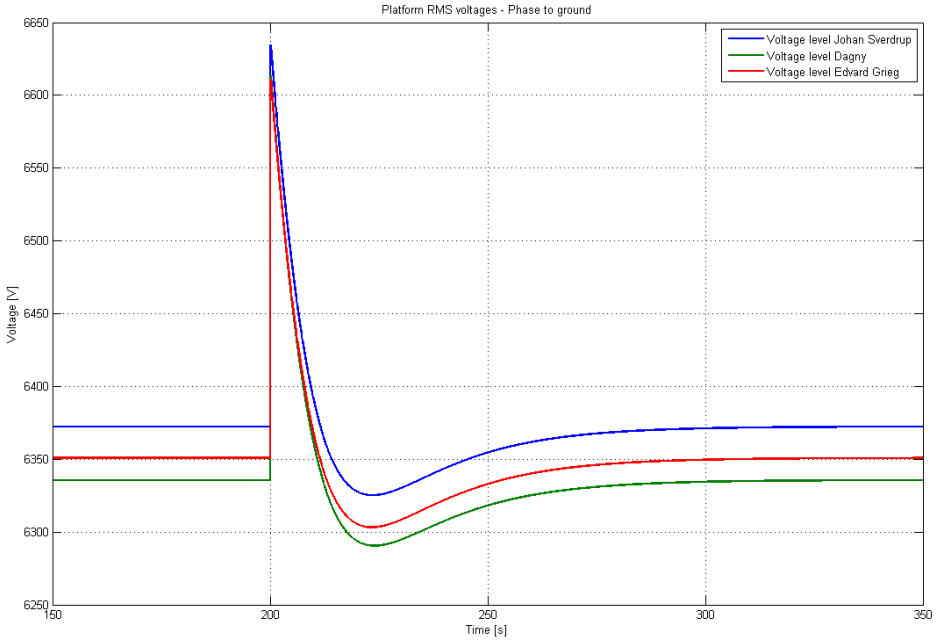

Figure 9.45: Platform RMS voltages during WPP production stop with 26 wind turbines and peak loads.

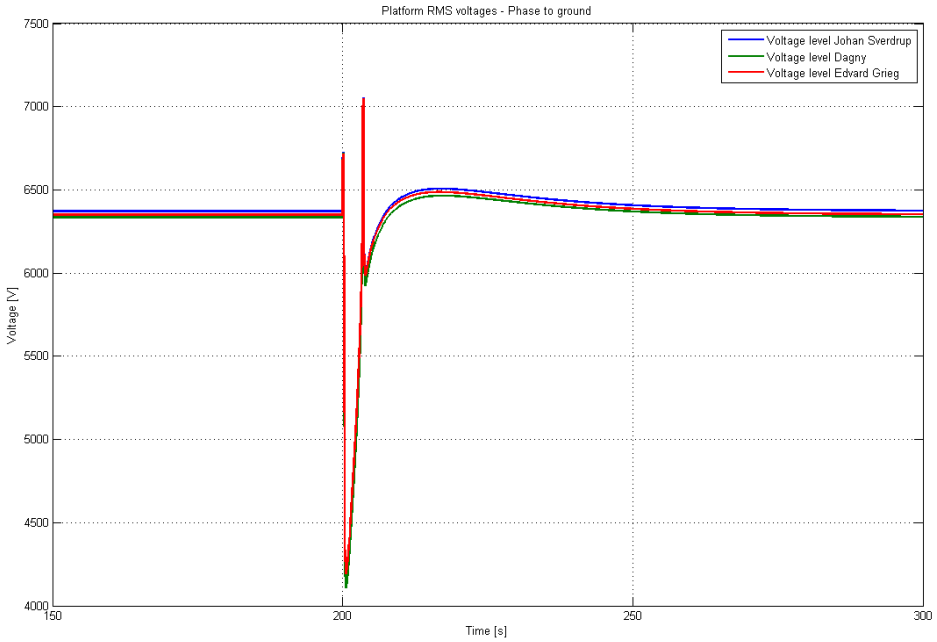

Figure 9.46: Platform RMS voltages during WPP production stop with 52 wind turbines and peak loads.

Appendix E - Estimations: Excel Sheets

System voltage [MV]	**0,11**					
Power Consumption						
	Total	Loss transmission	Johan Sverdrup	Dagny	Edvard Grieg & Ivar Aasen	New Discovery
Case 1, peak [MW]	306,0	10,5	186,7	31,0	77,8	
Case 2, avarage [MW]	181,5	10,5	93,3	31,0	46,7	
Case 4, extra platform [MW]	342,5	16,0	186,7	31,0	77,8	31
Distance [km]			0	60	20	30
Load currents						
	DPT1 / DPT2	Johan Sverdrup	Dagny	Edvard Grieg & Ivar Aasen	New Discovery	
Case 1, peak [A]	775	980	163	408		
Case 2, avarage [A]	449	490	163	245		
Case 4, extra platform [A]	857	980	163	408	163	

Estimated wind power production and short circuit calculation

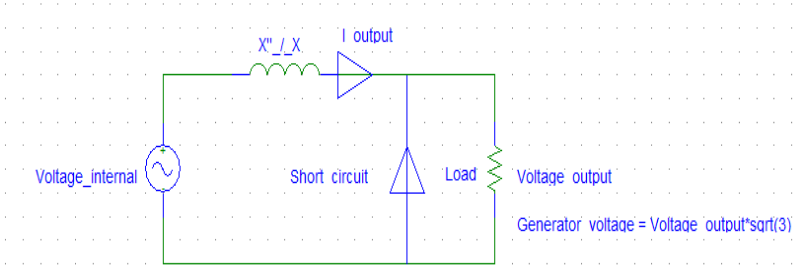

modeled as the the short circuit of a synchronous generator. Where X" is the total sub-transient reactance of the generator, the wind turbine transformer and the the collector line reactance. The internal voltage of the generator can be calculated from full load conditions.

		Power [MW]	Number of HywindX turbines
Case 1, 25 % of max load		78	13
Case 2, 50 % of max load		156	26
Case 3, 100 % of max load		312	52
HywindX			
Generator Voltage [kV]		0.69	
Power [MW]		6	
Impedance [ohm]		0.08	
Reactance [p.u]		1.3	
Sub-transient reactance [p.u]		0.2	
Sub-transient reactance [ohm]		0.016	
Transient reactance [p.u]		0.25	
Transient reactance [ohm]		0.020	
Internal Generator voltage [kV]		0.98	
Transformer WT			
Voltage primary side [kV]		33	
reactance [p.u]		0.05	
Capacity [MW]	Equal to wind turbine		
Distribution System Transformer 3			
Voltage primary side [kV]		110	
Transformer reactance [p.u]		0	

Three phase symmetrical short circuit, sub-transient

	Total Reactance secondary side DST3 [ohm]	Internal voltage seen from secondary side DST3 [kV]	Short Circuit current secondary side DST3 [kA]
	45.38	46.94	1.035

	HywindX, Short Circuit current primary side DST3 [A]	Estimated Load current [A]
Case 1, 25 % of max load	4035	409
Case 2, 50 % of max load	8069	819
Case 3, 100 % of max load	16138	1638

Three phase symmetrical short circuit, transient

	Total Reactance secondary side DST3 [ohm]	Internal voltage seen from secondary side DST3 [kV]	Short Circuit current secondary side DST3 [kA]
	54.45	46.94	0.862

	HywindX, Short Circuit current primary side DST3 [A]
Case 1, 25 % of max load	3362
Case 2, 50 % of max load	6724
Case 3, 100 % of max load	13449